NASA TECHNICAL NOTE

NASA TN D-5965

LOW-SPEED WIND-TUNNEL INVESTIGATION OF ALL-FLEXIBLE TWIN-KEEL TENSION-STRUCTURE PARAWINGS

by Paul G. Fournier

Langley Research Center
Hampton, Va. 23365

1. Report No. NASA TN D-5965	2. Government Accession No.	3. Recipient's Catalog No.
4. Title and Subtitle LOW-SPEED WIND-TUNNEL INVESTIGATION OF ALL-FLEXIBLE TWIN-KEEL TENSION-STRUCTURE PARAWINGS		5. Report Date October 1970
		6. Performing Organization Code
7. Author(s) Paul G. Fournier		8. Performing Organization Report No. L-7035
9. Performing Organization Name and Address NASA Langley Research Center Hampton, Va. 23365		10. Work Unit No. 126-13-10-03
		11. Contract or Grant No.
12. Sponsoring Agency Name and Address National Aeronautics and Space Administration Washington, D.C. 20546		13. Type of Report and Period Covered Technical Note
		14. Sponsoring Agency Code

15. Supplementary Notes

16. Abstract

Low-speed wind-tunnel tests were made to determine the static aerodynamic characteristics of several tension-structure all-flexible twin-keel parawings having keel cant angles from 0° to 20°. Of the configurations tested, those having 5° to 15° canted keels showed higher values of lift-drag ratio throughout most of the resultant-force range, especially at the higher values of resultant-force coefficient. The overall performance of the basic model was not improved by the addition of either a lower surface scoop or keel mounted upper surface ram-air-inflated tubes. Narrowing the center panel of the basic model did not change the overall performance, whereas widening the center panel resulted in somewhat lower performance. Limited increase in keel-to-payload separation distance resulted in improved performance.

17. Key Words (Suggested by Author(s)) All-flexible parawing Twin-keel parawing Keel cant angle Ram air inflation Low-speed aerodynamics	18. Distribution Statement Unclassified — Unlimited	
19. Security Classif. (of this report) Unclassified	20. Security Classif. (of this page) Unclassified	21. No. of Pages 84	22. Price* $3.00

LOW-SPEED WIND-TUNNEL INVESTIGATION OF ALL-FLEXIBLE

TWIN-KEEL TENSION-STRUCTURE PARAWINGS

By Paul G. Fournier
Langley Research Center

SUMMARY

Low-speed wind-tunnel studies were made to obtain the static aerodynamic characteristics of several tension-structure, all-flexible, twin-keel parawings. These all-flexible parawings were made of nonporous fabric and were attached to a mounting bar by means of multiple suspension lines.

The basic parawing had parallel keels (0° keel cant angle), 45° leading-edge sweep of the flat planform, nose cutoff at 20 percent keel length aft of the theoretical leading-edge apex and contoured, and a center-panel width of 40 percent keel length. Planform variations investigated included keel cant angles of 0°, 5°, 10°, 15°, and 20°, center-panel width, details of nose tie lines for a parawing with 15° cant angle, and added air scoop and ram-air-inflated fabric tubes on the keels. Tests were also made with several keel-payload separation distances.

Relatively small changes in maximum resultant-force coefficient accompanied an increase in keel cant angle from 0° to 15°. Increasing the cant angle to 20°, however, decreased the maximum resultant-force coefficient.

An investigation of the effects of center-panel width for the model with 15° canted keels indicated that both increasing or decreasing the width caused a reduction in maximum lift-drag ratio from the value for the basic center-panel width. Maximum resultant-force coefficients were highest for the smallest center-panel width investigated and decreased with increasing width.

There was no appreciable benefit to maximum lift-drag ratio from the addition of a lower surface scoop on the parawing center panel or the addition of upper surface ram-air-inflated tubes at the keels of the basic parallel twin-keel model.

For a keel-payload separation distance of approximately 1.00 keel length, values of maximum lift-drag ratio increased from 2.78 to 3.27 as the keel cant angle was varied from 0° to 15°. Values of maximum lift-drag ratio decreased when the cant angle of the keels was increased from 15° to 20°. Increasing the keel-payload separation to 1.25 keel length increased the maximum lift-drag ratio of the model with 15° cant angle to a value of 3.41. A modification to the line attachment at the formed nose on the center panel of this parawing increased the maximum lift-drag ratio to 3.48.

INTRODUCTION

Many research investigations of parawings have been conducted by the National Aeronautics and Space Administration in the past several years. This work has been concerned primarily with rigid frame paragliders having widely varying geometric, structural, and aerodynamic characteristics. (See refs. 1 to 4.) Recent parawing research has concentrated on all-fabric lifting surfaces having no structural members or stiffness. (See refs. 5 to 9.) These all-flexible parawings are capable of providing gliding, controllable flight by proper rigging of multiple suspension lines which connect the parawing to the payload. This type of parawing shows considerable promise for use in applications where compact storage and weight requirements dictate the use of a parachute-like tension structure and where significant glide capability is necessary.

Investigations of all-flexible parawings have shown that twin-keel (three lobes) configurations have higher lift-drag ratios than the single-keel (two lobes) configurations because the twin-keel parawings are able to operate at lower angles of attack. The twin-keel parawing is a refined version of the earlier all-flexible single-keel parawing. The refinements included the addition of a rectangular center panel to increase the aspect ratio of the basic single-keel configuration and the contouring of the nose portion of the center panel to produce an airfoil-like leading edge.

The present investigation was conducted for the purpose of determining the aerodynamic characteristics and rigging for an advanced series of twin-keel, all-flexible parawings. These tests were a continuation of the series of twin-keel parawings reported in references 8 and 9 and were an attempt to improve the performance of these types of parawings. The parawings in this paper have identification numbers that are a continuation of the numbering system of models presented in reference 8.

The basic twin-keel parawing configuration had parallel keels (0° keel cant angle), 45° leading-edge sweep of the flat planform, nose cutoff at 20 percent keel length aft of the theoretical leading-edge apex and contoured, and a center-panel width of 40 percent keel length. Planform variations investigated included keel cant angles of 0°, 5°, 10°, 15°, and 20°, center-panel width, details of nose tie lines for a wing with 15° cant angle, and added air scoop and ram-air-inflated fabric tubes on the keels. The models with the various keel cant angles were tested at several keel-payload separation distances.

These wind-tunnel tests were conducted with the tethered method of testing in which the confluence of lines was attached to the tunnel sting-support system and the model flown in tethered flight as described in reference 8. It is believed that this method of testing does simulate, as near as possible, free flight. The attitude of the parawing was varied during the tests by shortening of the control lines. The investigation was made in the 17-foot (5.18 meters) test section of the Langley 300-MPH 7- by 10-foot tunnel.

SYMBOLS

The data presented are referred to the stability axes. The positive direction of forces, moment, and angle are shown in figure 1. The moment reference location was at the confluence of lines and is shown in figure 2.

A	aspect ratio, b_o^2/S
b_o	span of parawing flat planform, inches (centimeters)
c	reference chord for pitching moments, l_k minus Nose cutoff, inches (centimeters)
C_D	drag coefficient, $\dfrac{\text{Drag}}{qS}$
C_L	lift coefficient, $\dfrac{\text{Lift}}{qS}$
C_R	resultant-force coefficient, $\sqrt{C_L^2 + C_D^2}$
C_m	pitching-moment coefficient, $\dfrac{\text{Pitching moment}}{qSc}$
L/D	lift-drag ratio, C_L/C_D
q	free-stream dynamic pressure, pounds per foot^2 (newtons per meter^2)
S	area of parawing-canopy flat planform, feet^2 (meters^2)
S_c	area of center panel, feet^2 (meters^2)
x	linear dimensions
l_k	length of keel of theoretical parawing-canopy flat planform (keel position for each model is shown in fig. 3 and detailed drawings preceding data figures), inches (centimeters)
$l_{k,1}$	actual length of keel of parawing-canopy flat planform (see fig. 3 and detailed drawings preceding data figures), inches (centimeters)

$x/l_{k,1}$ line attachment point along actual parawing keel or leading edge

l/l_k nondimensional length of keel and leading-edge suspension lines measured from parawing to attachment points shown in figure 2

α_w parawing angle measured from vertical normal to wind stream to a specified keel suspension line (eighth keel line was used to measure parawing angle and is indicated in the detailed drawing preceding data figures for each model), degrees

$\Delta l/l_k$ incremental nondimensional shortening of length of control lines

Λ_o angle of sweepback of leading edge of wing canopy flat planform, degrees

Λ_k keel-cant angle, degrees

Subscripts:

max   maximum

le leading edge

DESCRIPTION OF MODELS

Flat planform drawings of the nine models tested are shown in figure 4. Detailed drawings giving pertinent dimensions immediately precede the data for each model and the planform geometric characteristics of all models are summarized in table I. The models were all of sewed construction and were made in accordance with the construction details of figure 3. The canopy material was 0.75 oz/yd^2 (25.4 g/m^2) resin-impregnated rip-stop nylon which had essentially zero porosity. All models were rigged with 130-lb (578 N) test dacron line. This type of line was used because of its low stretch characteristics. Minimizing the line stretch eliminated or reduced the required changes in line length to correct for elongation during the test runs and reduced the time needed to make accurate measurements of line lengths after the tests. The model-support fixture is shown in figure 2. All suspension lines were held by the clamping block except the aft keel lines and the wing tip lines, which were attached to a central eyebolt and outboard eyebolts on the cross bar, respectively. The aft keel lines and wing tip lines were used for control. The line lengths for each test are presented in table II.

All models tested had evenly spaced line attachment points along the keel and leading edge, and the distance to these attachment points is given in percent of the actual keel length $l_{k,1}$. All models had a contoured nose (fig. 5(a)).

Photographs of the models tested are presented in figure 6. The basic twin-keel parawing configuration, model 5 (fig. 6(a)), had parallel keels (0° keel cant angle), 45° leading-edge sweep of the flat planform, nose cutoff at 20 percent keel length aft of the theoretical leading-edge apex and contoured, and a center panel width of 40 percent keel length. The first series of parawings tested (models 17 and 18) had the same basic planform as the basic twin-keel model 5, which was also tested in reference 8. These parawings had parallel keels. Model 17 had a ram-air-inflated triangular scoop on the undersurface of the parawing (fig. 6(c)) and model 18 had a ram-air-inflated tube on the upper surface of the parawing at each keel (fig. 6(d)).

The second series of parawings (models 19, 20, 21, and 24), figure 6(e), had the same outer panels and center-panel width at the nose as the basic parallel twin-keel model 5, but each outer panel was canted outward from the nose 5°, 10°, 15°, or 20°, respectively. The third series of parawings (models 22 and 23), figure 6(f), had the same outer panels as model 21, 15° canted keel, but the center panels were narrowed or widened one-third of the basic width. Details of the contoured nose construction, along with modifications made to the basic line attachment at the nose along the keel, are presented in figure 5. The basic contoured nose was formed by turning the nose of the parawing flat planform under and tying the nose tie strings at the locations shown in figure 5(a). For the basic configuration, the nose of the canopy, at the keels, was tied to the first keel suspension line as indicated in the upper left of figure 5(b). Modifications to the nose contouring included moving the first keel line to the nose as shown in figure 6(b) and the upper right of figure 5(b), addition of a suspension line at the nose (lower left of fig. 5(b)), and an increased length of the nose tie at the keel (lower right of fig. 5(b)).

EXPERIMENTAL PROCEDURE

Static wind-tunnel tests were conducted in the 17-ft (5.18 m) test section of the Langley 300-MPH 7- by 10-foot tunnel. Tests were made at a dynamic pressure of 2.0 lb/ft^2 (95.8 N/m^2).

Data were obtained by means of a six-component strain-gage balance. Measurements of wing angle of attack were made visually by sighting the reference suspension line through a window-mounted protractor. The data presented in this report are referred to the stability-axis system shown in figure 1.

These wind-tunnel tests were conducted with the tethered method of testing in which the confluence of lines was attached to the tunnel sting-support system and the model flown in tethered flight. The models could not conveniently be tested in the wind tunnel with a point suspension system as used in many free-gliding flight tests because of the difficulty of maintaining a trim flying condition in the tunnel. The control lines (aft keel and tip lines) were displaced from the confluence of lines to give the stability needed for testing in the wind tunnel (fig. 2).

Tests were made with the model at several attitudes (α_w) relative to the sting system by use of the aft keel control lines and/or the leading-edge tip control lines. Initially the models were rigged so that the nose would be on the verge of collapse. Then the attitude of the model was systematically increased by incremental shortening of the control lines until longitudinal and lateral oscillations prevented further testing.

CORRECTIONS

Jet-boundary corrections to angle of attack (model attitude, α_w), drag coefficients, and blockage corrections to dynamic pressure as determined from references 10 and 11 have been applied to the wind-tunnel results. The drag of the line attachment mount was negligible and was not subtracted from the total drag.

PRESENTATION OF DATA

As mentioned previously, the data for each model are preceded by a detailed drawing of the model. As a matter of convenience in locating the data source and model definition for the various models, the following table is presented. The data consist of basic longitudinal aerodynamic characteristics through a range of control-line settings (parawing angle-of-attack variation). The data figure also presents variation of lift-drag ratio with resultant-force coefficient. Comparison of performance, variation of L/D with C_R, is an upper envelope of the results of the basic data obtained for the different control settings.

Model	Configuration	Photo	Sketch	Basic data	Scoop and ram-air-inflated tubes	Keel cant angle	Nose line attachments and modification	Center-panel width	Payload distance
				Figures					
5	Basic parawing $\Lambda_k = 0^o$	6(a)	7	8, 9		X			$1.00\ell_k$
				10, 11		X			$1.25\ell_k$
5	First keel line moved to nose	6(b)	12	13, 14			X		$1.00\ell_k$
17	Lower surface scoop added	6(c)	15	16, 17	X				$1.00\ell_k$
18	Ram-air-inflated tubes added	6(d)	18	19, 20	X				$1.00\ell_k$
19	$\Lambda_k = 5^o$	6(e)	21	22, 23		X			$1.00\ell_k$
20	$\Lambda_k = 10^o$	6(e)	24	25, 26		X			$1.00\ell_k$
				27, 28		X			$1.25\ell_k$
21	$\Lambda_k = 15^o$	6(e)	29	30, 31		X			$1.00\ell_k$
				32, 33		X			$1.25\ell_k$
21	Added keel line at nose $\Lambda_k = 15^o$	---	34	35, 36			X		$1.25\ell_k$
				37, 38			X		$1.50\ell_k$
22	1/3 narrower center panel $\Lambda_k = 15^o$	6(f)	39	40, 41				X	$1.00\ell_k$
23	1/3 wider center panel $\Lambda_k = 15^o$	6(f)	42	43, 44				X	$1.00\ell_k$
				45, 46				X	$1.25\ell_k$
24	$\Lambda_k = 20^o$	6(e)	47	48, 49		X			$1.25\ell_k$
				50, 51		X			$1.50\ell_k$
Summary plots presented in figures					52	53 61	54	55 61	56, 57, 58, 59, 60

DISCUSSION

The twin-keel parawing is a refined version of the earlier all-flexible single-keel parawing as discussed previously in detail. The refinements included the addition of a rectangular center panel and the contouring of the nose portion of the center panel to produce an airfoil-like leading edge. The basic twin-keel parawing of this investigation had parallel keels (0° keel cant angle), 45° leading-edge sweep of the flat planform, nose cutoff at 20 percent keel length aft of the theoretical leading-edge apex and contoured, and a center-panel width of 40 percent keel length.

Added Structure

Effect of scoop and ram-air-inflated tubes.- An attempt to increase the performance of the basic parallel twin-keel parawing was investigated by adding a triangular scoop on the lower surface of the center panel, model 17 (fig. 15), or by adding ram-air-inflated tubes on the upper surface of the parawing along the keels, model 18 (fig. 18). Similar to the approach taken in reference 5, these additions were an attempt to make the parawing more rigid and to prevent the wing from collapsing at the lower wing angle α_w so that higher lift-drag ratios may be obtained. A comparison showing the effect of these additions on the variation of L/D with C_R for a keel-payload separation distance of $1.00 l_k$ is given in figure 52.

In general, the addition of either the scoop or the ram-air-inflated tubes did not improve maximum L/D for these wings. Comparison of figures 8, 16, and 19 show that the basic parawing model 5 had the lowest values of C_L available.

Planform Variations

Effect of keel cant angle.- Variations in parawing keel cant angle of 5°, 10°, 15°, and 20° from the basic parallel (0° keel cant angle) twin-keel parawing were investigated. The nose width of the center panel was kept the same as the outer panels were canted outward to increase the wing aspect ratio. Envelopes of the variation of L/D with C_R are presented in figure 53 for keel-payload separation distances of 1.00 and $1.25 l_k$. The results of figure 53(a) for $l/l_k = 1.00$ show a significant increase of maximum lift-drag ratio when keel cant angle is increased from 0° to 5°. Increasing the cant angle to 10° and 15° provided higher maximum lift-drag ratios and somewhat lower values of maximum resultant-force coefficient than obtained with the 5° cant angle.

Effects of keel-cant angle for a keel-payload separation l/l_k of 1.25, presented in figure 53(b), show the same trends as for $l/l_k = 1.00$; however, increasing the cant angle from 15° to 20° reduced the maximum lift-drag ratio. A summary of effects of keel cant angle is presented in figure 61, which also includes data for cant angles of 15° and 20° for

a keel-payload distance l/l_k of 1.50. All data for 20° cant angle show lower values of maximum lift-drag ratio and maximum resultant-force coefficient than for 15° cant angle. It is apparent, therefore, that the 20° cant angle was excessive, and a desirable cant angle for application to design would be about 15°.

Several modifications and adjustments were made to the details of the formed nose of the wing center panel, as shown in figure 5, in attempts to improve the nose shape and parawing performance. Most of these adjustments produced little or no change in aerodynamic characteristics. Two examples are presented in figures 13 and 14 and 35 to 38. The added nose line to the 15° canted keel parawing with $l/l_k = 1.25$ increased maximum lift-drag ratio from 3.41 to 3.48. (See figs. 35 to 38.)

Effect of center-panel width.- Parawings with center panels one-third narrower and one-third wider than the width of the basic center panel of twin-keel parawing model 21 (15° keel cant angle) were investigated. A comparison showing the effect of center-panel width on the upper envelope of the variation of L/D with C_R for a keel-payload separation distance of $1.00l_k$ is given in figure 55, and a summary of results is given in figure 61. The results of figure 61 show that either an increase or a decrease in the center-panel width from the basic width caused a loss in maximum lift-drag ratio. Maximum resultant-force coefficients were highest for the smallest center-panel width investigated and decreased with increasing width of the center panel.

Keel-Payload Distance

Keel-payload distance was taken as the length of the suspension line that was used for the reference wing angle α_w – that is, the eighth keel line. The keel-payload distances were approximately $1.00l_k$, $1.25l_k$, and $1.50l_k$. In general, an increase in keel-payload distance increased the values of L/D at a given value of C_R (figs. 56 to 60) and agree with results of references 1 and 3. With regard to maximum lift-drag ratio (fig. 61), the largest separation distance l/l_k of 1.50 was not as desirable as the intermediate value of $l/l_k = 1.25$. It can be reasoned, therefore, that increasing the line lengths from the shortest lengths tested to the intermediate length allowed a favorable change in canopy shape. Further increases in line length from the intermediate length failed to provide improvements in canopy shape sufficient to overcome the added drag of the additional line length.

CONCLUDING REMARKS

Low-speed wind-tunnel tests were made to determine the static aerodynamic characteristics of several tension-structure all-flexible twin-keel parawings. The addition to

the basic parallel keel model of either a lower surface scoop or upper surface ram-air-inflated tubes at the keels did not improve the overall performance of these wings over the original basic twin-keel parawing. Of the configurations tested, those having 5° to 15° canted keels showed higher values of lift-drag ratio throughout most of the resultant-force range, especially at the higher values of resultant-force coefficient. In general, there was no great change in the value of lift-drag ratio for a given resultant-force coefficient between the model with the narrow center panel and the basic width center panel; whereas, the model with the widened center panel indicated somewhat lower lift-drag ratio and less usable range of resultant-force coefficient. An increase in the keel-to-payload distance from 1.00 keel length to 1.25 keel length indicated an improvement in performance; however, a further increase to 1.50 keel length did not increase maximum lift-drag ratio but did give an increase at a given resultant-force coefficient over most of the test range.

Langley Research Center,
National Aeronautics and Space Administration,
Hampton, Va., June 3, 1970.

REFERENCES

1. Polhamus, Edward C.; and Naeseth, Rodger L.: Experimental and Theoretical Studies of the Effects of Camber and Twist on the Aerodynamic Characteristics of Parawings Having Nominal Aspect Ratios of 3 and 6. NASA TN D-972, 1963.

2. Naeseth, Rodger L.; and Gainer, Thomas G.: Low-Speed Investigation of the Effects of Wing Sweep on the Aerodynamic Characteristics of Parawings Having Equal-Length Leading Edges and Keel. NASA TN D-1957, 1963.

3. Croom, Delwin R.; Naeseth, Rodger L.; and Sleeman, William C., Jr.: Effects of Canopy Shape on Low-Speed Aerodynamic Characteristics of a 55° Swept Parawing With Large-Diameter Leading Edges. NASA TN D-2551, 1964.

4. Bugg, Frank M.: Effects of Aspect Ratio and Canopy Shape on Low-Speed Aerodynamic Characteristics of 50.0^O Swept Parawings. NASA TN D-2922, 1965.

5. Naeseth, Rodger L.; and Fournier, Paul G.: Low-Speed Wind-Tunnel Investigation of Tension-Structure Parawings. NASA TN D-3940, 1967.

6. Bugg, Frank M.; and Sleeman, William C., Jr.: Low-Speed Tests of an All-Flexible Parawing for Landing a Lifting-Body Spacecraft. NASA TN D-4010, 1967.

7. Fournier, Paul G.; and Sleeman, William C., Jr.: Wind-Tunnel Studies of Effects of Construction Methods, Design Details, and Canopy Slots on the Aerodynamic Characteristics of Small-Scale All-Flexible Parawings. NASA TN D-5974, 1970.

8. Naeseth, Rodger L.: Low-Speed Wind-Tunnel Investigation of a Series of Twin-Keel All-Flexible Parawings. NASA TN D-5936, 1970.

9. Ware, George M.: Wind-Tunnel Investigation of the Aerodynamic Characteristics of a Twin-Keel Parawing. NASA TN D-5199, 1969.

10. Gillis, Clarence L.; Polhamus, Edward C.; and Gray, Joseph L., Jr.: Charts for Determining Jet-Boundary Corrections for Complete Models in 7- by 10-Foot Closed Rectangular Wind Tunnels. NACA WR L-123, 1945. (Formerly NACA ARR L5G31.)

11. Herriot, John G.: Blockage Corrections for Three-Dimensional-Flow Closed-Throat Wind Tunnels, With Consideration of the Effect of Compressibility. NACA Rep. 995, 1950. (Supersedes NACA RM A7B28.)

TABLE I.- GEOMETRIC CHARACTERISTICS OF MODELS

$$\left[l_{k,1} = 60.00 \text{ in.} \quad (152.40 \text{ cm}) \quad \text{for all models} \right]$$

Model	Λ_k, deg	l_k in.	l_k cm	c in.	c cm	b_o in.	b_o cm	S ft^2	S m^2	S_c ft^2	S_c m^2	A, b_o^2/S
5,17,18	0	75.00	190.50	60.00	152.40	114.83	291.67	30.173	2.803	12.500	1.161	3.04
19	5	72.36	183.79	59.77	151.82	121.92	309.68	32.302	3.001	14.624	1.359	3.20
20	10	69.59	176.76	59.09	150.09	128.50	326.39	34.261	3.183	16.584	1.540	3.35
21	15	66.62	169.22	57.95	147.19	133.92	340.16	36.001	3.345	18.323	1.702	3.46
22	15	63.73	161.87	57.95	147.19	123.92	314.76	31.976	2.971	14.298	1.329	3.34
23	15	69.51	176.56	57.95	147.19	143.92	365.56	40.026	3.719	22.347	2.076	3.59
24	20	63.37	160.96	56.38	143.20	139.76	352.44	37.454	3.480	19.779	1.838	3.57

TABLE II.- LINE LOCATIONS AND LENGTHS

Line	$x/l_{k,1}$	l/l_k for model (figure) –																
		5 (8,9)	5 (10,11)	5 (13,14)	17 (16,17)	18 (19,20)	19 (22,23)	20 (25,26)	20 (27,28)	21 (30,31)	21 (32,33)	21 (35,36)	21 (37,38)	22 (40,41)	23 (43,44)	23 (45,46)	24 (48,49)	24 (50,51)
									Keel									
0	0	----	----	0.974	----	----	----	----	----	----	----	1.447	----	----	----	----	----	----
1	.083	0.973	1.203	----	0.951	0.972	1.074	1.078	1.328	1.158	1.451	1.451	1.733	1.087	1.068	1.308	1.508	1.758
2	.167	.974	1.220	.998	.969	.984	1.072	1.102	1.352	1.153	1.447	1.447	1.729	1.104	1.108	1.348	1.493	1.750
3	.250	.980	1.229	1.002	.969	.986	1.058	1.092	1.342	1.148	1.444	1.444	1.721	1.101	1.104	1.343	1.490	1.744
4	.333	.972	1.226	.993	.956	.979	1.060	1.084	1.334	1.134	1.428	1.428	1.710	1.089	1.095	1.334	1.473	1.726
5	.417	.976	1.222	.995	.947	.979	1.056	1.076	1.326	1.128	1.420	1.420	1.700	1.082	1.084	1.323	1.462	1.715
6	.500	.974	1.224	.997	.946	.978	1.051	1.066	1.316	1.119	1.413	1.413	1.695	1.074	1.075	1.314	1.454	1.707
7	.583	.981	1.227	.995	.947	.980	1.051	1.061	1.311	1.111	1.407	1.407	1.688	1.067	1.066	1.306	1.437	1.688
*8	.667	.974	1.224	.976	.932	.975	1.039	1.054	1.304	1.102	1.396	1.396	1.673	1.058	1.058	1.298	1.420	1.674
9	.750	.966	1.214	.967	.926	.967	1.029	1.028	1.278	1.077	1.372	1.372	1.653	1.035	1.046	1.286	1.393	1.647
10	.833	.958	1.207	.959	.914	.957	1.015	1.015	1.265	1.059	1.353	1.353	1.634	1.016	1.026	1.265	1.357	1.612
11	.917	.933	1.180	.932	.891	.933	.992	.989	1.239	1.016	1.310	1.310	1.590	.975	.984	1.223	1.325	1.577
12	1.000	.865	1.101	.865	.818	.867	.941	.922	1.172	.950	1.258	1.258	1.506	.913	.888	1.121	1.261	1.518
									Leading edge									
1	0.167	0.928	1.182	0.951	0.913	0.952	1.037	1.052	1.302	1.112	1.404	1.404	1.683	1.069	1.068	1.307	1.490	1.743
2	.333	.907	1.159	.908	.878	.903	1.013	1.008	1.259	1.075	1.368	1.368	1.647	1.034	1.033	1.273	1.452	1.709
3	.500	.888	1.141	.904	.853	.890	.983	.973	1.223	1.027	1.319	1.319	1.599	.988	.988	1.228	1.382	1.638
4	.677	.843	1.093	.844	.805	.844	.936	.919	1.169	.962	1.255	1.255	1.534	.924	.925	1.164	1.306	1.560
5	.833	.778	1.019	.779	.743	.778	.859	.840	1.090	.868	1.161	1.161	1.442	.835	.822	1.062	1.196	1.450
6	1.000	.637	.887	.630	.562	.629	.706	.665	.915	.683	.983	.983	1.260	.659	.647	.886	.977	1.259

*α_w reference line.
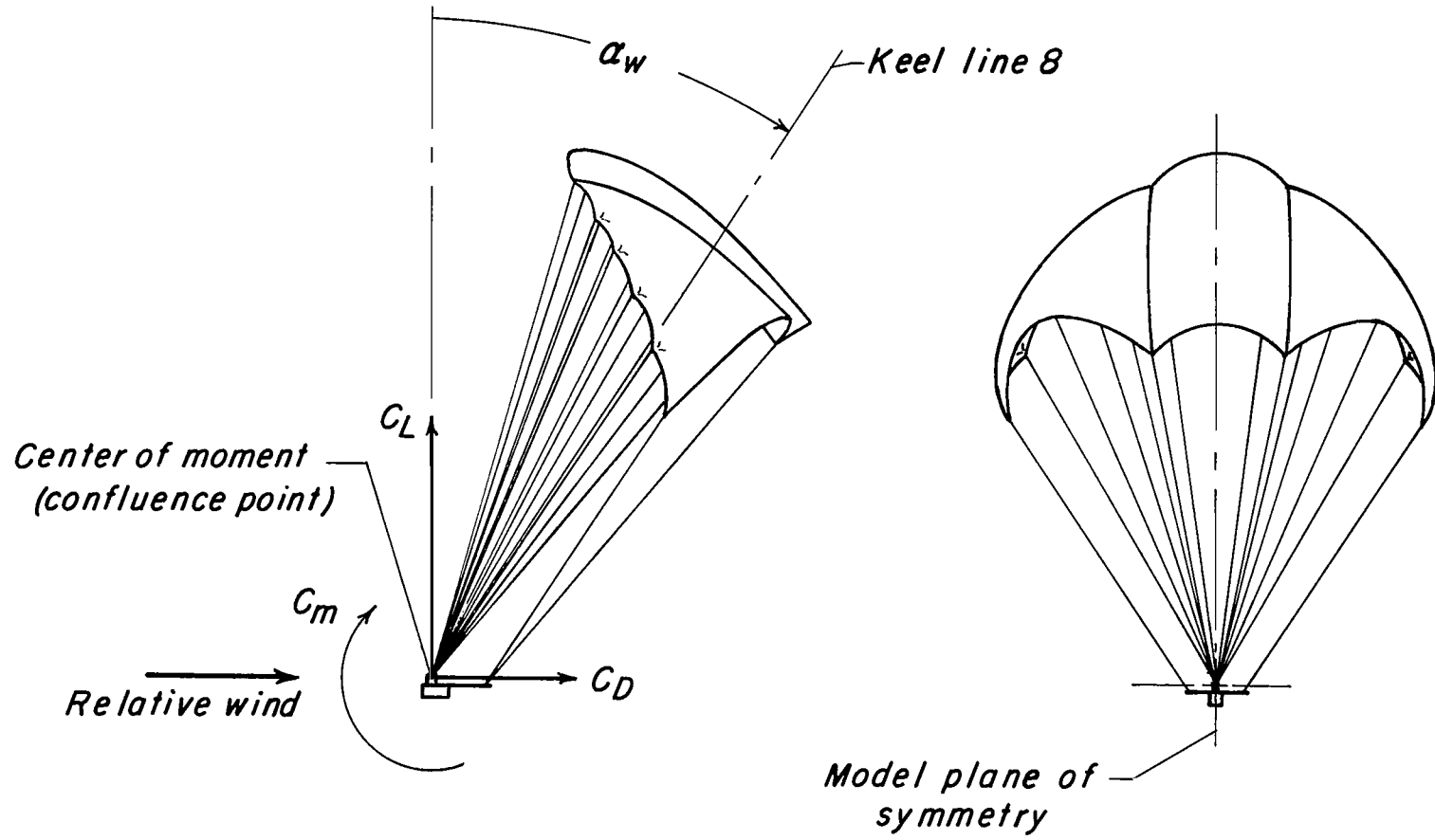
Figure 1.- Sketch showing positive direction of forces, moment, and angle used in the presentation of the data.

Line clamp block

Aft keel control line location

Wing tip control line location

H_1

Center of moment (Confluence point)

H_2

H_3

Balance cage

Strut
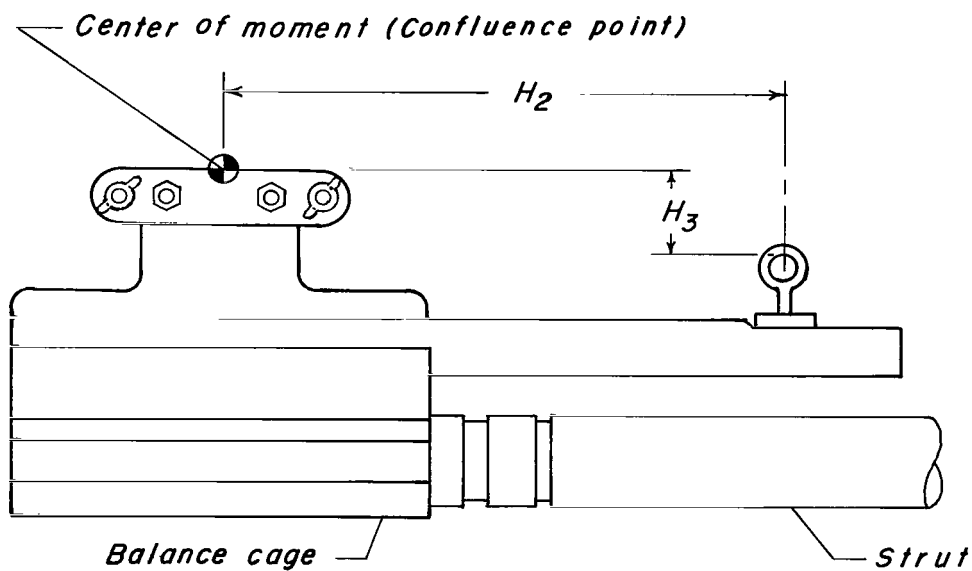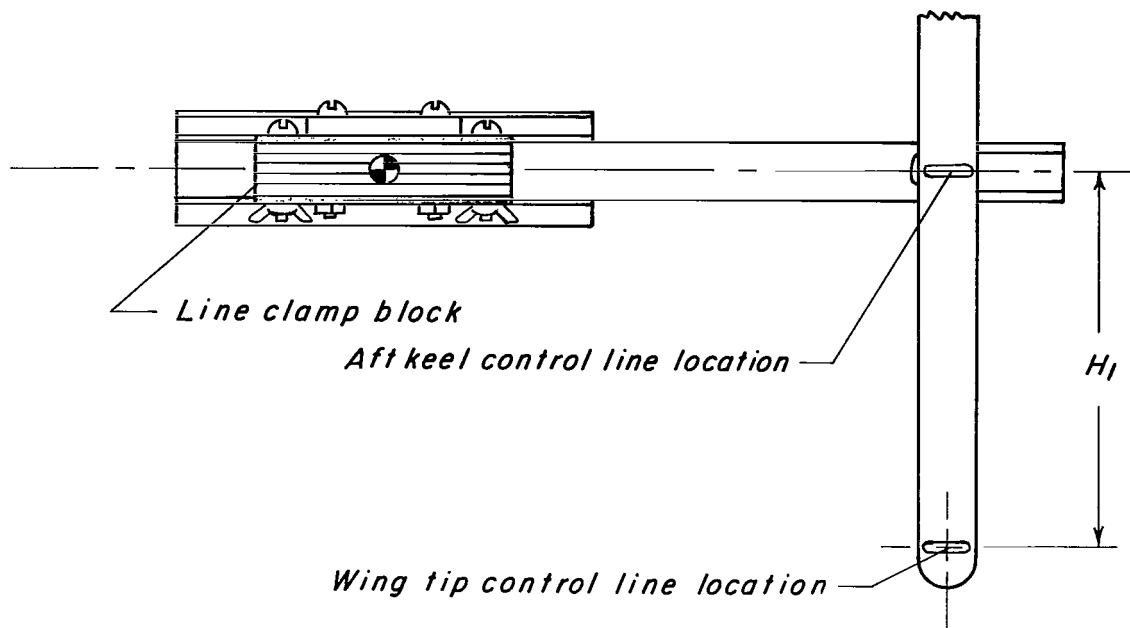
$H_1 = 5.000$ in. (12.700 cm) $H_2 = 7.125$ in. (18.098 cm) $H_3 = 1.035$ in. (2.639 cm)

Figure 2.- Parawing line attachments to the balance used for tethered method of testing.

15
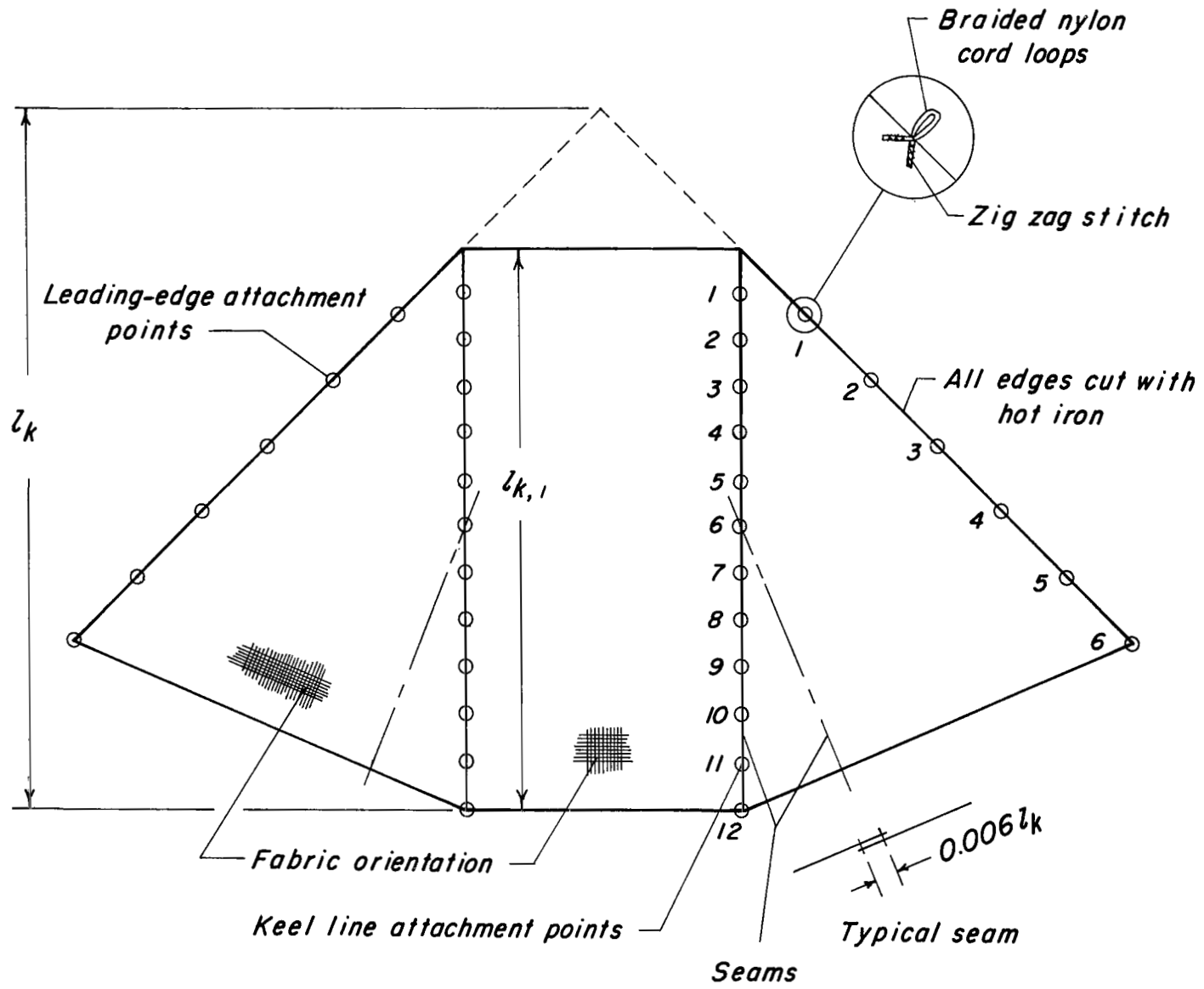
Figure 3.- Typical construction details shown for the parallel twin-keel model 5. Sewed construction.
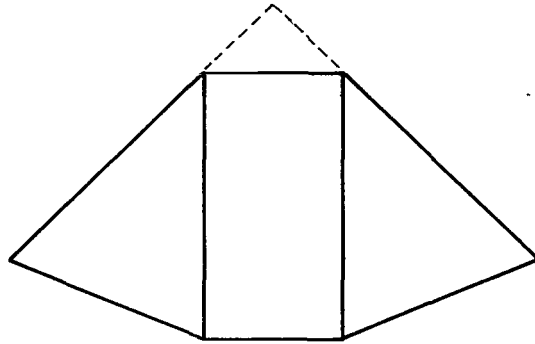
Model 5
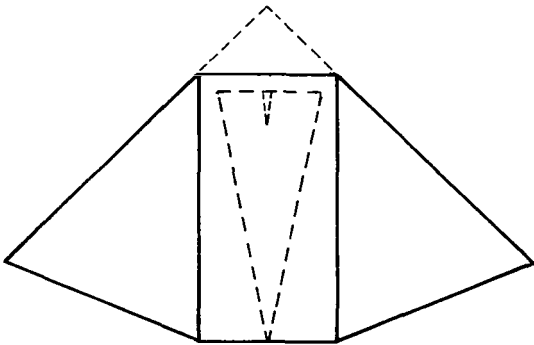
Lower surface scoop
Model 17
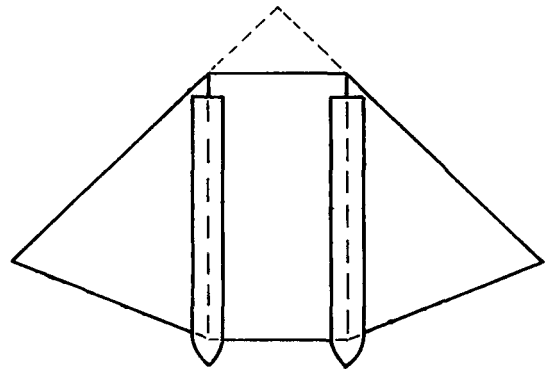
Upper surface
ram-air-inflated tubes
Model 18

(a) Parallel keel configurations.

Figure 4.- Planform of models.
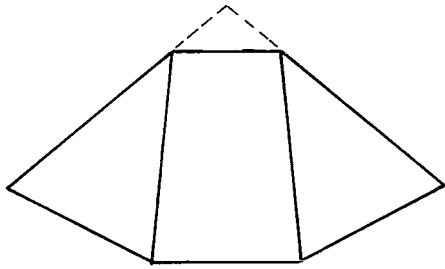
5° canted keels
Model 19
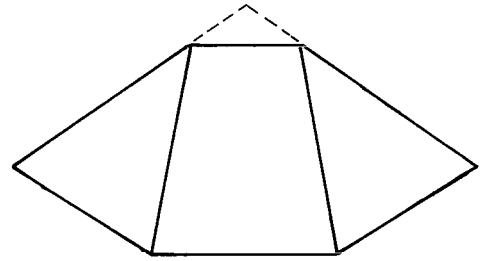
10° canted keels
Model 20
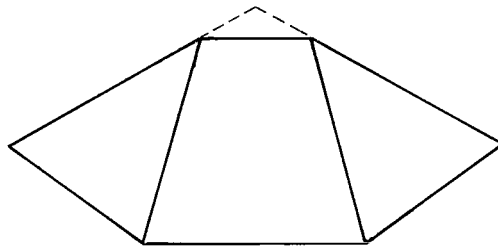
15° canted keels
Model 21
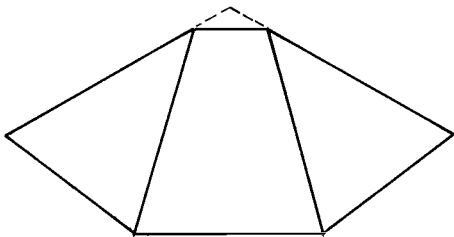
15° canted keels with
narrowed center panel
Model 22
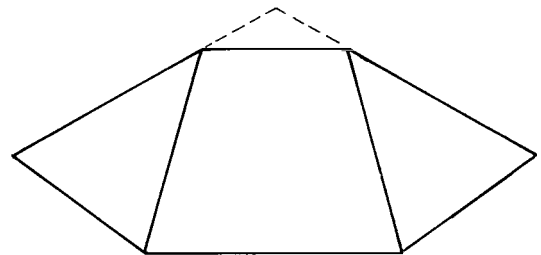
15° canted keels with
widened center panel
Model 23
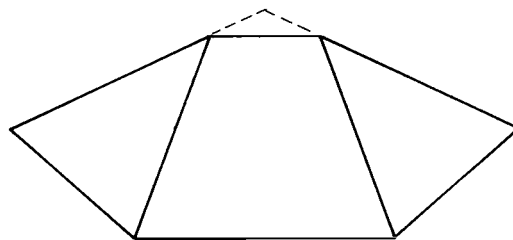
20° canted keels
Model 24

(b) Canted keel configurations.

Figure 4.- Concluded.
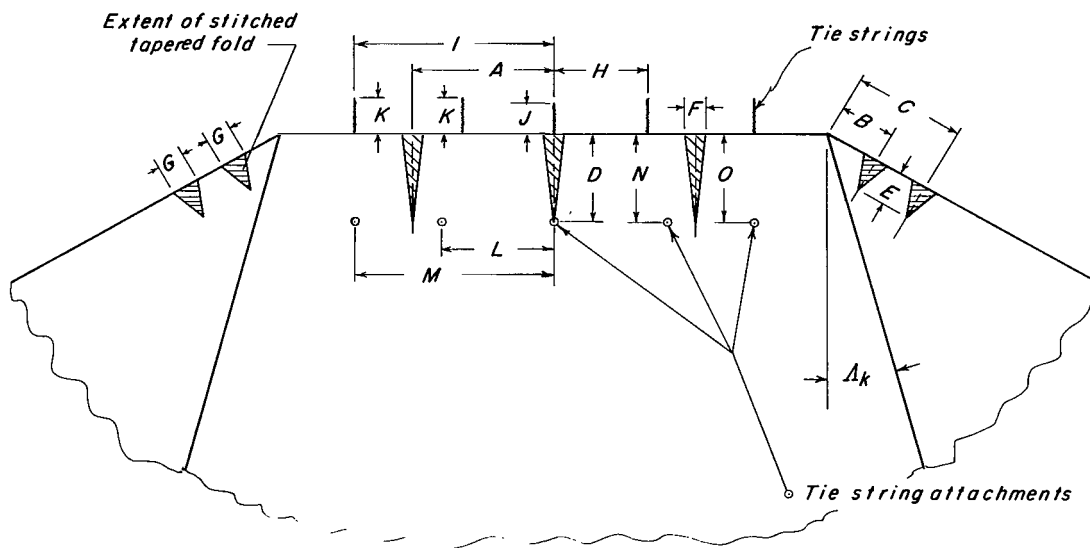
Dimensions in fraction of actual keel length, $l_{k,1}$

Letter dimension	Model 5 l_k=75.00 in. (190.50 cm)	Model 17 l_k=75.00 in. (190.50 cm)	Model 18 l_k=75.00 in. (190.50 cm)	Model 19 l_k=72.36 in. (183.79 cm)	Model 20 l_k=69.59 in. (176.76 cm)	Model 21 l_k=66.62 in. (169.21 cm)	Model 22 l_k=63.73 in. (161.87 cm)	Model 23 l_k=69.51 in. (176.56 cm)	Model 24 l_k=63.37 in. (160.92 cm)
Λ_k	0^0	0^0	0^0	5^0	10^0	15^0	15^0	15^0	20^0
A	0.129	0.129	0.129	0.129	0.129	0.129	0.083	0.162	0.129
B	.050	.050	.050	.050	.050	.050	.050	.050	.050
C	.100	.100	.100	.100	.100	.100	.100	.100	.100
D	.082	.082	.082	.082	.082	.082	.082	.082	.082
E	.032	.032	.032	.032	.032	.032	.032	.032	.032
F	.021	.020	.020	.020	.020	.020	.020	.020	.021
G	.025	.025	.025	.025	.025	.025	.025	.025	.025
H	.082	.086	.086	.086	.086	.086	.100	.181	.087
I	.182	.183	.183	.183	.183	.183	----	----	.185
J	.029	.029	.029	.029	.029	.029	.029	.029	.033
K	.033	.033	.033	.033	.033	.033	.033	.033	.033
L	.103	.092	.103	.103	.113	.103	.100	.179	.100
M	.182	.182	.182	.183	.194	.182	----	----	.175
N	.082	.082	.082	.082	.082	.082	.082	.082	.066
O	.082	.082	.082	.082	.082	.082	----	----	.066

(a) Dimensions of darts and ties.

Figure 5.- Details of contoured nose of twin-keel parawing.

19

Wind direction

Keel line 1 attachment loop

Canopy

Keel line 1

1.625 in. (4.13 cm)
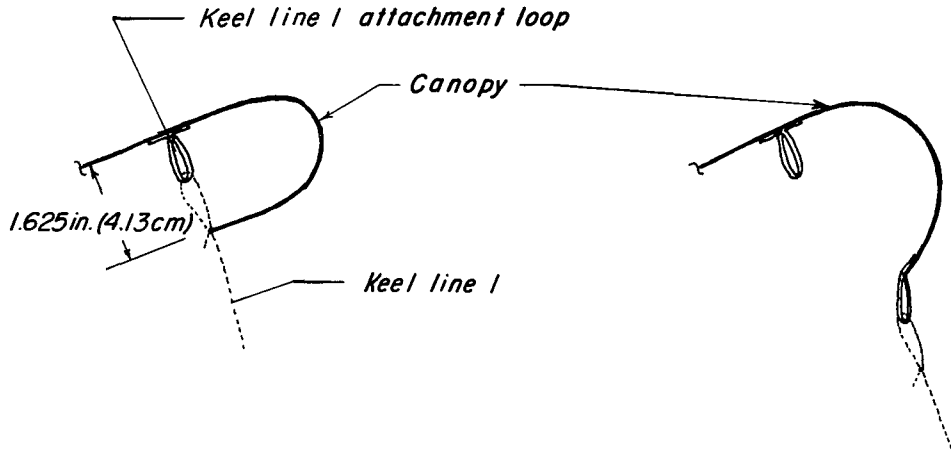
Models 5,18,19,20,21,22,23 and 24

Model 5 with modified line
arrangement at the nose
(Keel line 1 moved to nose)

Keel line 1

Line at nose
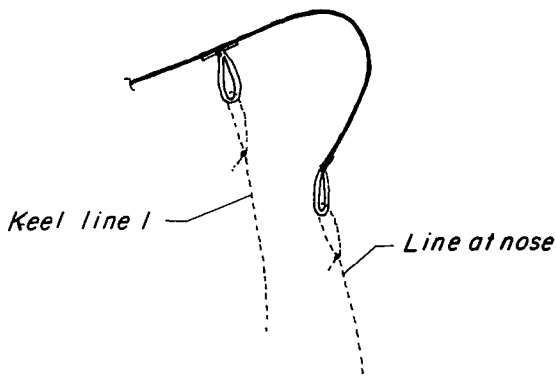
Model 21 with modified line
arrangement of the nose
(Added nose line)

1.625 in. (4.13 cm)

Nose tie

1.625 in. (4.13 cm)
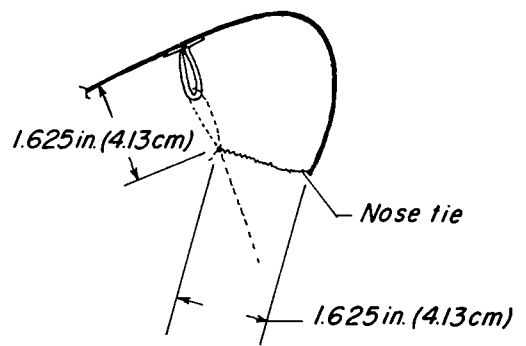
Model 17

(b) Chordwise section view through the keel at the nose during flight shaped conditions.

Figure 5.- Concluded.
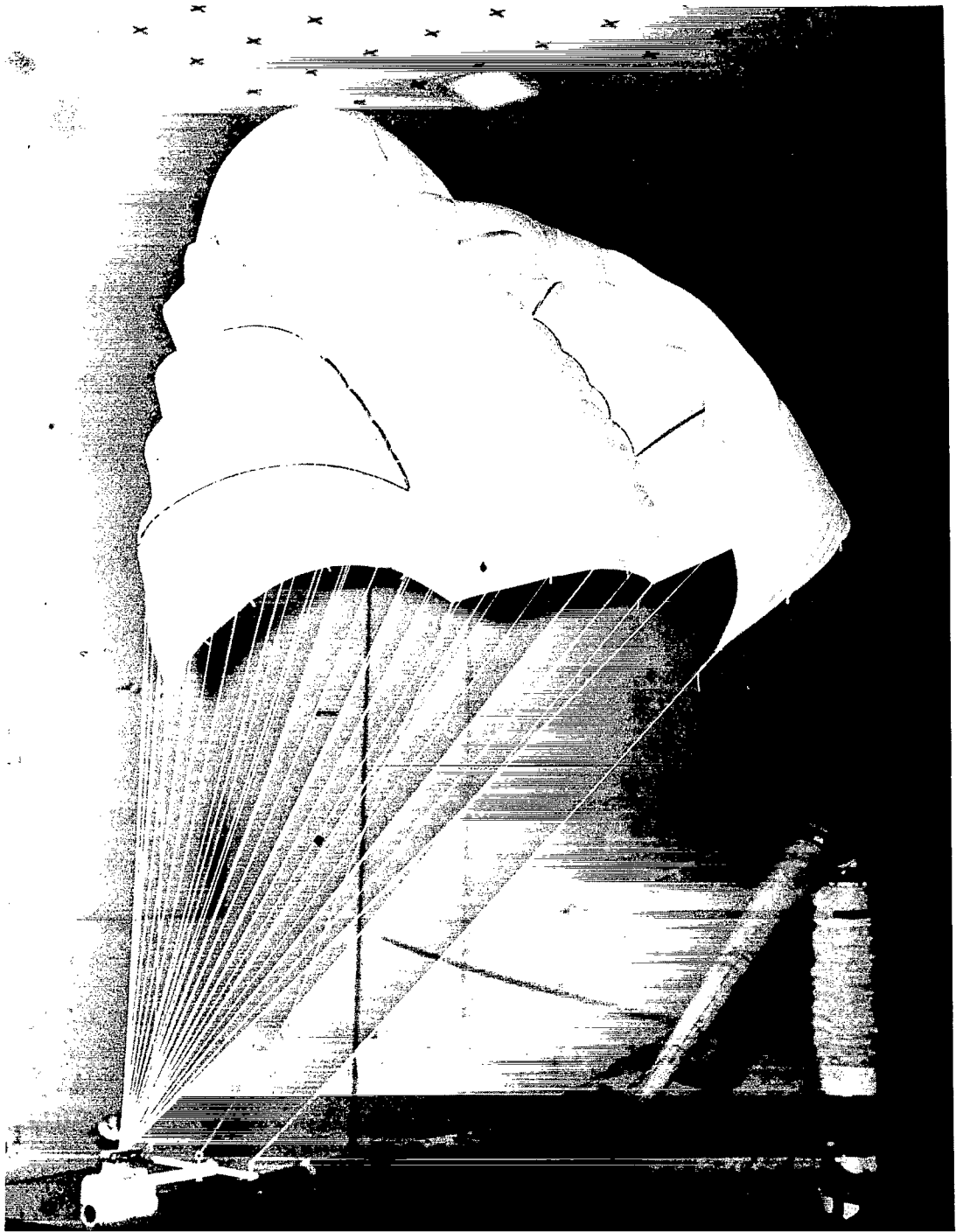
(a) Model 5, basic parallel keel (0° keel cant angle), with standard rigging.　　　　L-70-1676

Figure 6.- Twin-keel parawings.

(b) Model 5 with first keel line moved to nose.   L-70-1677

Figure 6.- Continued.
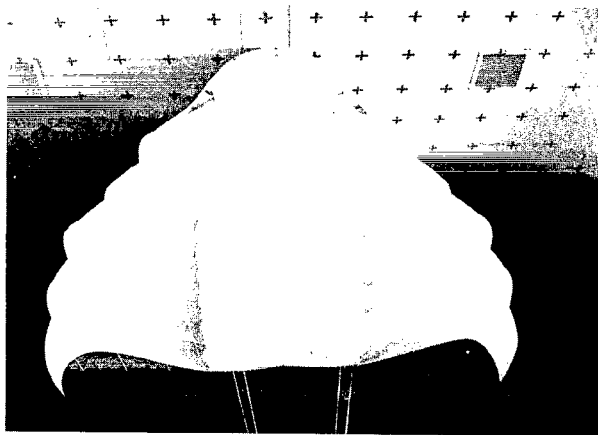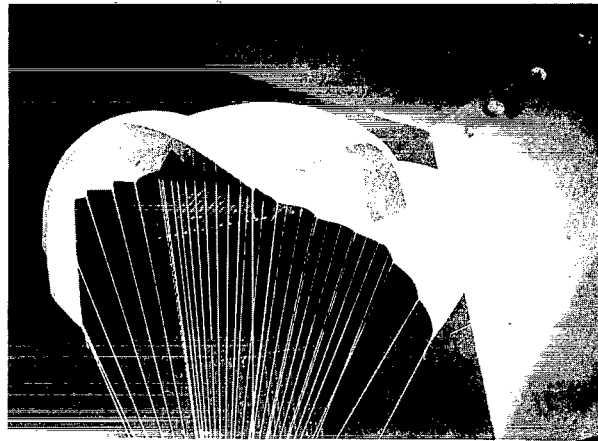
(c) Model 17, lower surface scoop added.   L-70-1678

Figure 6.- Continued.
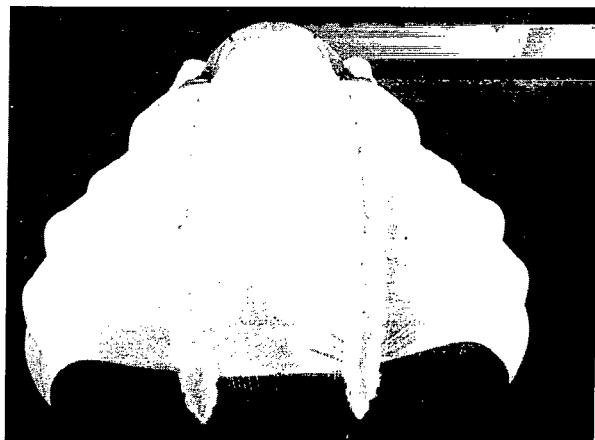
(d) Model 18, upper surface ram-air-inflated tubes added.　　　L-70-1679

Figure 6.- Continued.
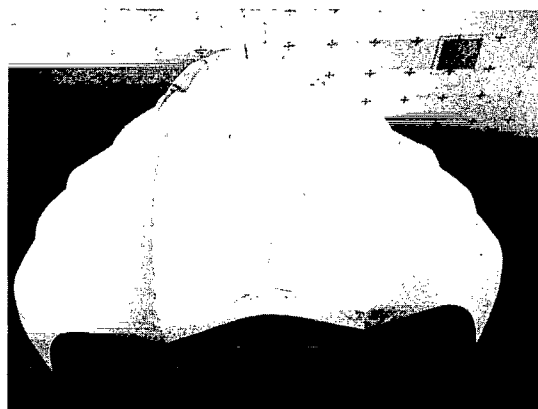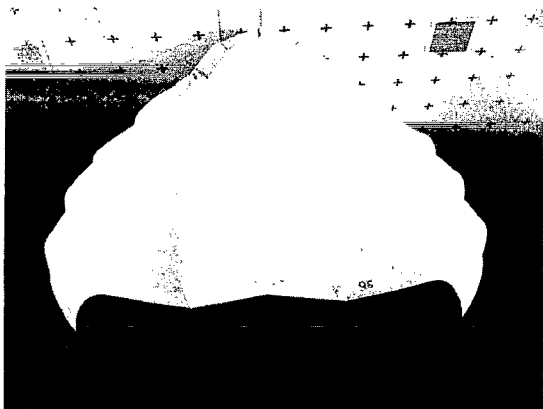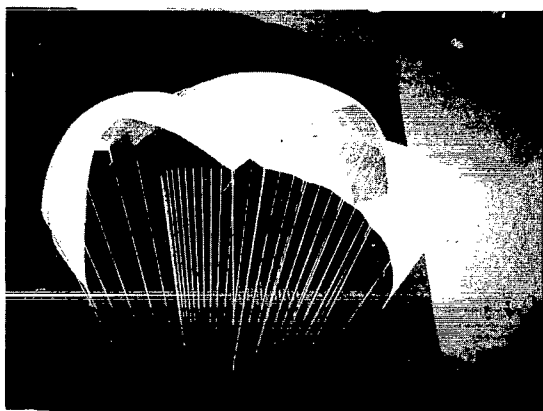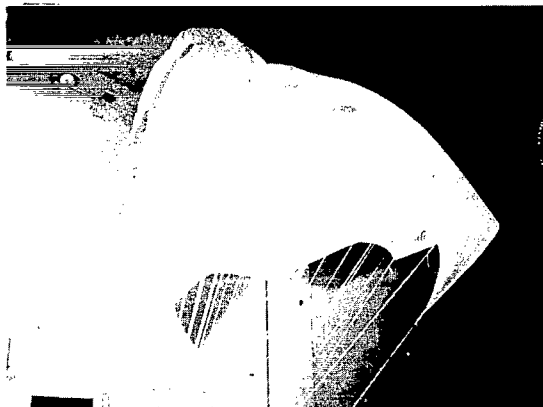
Model 19 , 5° Canted keels   *Model 20 ,10° Canted keels*

(e) Canted keel configurations.

Figure 6.- Continued.
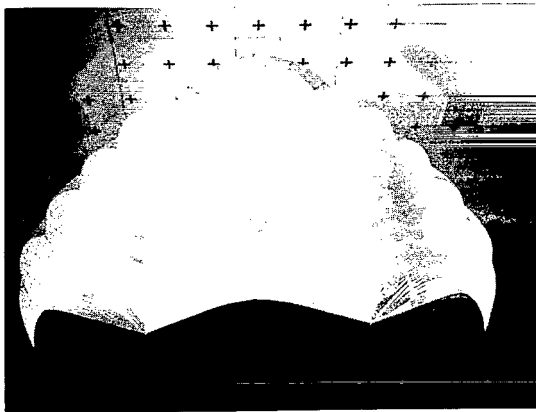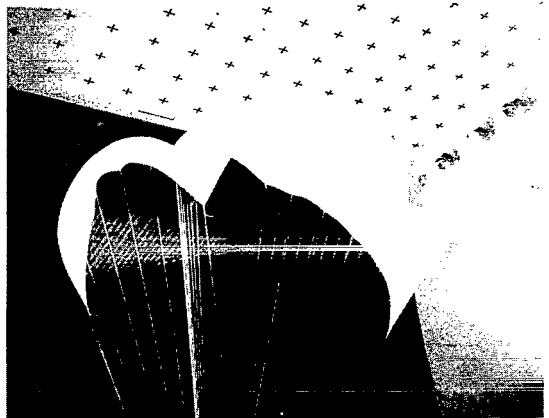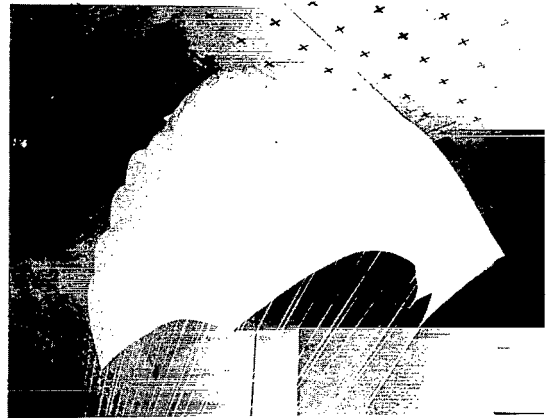
Model 21, 15° Canted keels   Model 24, 20° Canted keels

(e) Concluded.

L-70-1680

Figure 6.- Continued.
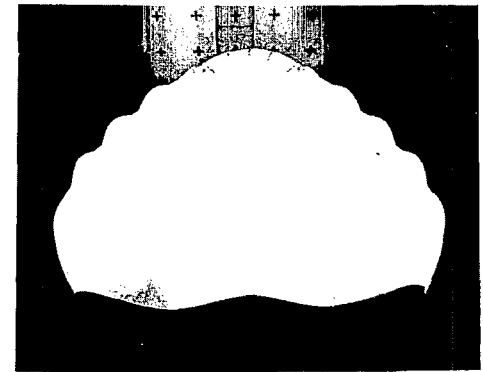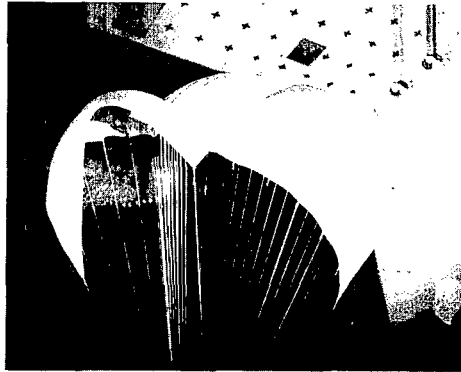
Model 22 , 15° Canted keels with narrowed center panel
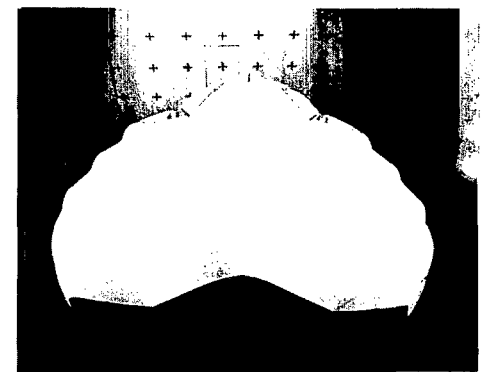
Model 23 , 15° Canted keels with widened center panel

(f) Modified center panel.   L-70-1682

Figure 6.- Concluded.
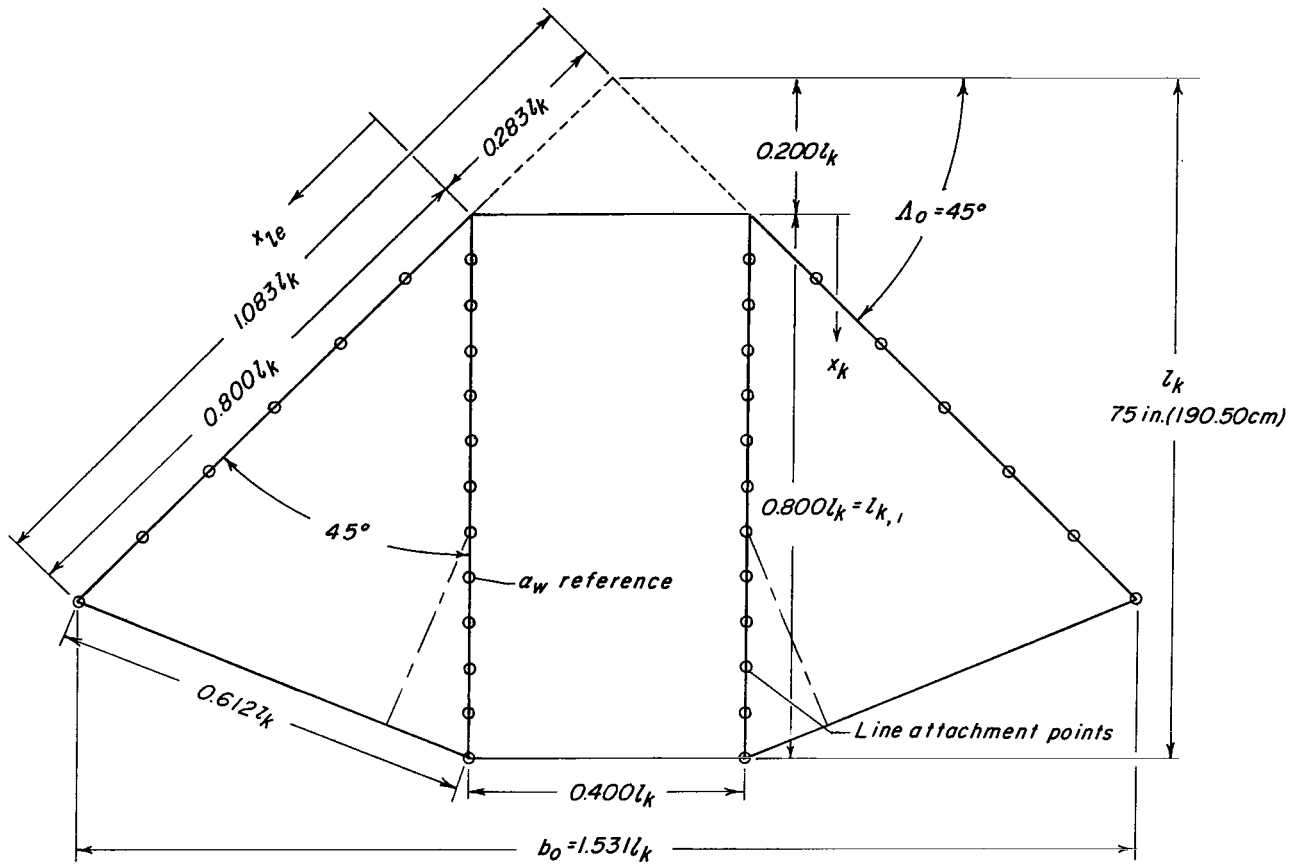
Figure 7.- Flat planform details of twin-keel parawing model 5.
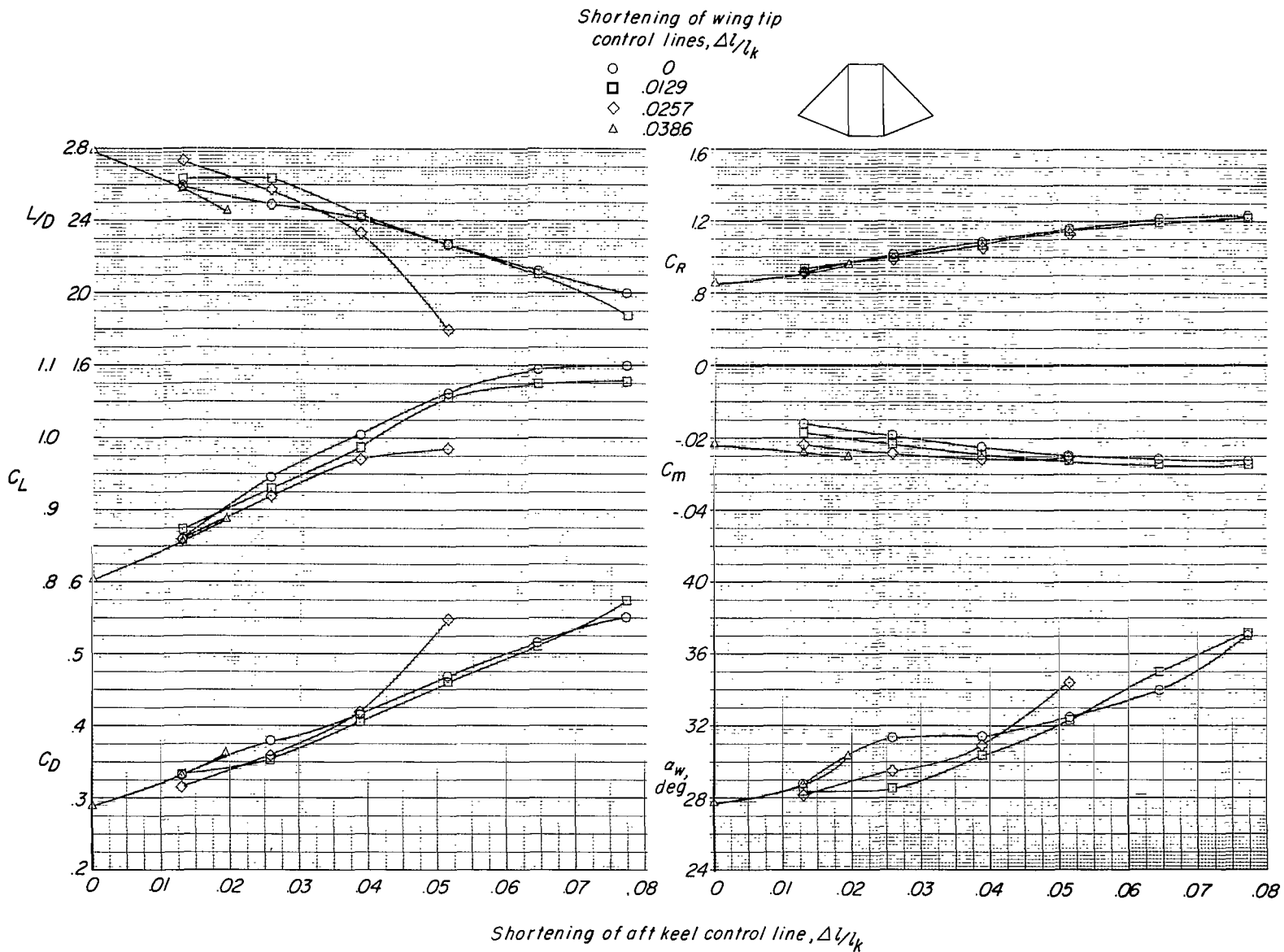
Figure 8.- Effect of aft keel control line shortening on the longitudinal aerodynamic characteristics of twin-keel model 5. Keel-to-payload separation distance ≈ $1.00l_k$.
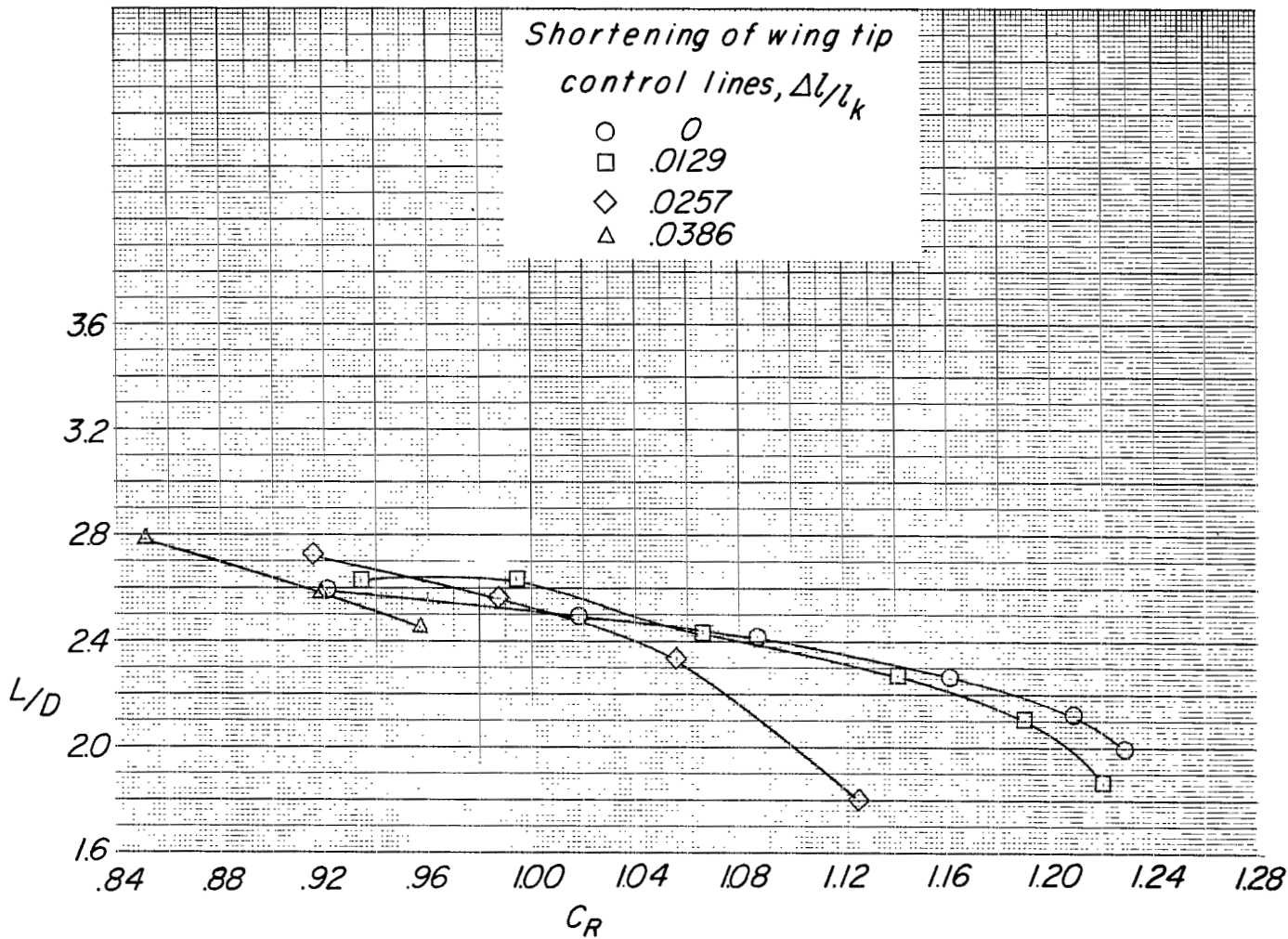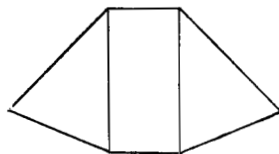
Figure 9.- Variation of L/D with C_R for same configuration as that used for figure 8.
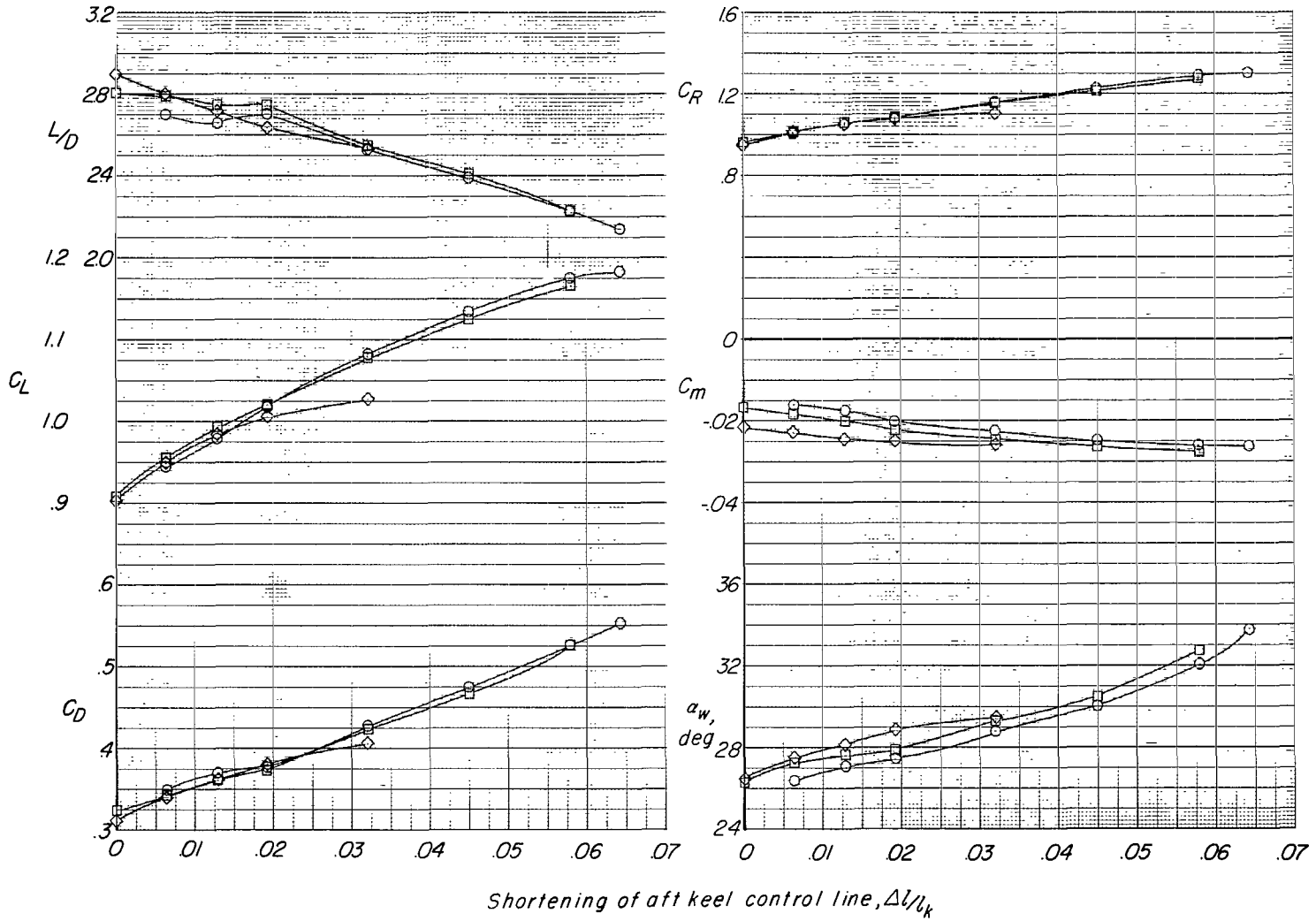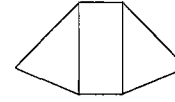
Figure 10.- Effect of aft keel control line shortening on the longitudinal aerodynamic characteristics of twin-keel model 5.
Keel-to-payload separation distance $\approx 1.25 l_k$.
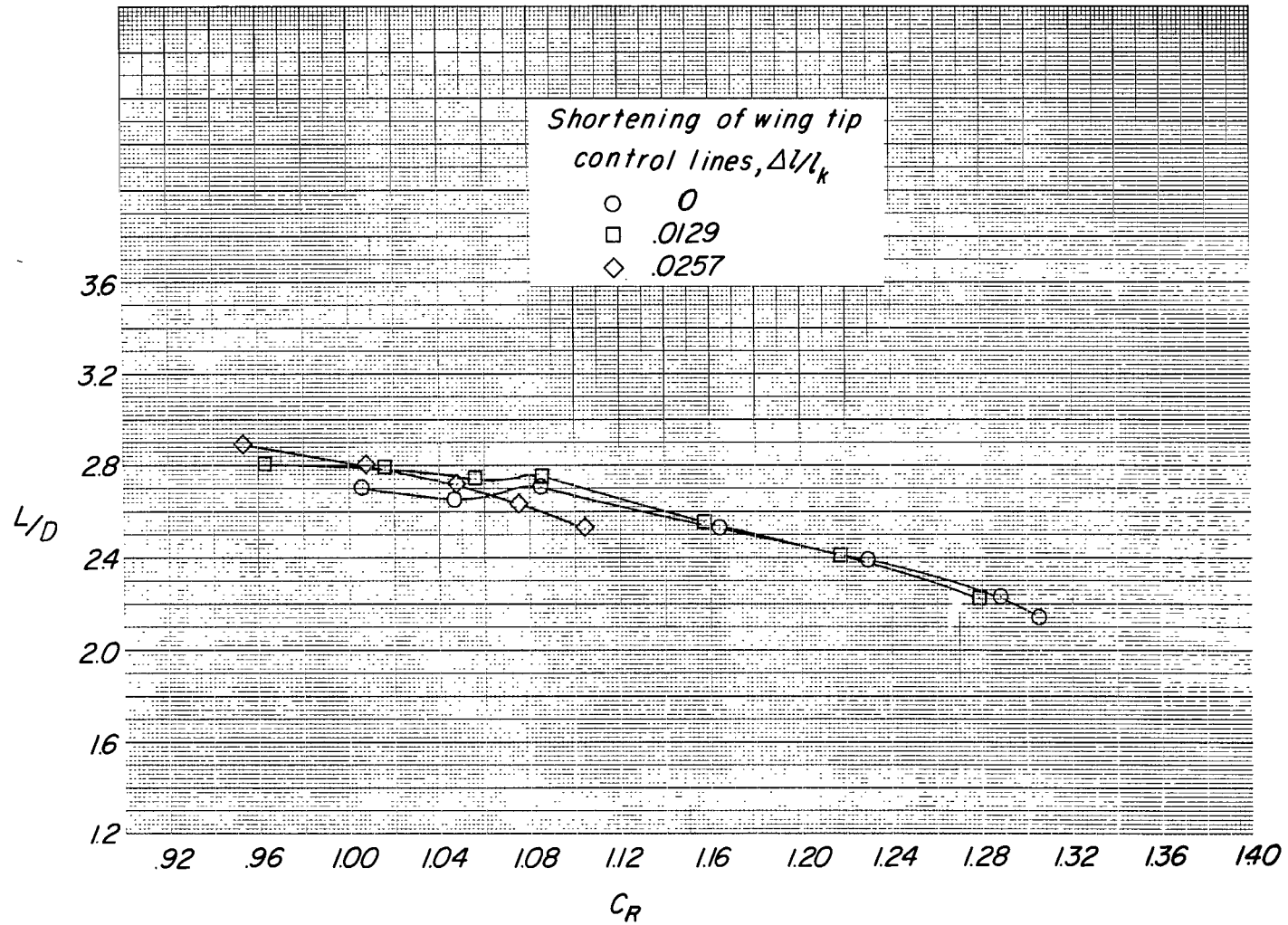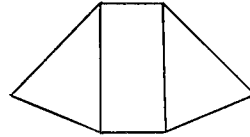
Figure 11.- Variation of L/D with C_R for same configuration as that used for figure 10.
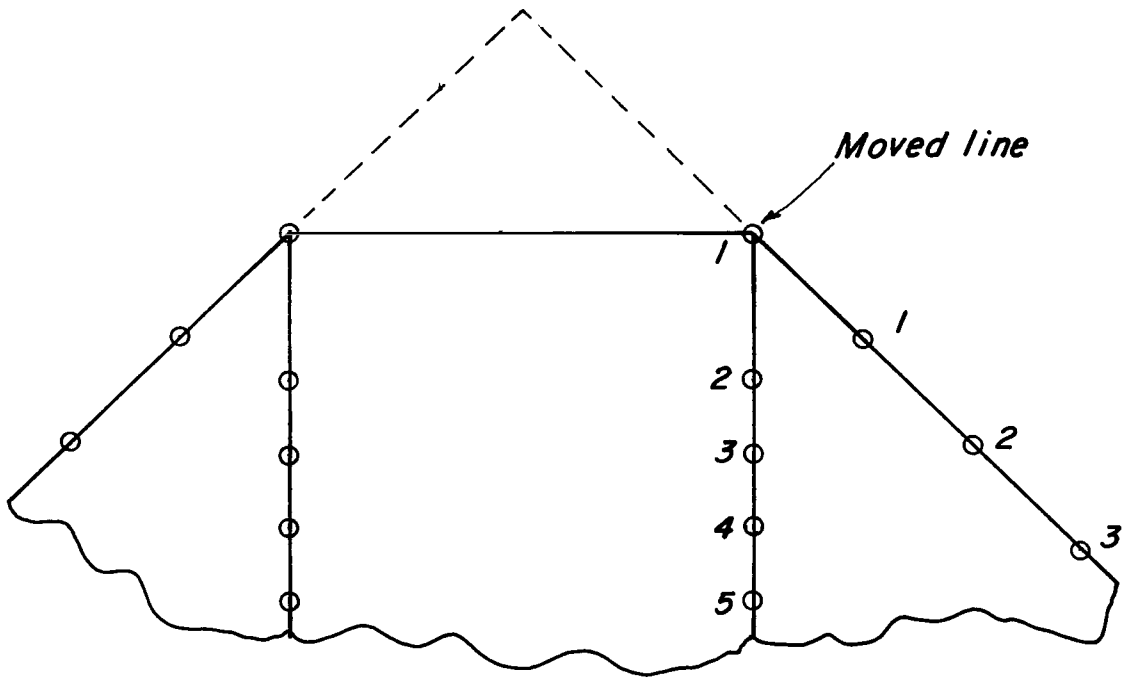
Figure 12.- Flat planform details of twin-keel parawing model 5, showing modified line arrangement at the nose. First keel line moved to nose.
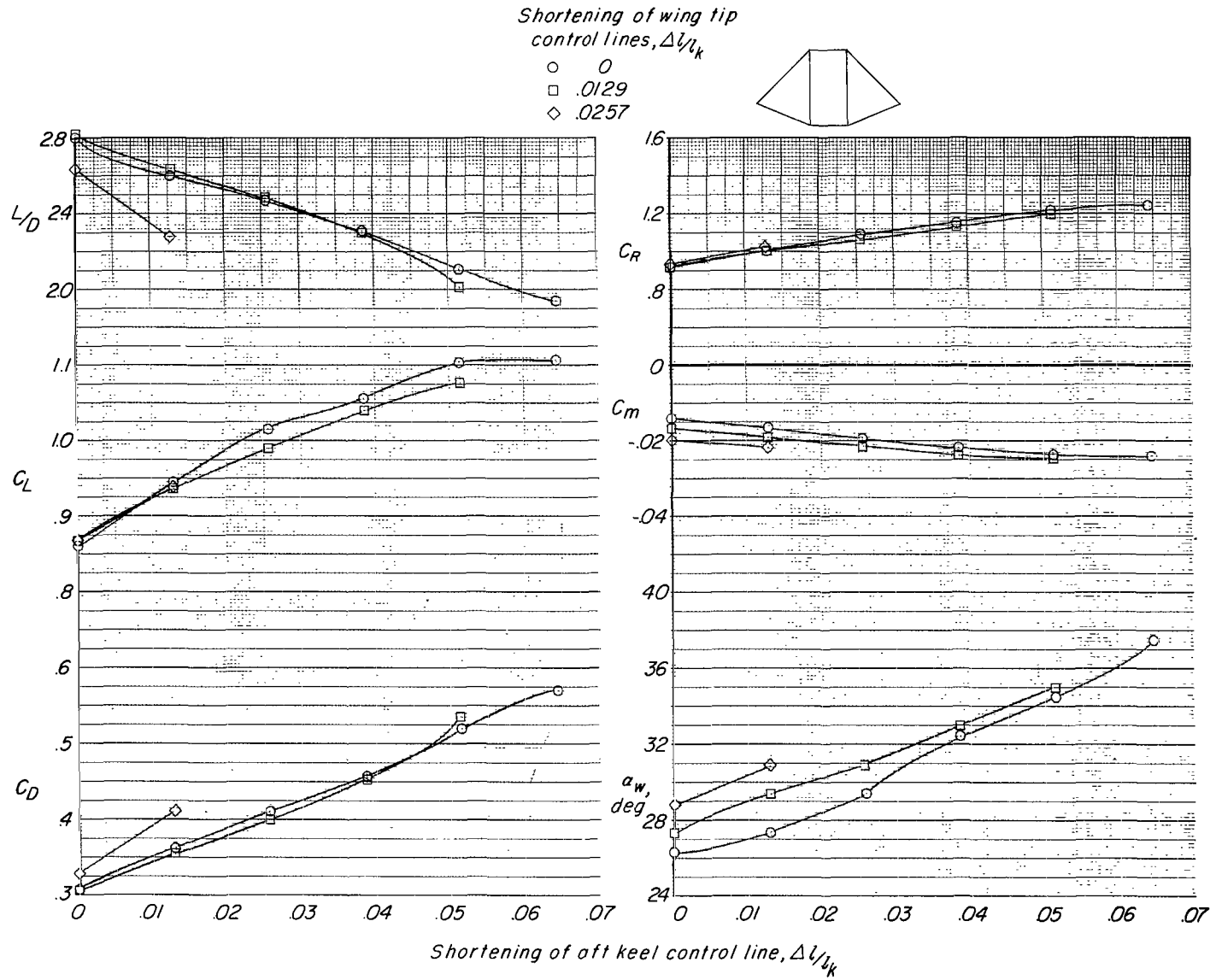
Figure 13.- Effect of aft keel control line shortening on the longitudinal aerodynamic characteristics of twin-keel model 5 with modified line arrangement at the nose. Keel-to-payload separation distance ≈ $1.00l_k$.
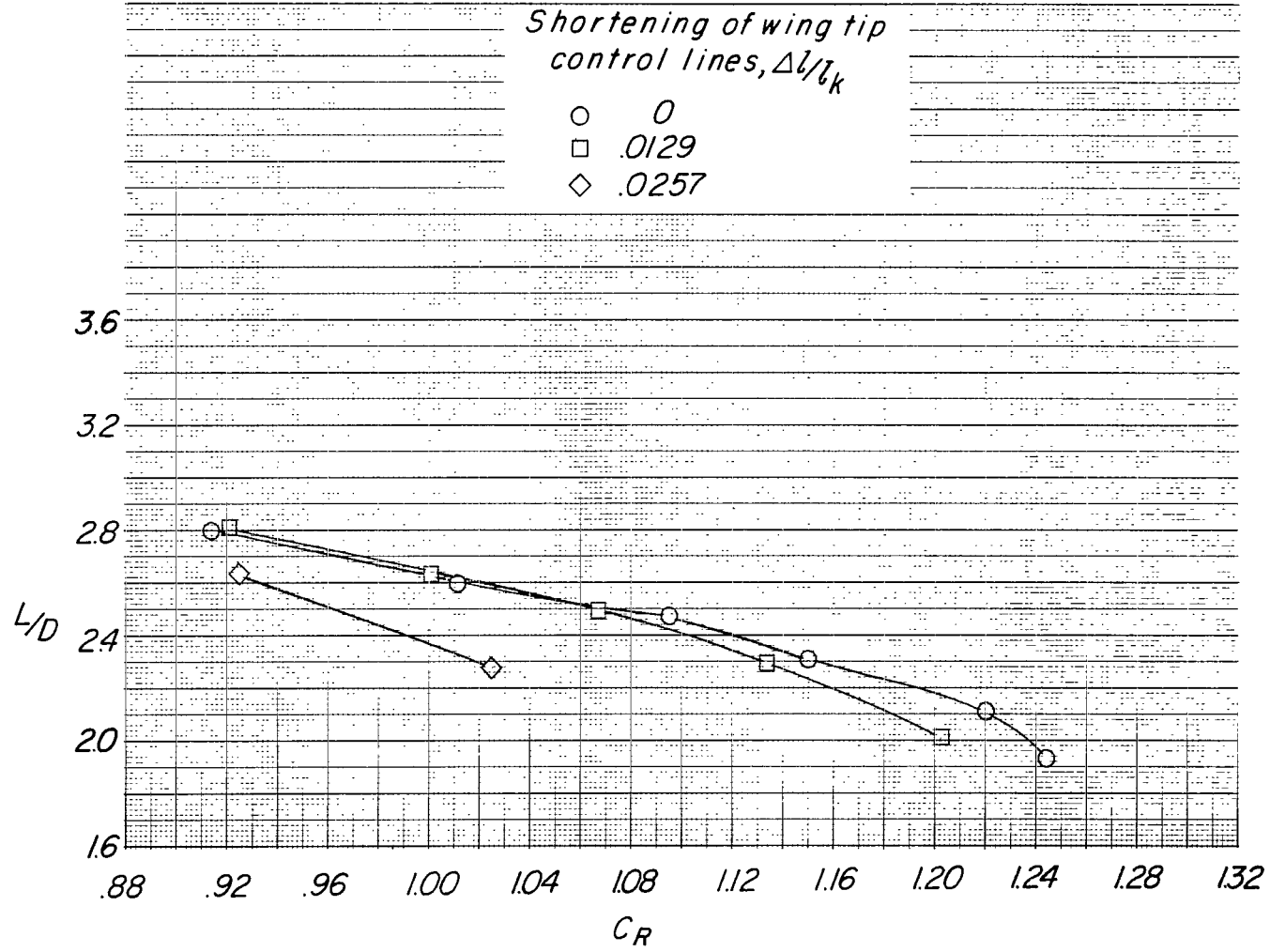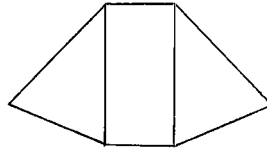
Figure 14.- Variation of L/D with C_R for same configuration as that used for figure 13.
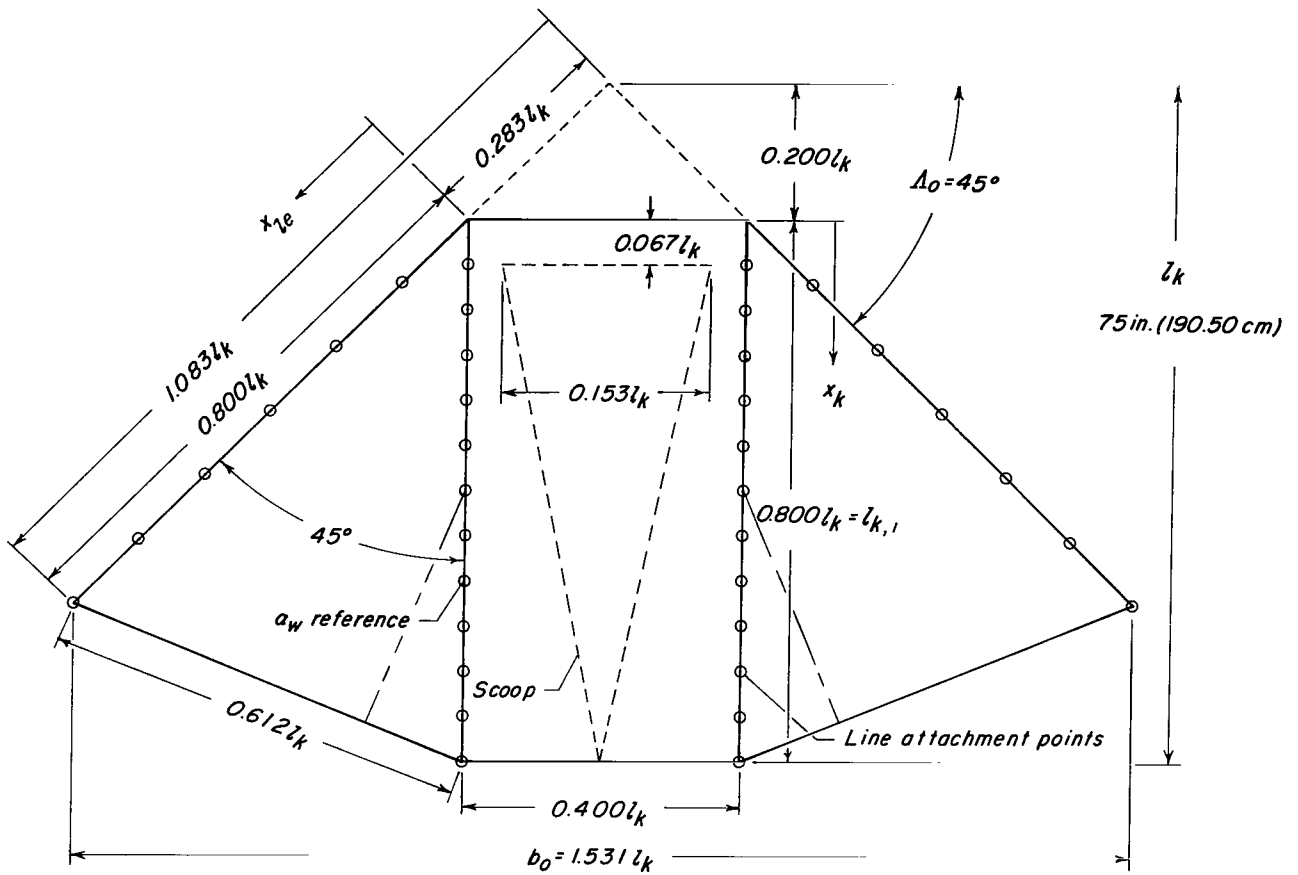
Keel	$x/l_{k,1}$	Leading edge
0.083		0.167
.167		.333
.250		.500
.333		.667
.417		.833
.500		1.000
.583		
.667		
.750		
.833		
.917		
1.000		

Line attachment location

(a) Planform.

Figure 15.- Flat planform details of twin-keel parawing model 17, with ram-air-inflated scoop on lower surface of center panel.

0.033l_k

0.120l_k

0.153l_k

0.013l_k

0.027l_k

0.047l_k

0.047l_k

0.080l_k

0.100l_k

Stitch tapered fold

Lower surface of wing
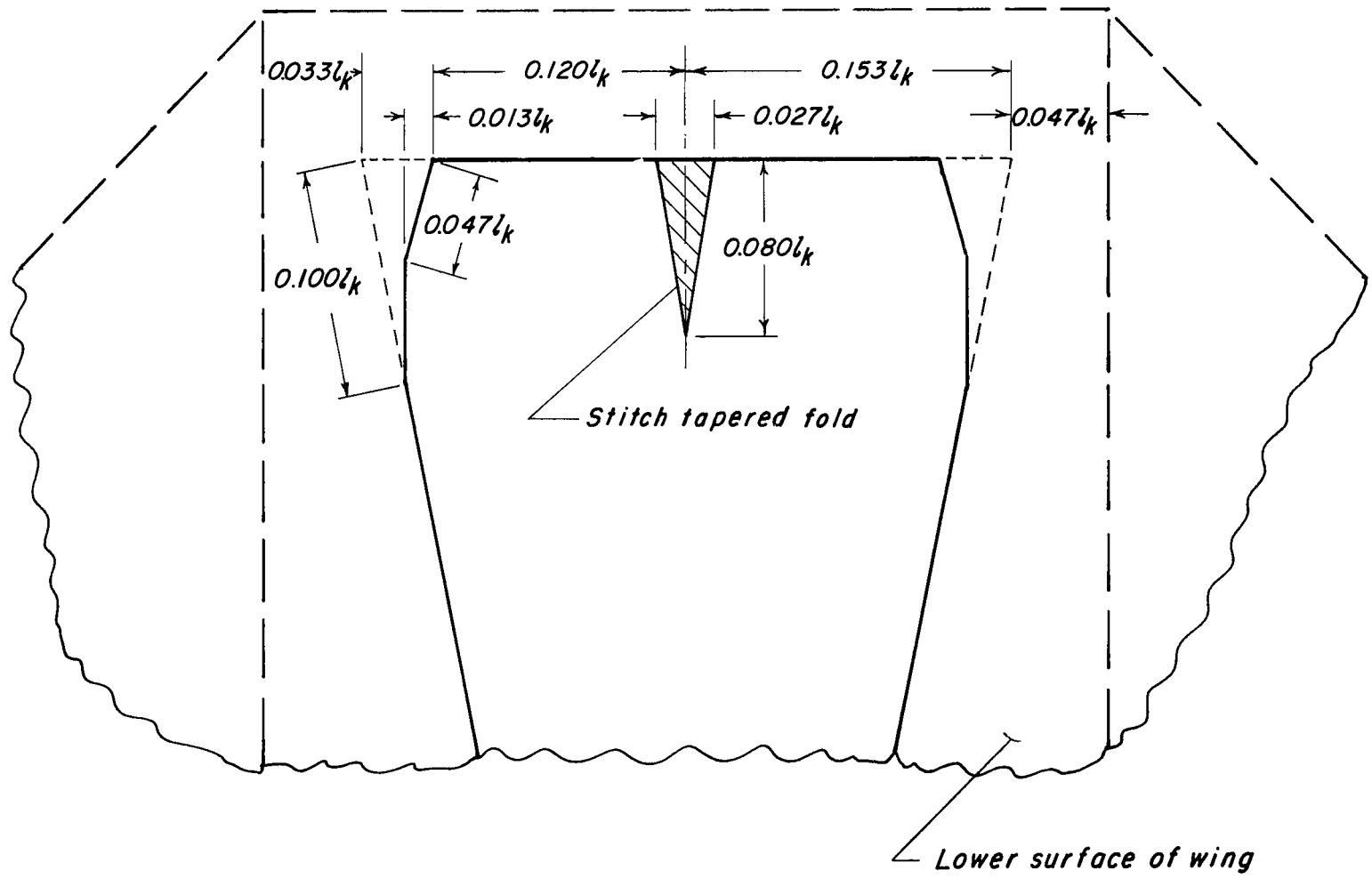
(b) Scoop details.

Figure 15.- Concluded.
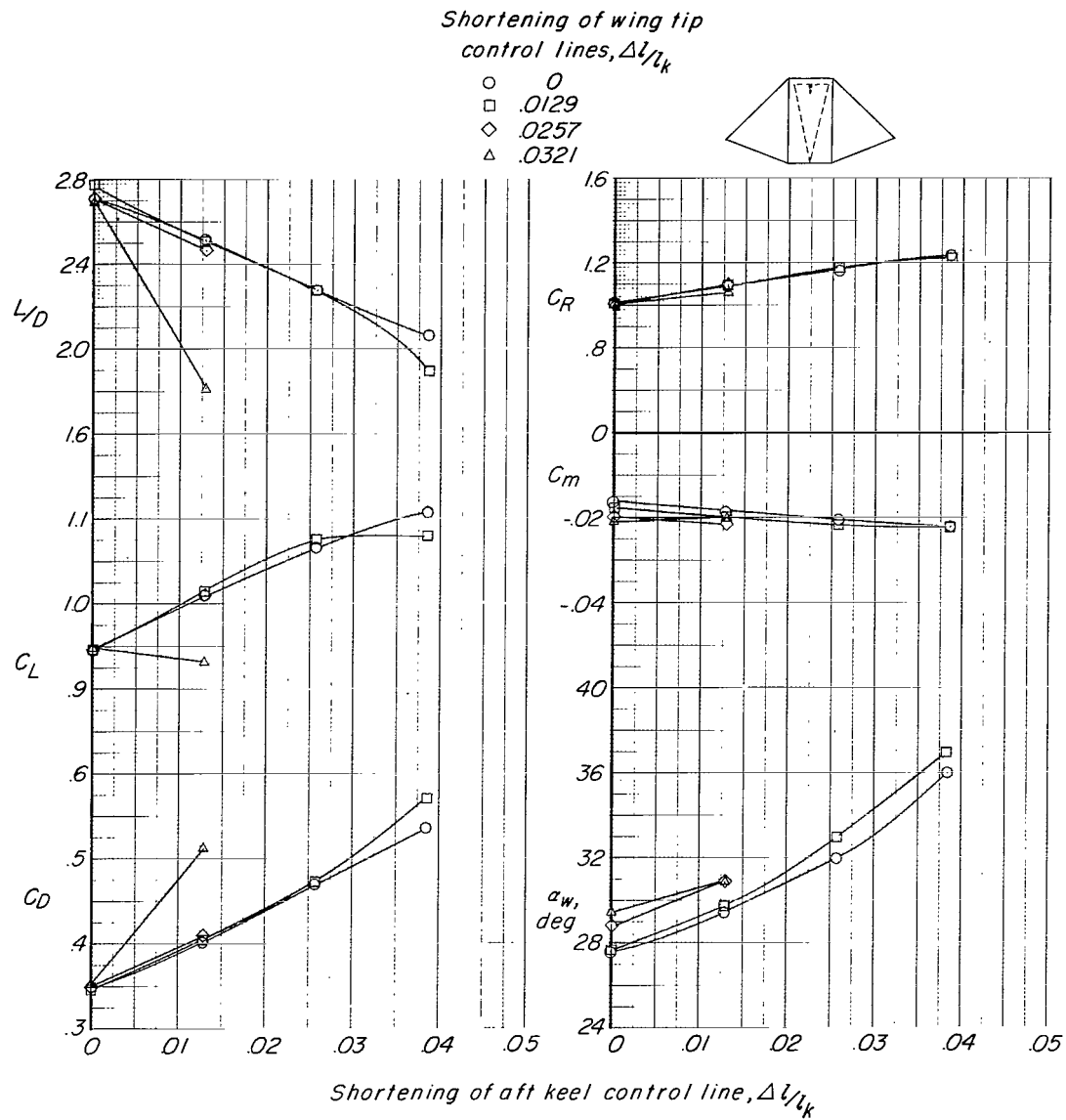
Figure 16.- Effect of aft keel control line shortening on the longitudinal aerodynamic characteristics of twin-keel model 17 with lower surface triangular scoop. Keel-to-payload separation distance $\approx 1.00 l_k$.
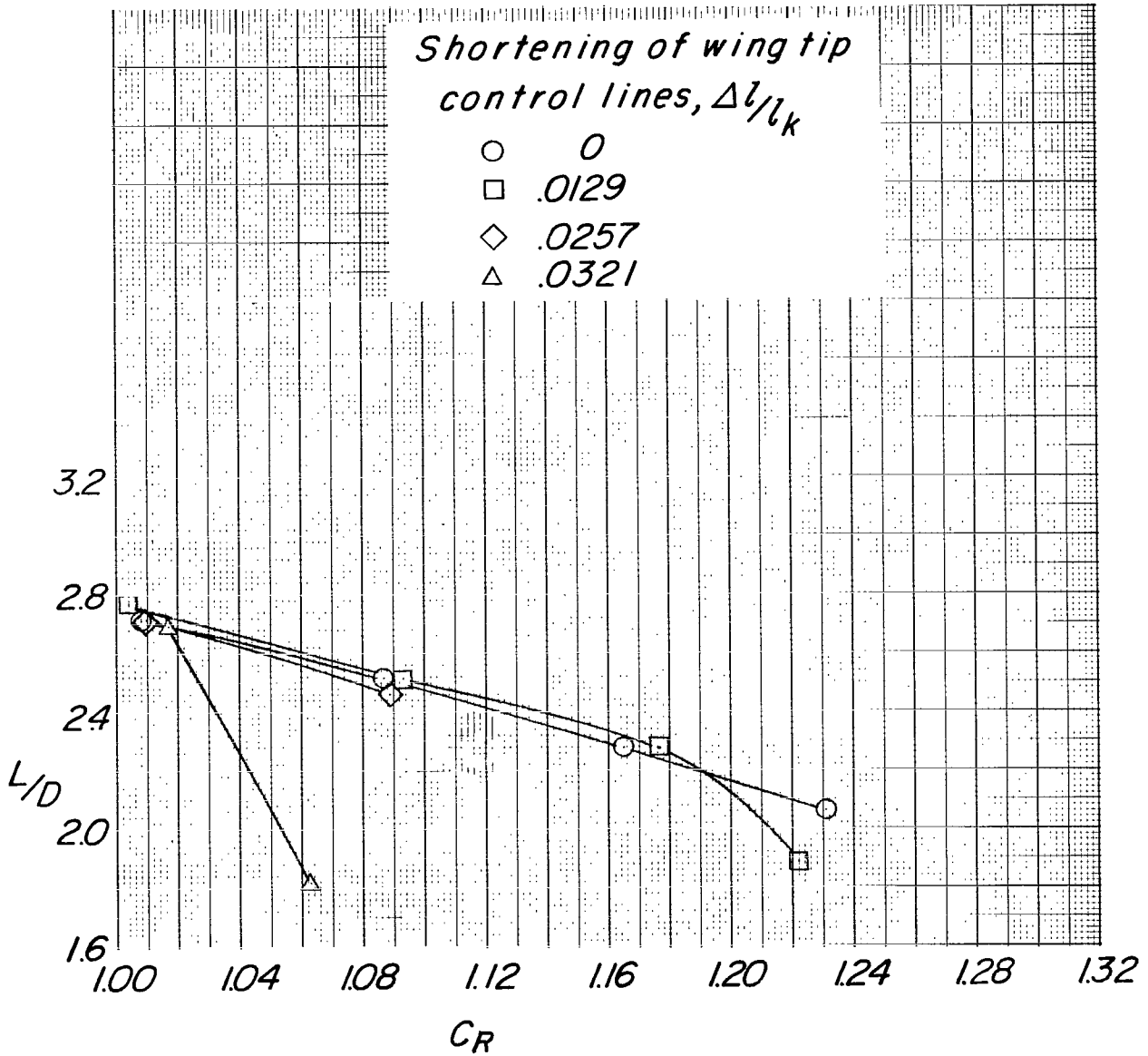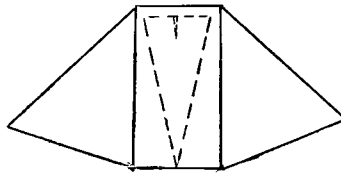
Figure 17.- Variation of L/D with C_R for same configuration as that used for figure 16.
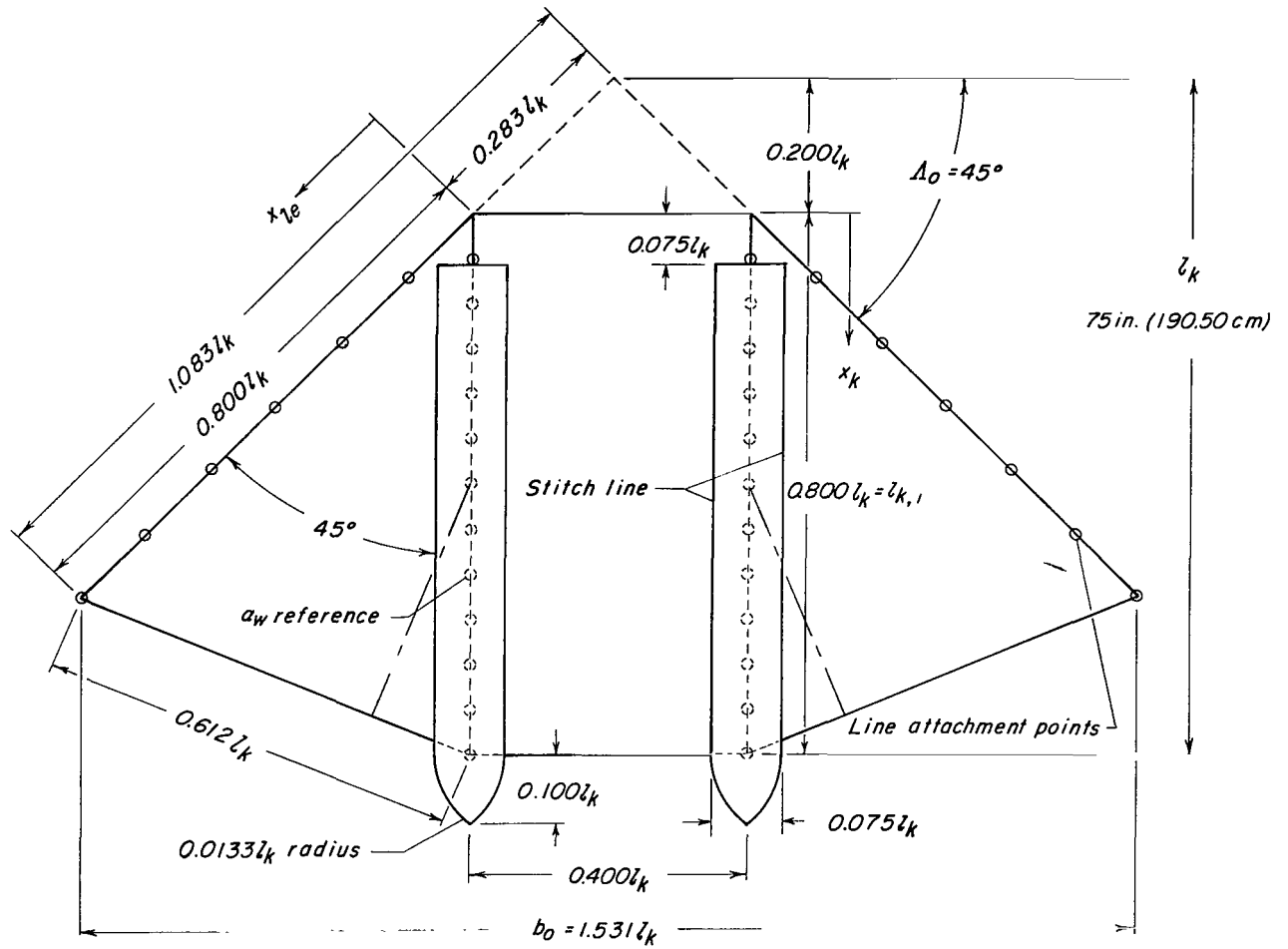
Keel	$x/l_{k,l}$	Leading edge
0.083		0.167
.167		.333
.250		.500
.333		.667
.417		.833
.500		1.000
.583		
.667		
.750		
.833		
.917		
1.000		

Line attachment location

Figure 18.- Flat planform details of twin-keel parawing model 18, with ram-air-inflated tubes on upper surface of wing.
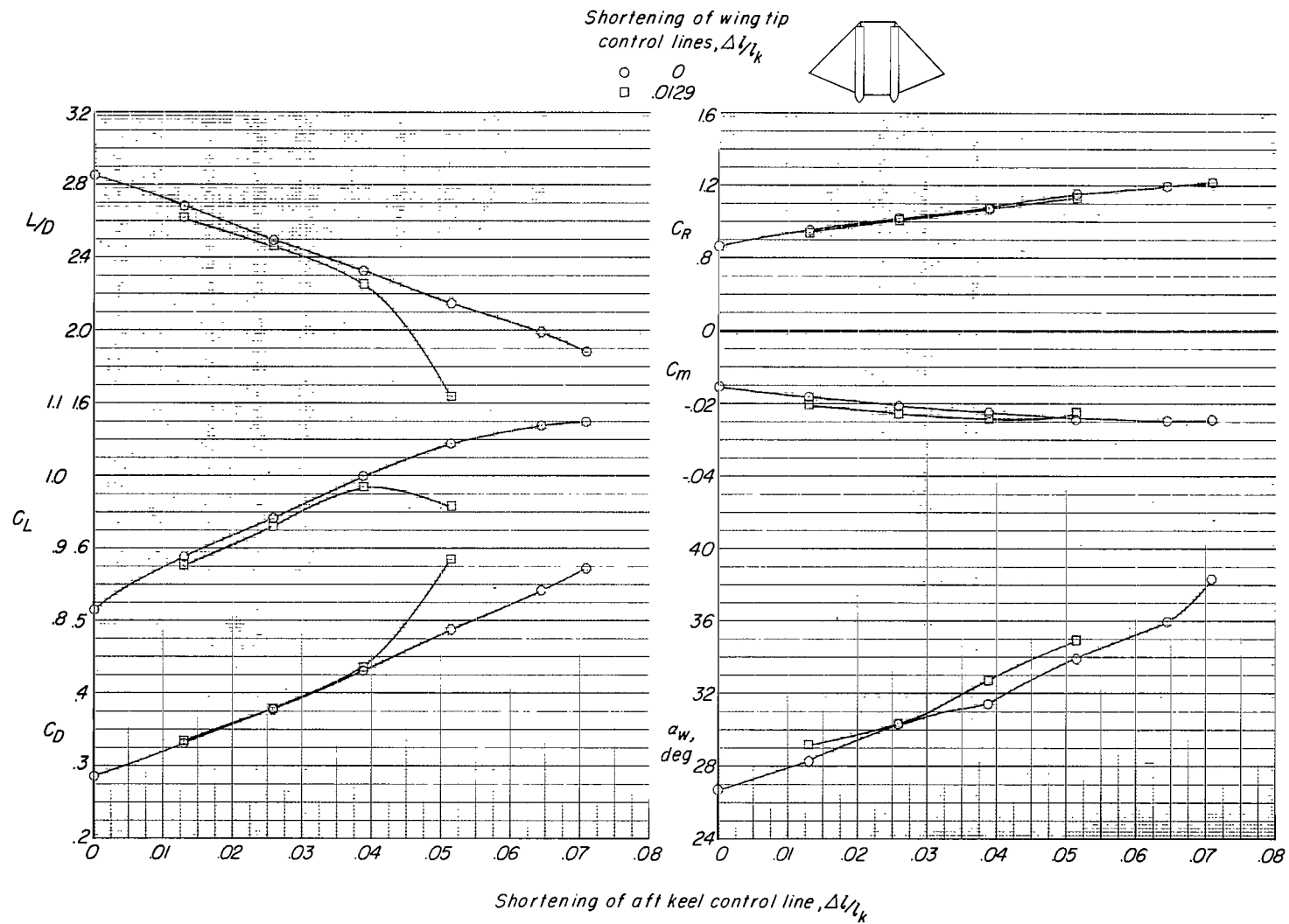
Figure 19.- Effect of aft keel control line shortening on the longitudinal aerodynamic characteristics of twin-keel model 18. Parallel keels with twin upper surface ram-air-inflated tubes. Keel-to-payload separation distance $\approx 1.00 l_k$.
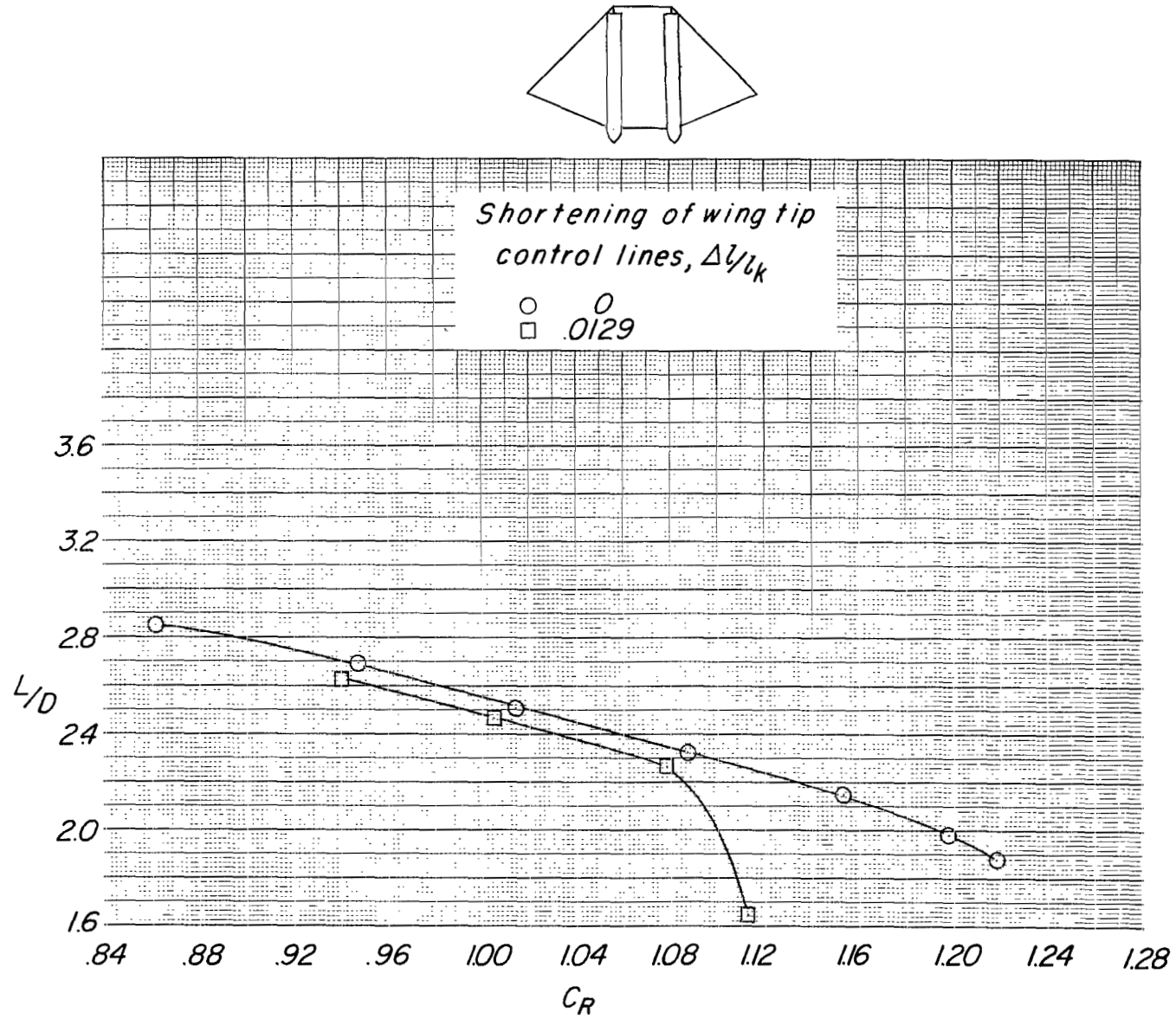
Figure 20.- Variation of L/D with C_R for same configuration as that used for figure 19.
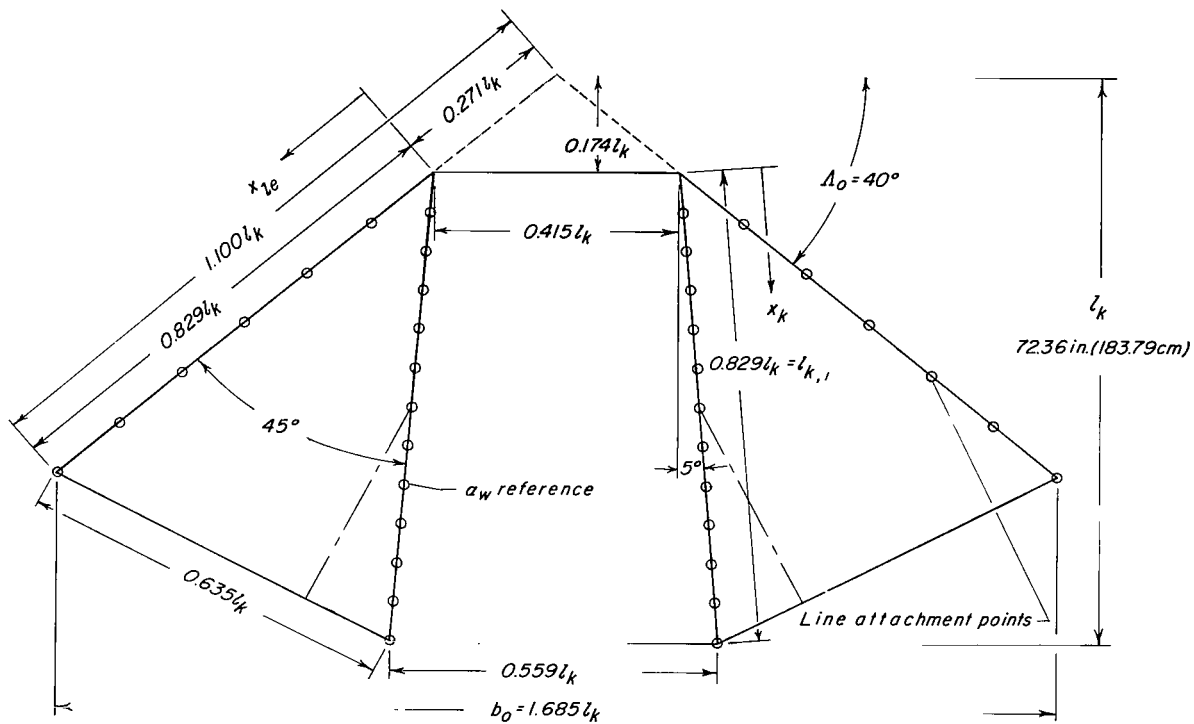
$x/l_{k,l}$	
Keel	Leading edge
0.083	0.167
.167	.333
.250	.500
.333	.667
.417	.833
.500	1.000
.583	
.667	
.750	
.833	
.917	
1.000	

Line attachment location

Figure 21.- Flat planform details of twin-keel parawing model 19.
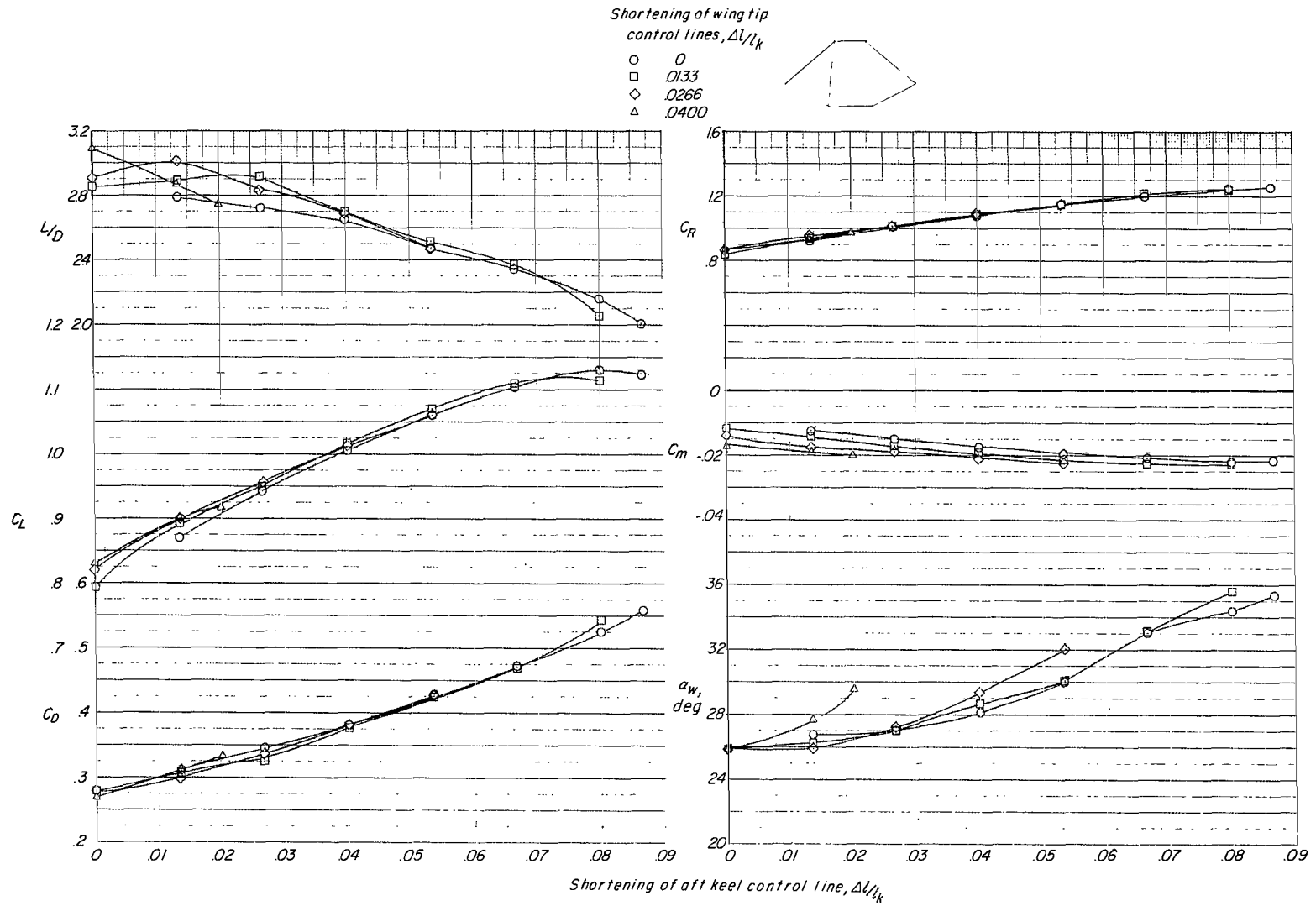
Figure 22.- Effect of aft keel control line shortening on the longitudinal aerodynamic characteristics of twin-keel model 19, 5° canted keels. Keel-to-payload separation distance ≈ $1.00l_k$.
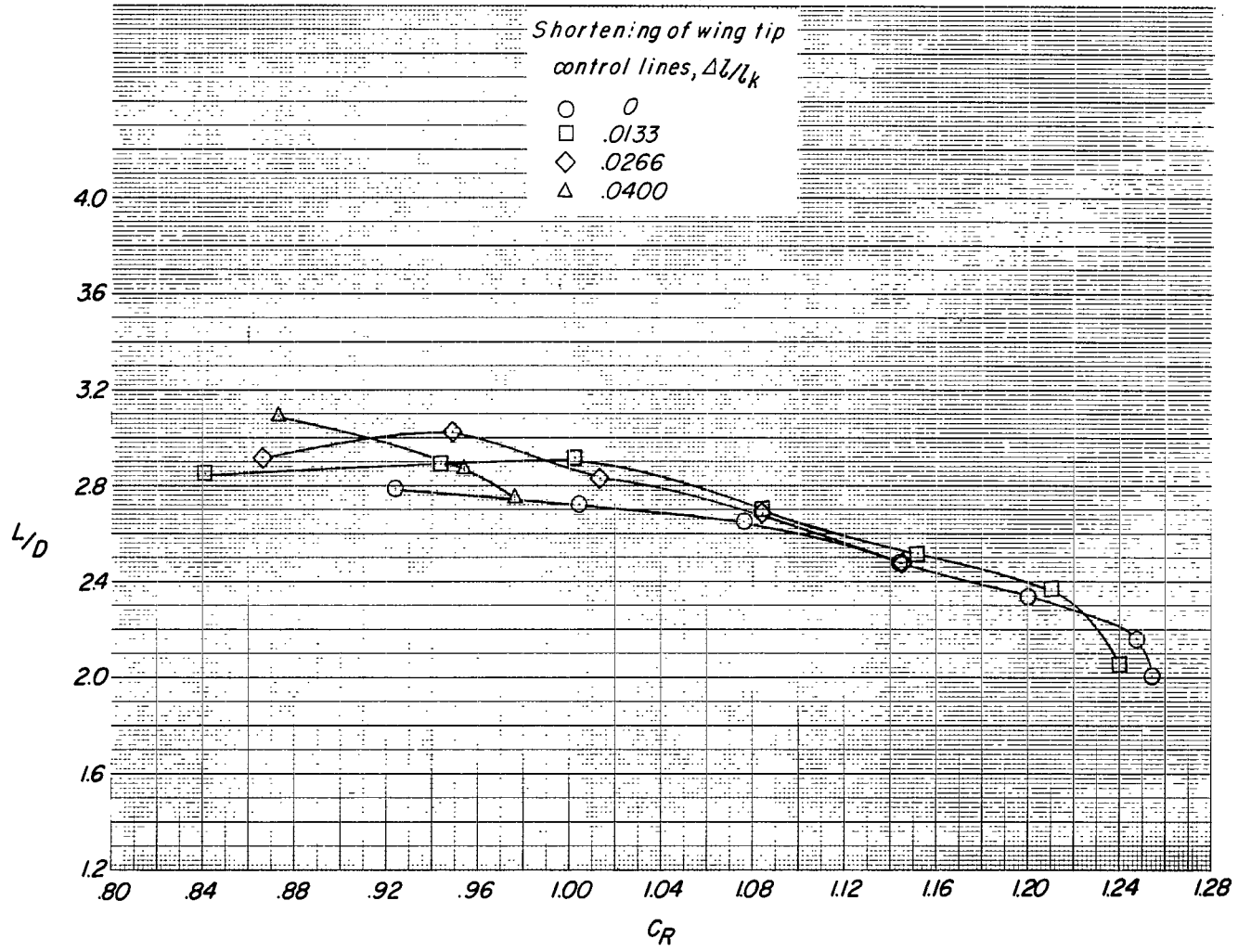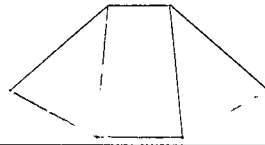
Figure 23.- Variation of L/D with C_R for same configuration as that used for figure 22.
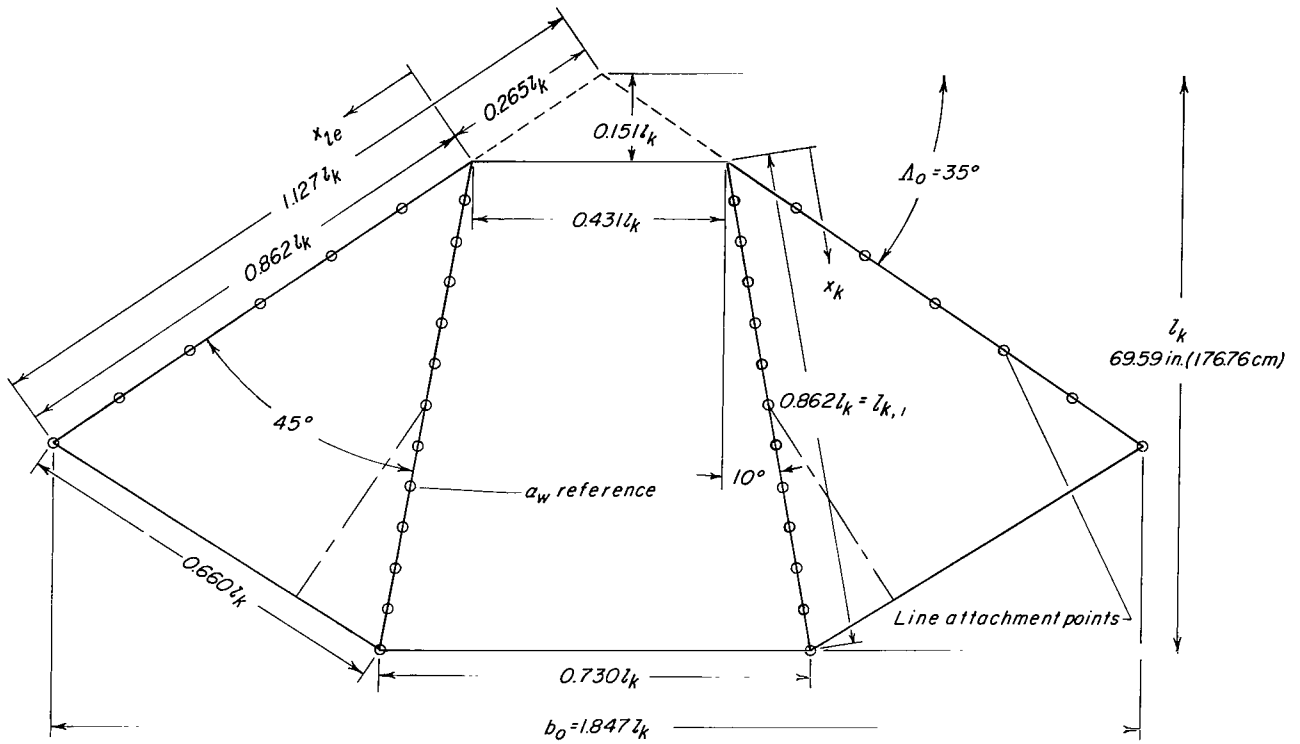
$0.265 l_k$

x_{le}

$1.127 l_k$

$0.862 l_k$

$0.151 l_k$

$0.431 l_k$

$\Lambda_0 = 35°$

x_k

l_k
69.59 in. (176.76 cm)

$45°$

a_w reference

$0.862 l_k = l_{k,1}$

$10°$

$0.660 l_k$

Line attachment points

$0.730 l_k$

$b_0 = 1.847 l_k$

Keel	$x/l_{k,1}$ Leading edge
0.083	0.167
.167	.333
.250	.500
.333	.667
.417	.833
.500	1.000
.583	
.667	
.750	
.833	
.917	
1.000	

Line attachment location

Figure 24.- Flat planform details of twin-keel parawing model 20.
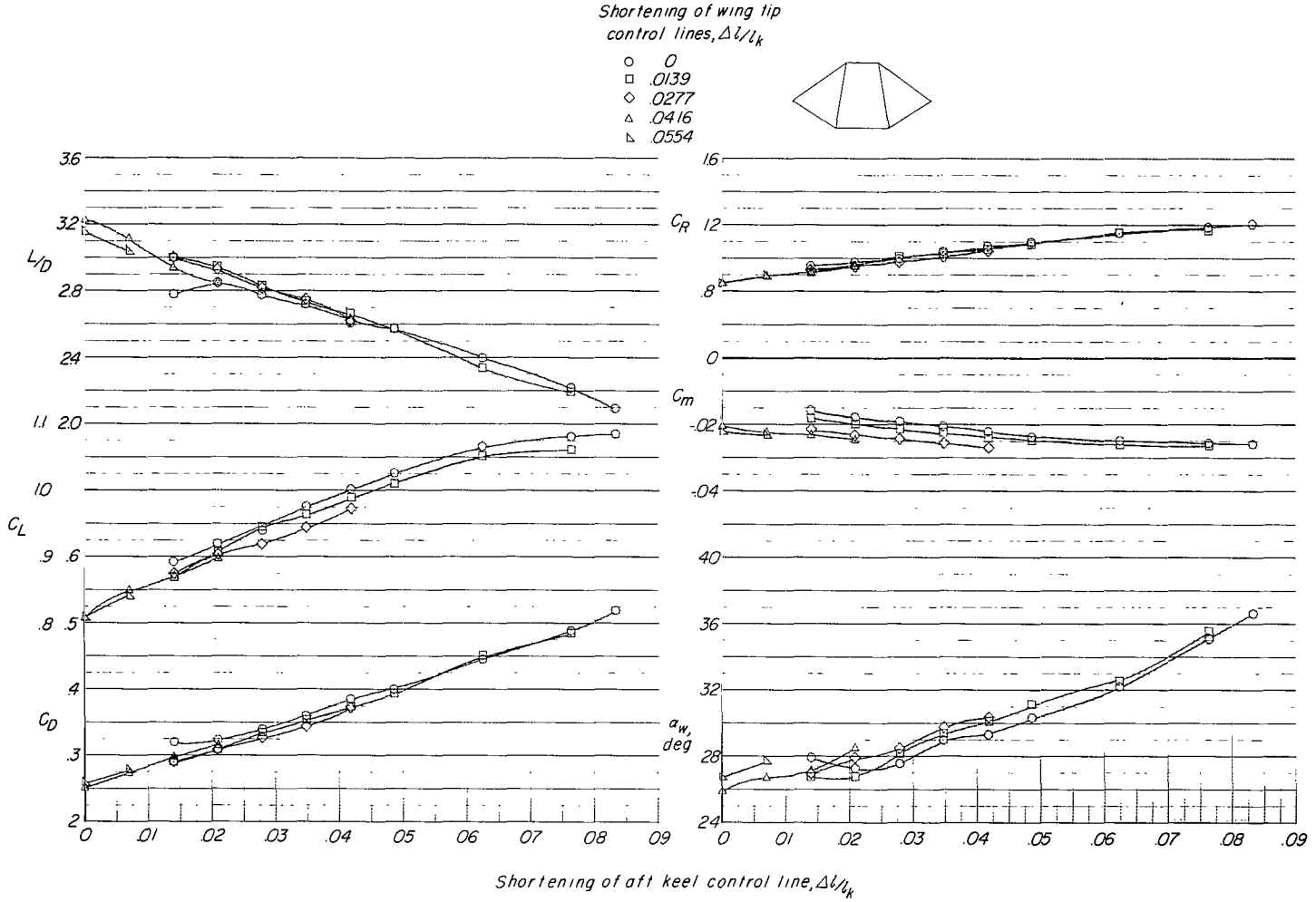
Figure 25.- Effect of aft keel control line shortening on the longitudinal aerodynamic characteristics of twin-keel model 20, 10^0 canted keels. Keel-to-payload separation distance $\approx 1.00 l_k$.
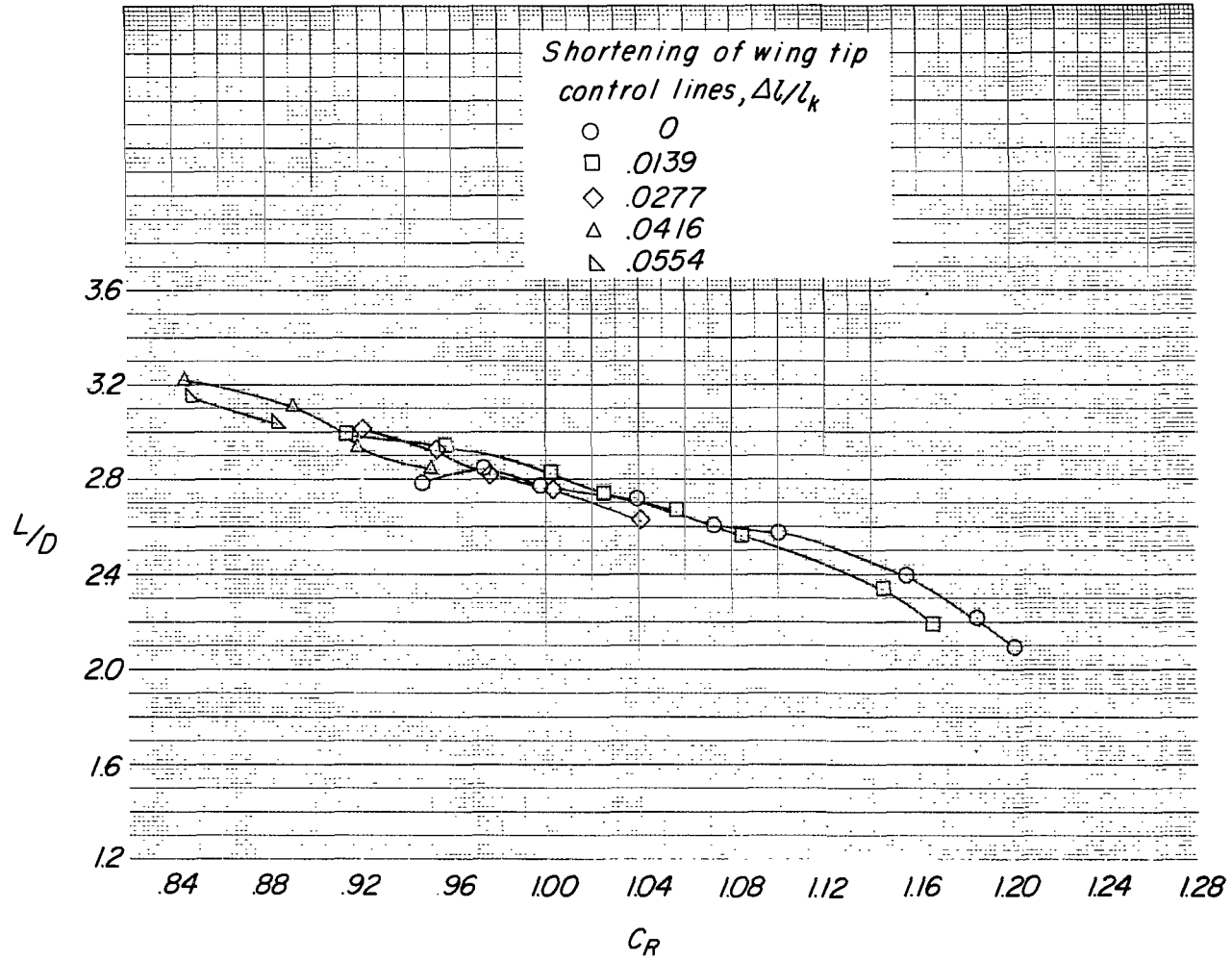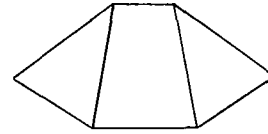
Figure 26.- Variation of L/D with C_R for same configuration as that used for figure 25.
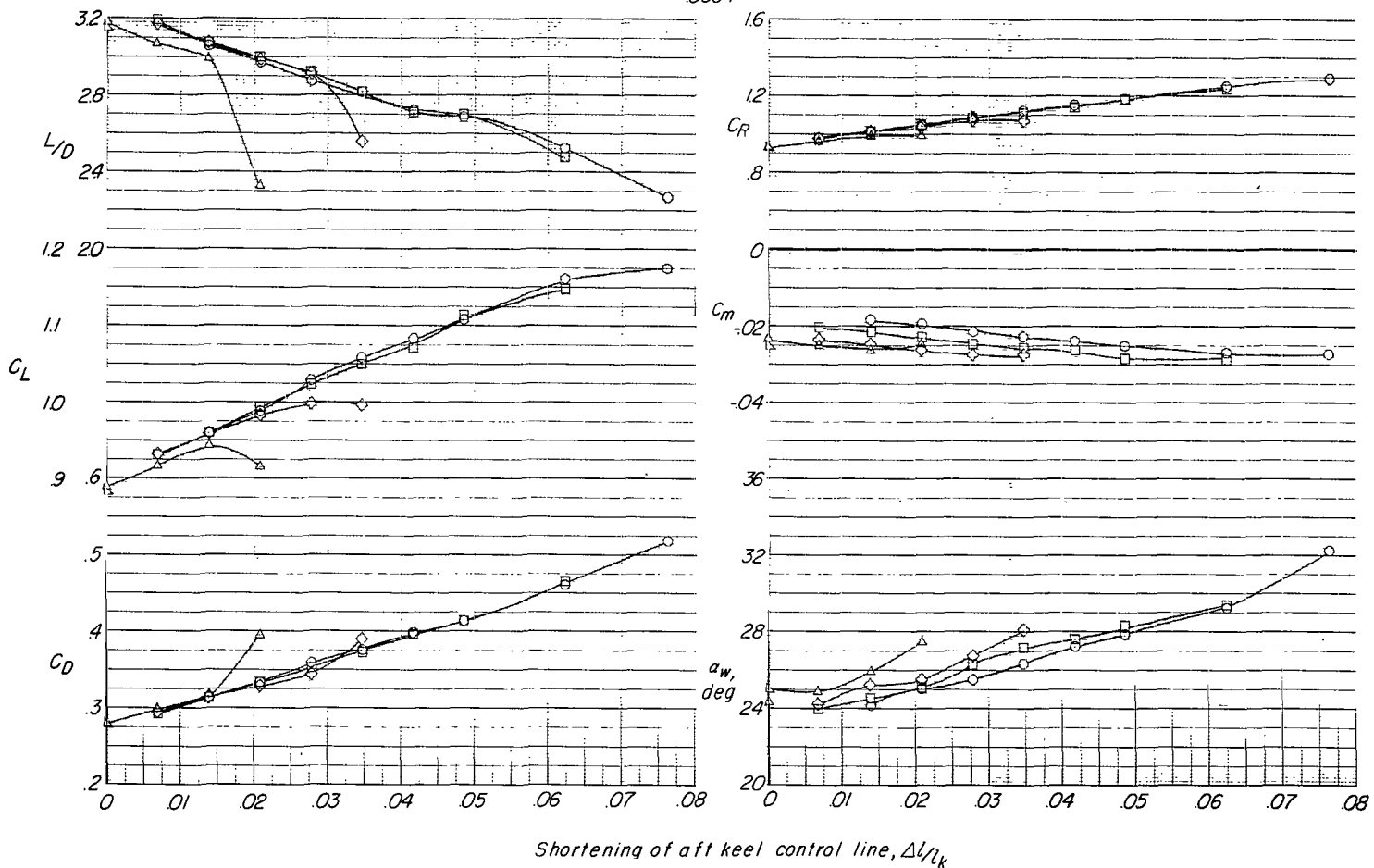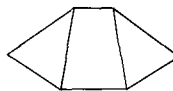
Figure 27.- Effect of aft keel control line shortening on the longitudinal aerodynamic characteristics of twin-keel model 20, 10^0 canted keels. Keel-to-payload separation distance $\approx 1.25l_k$.
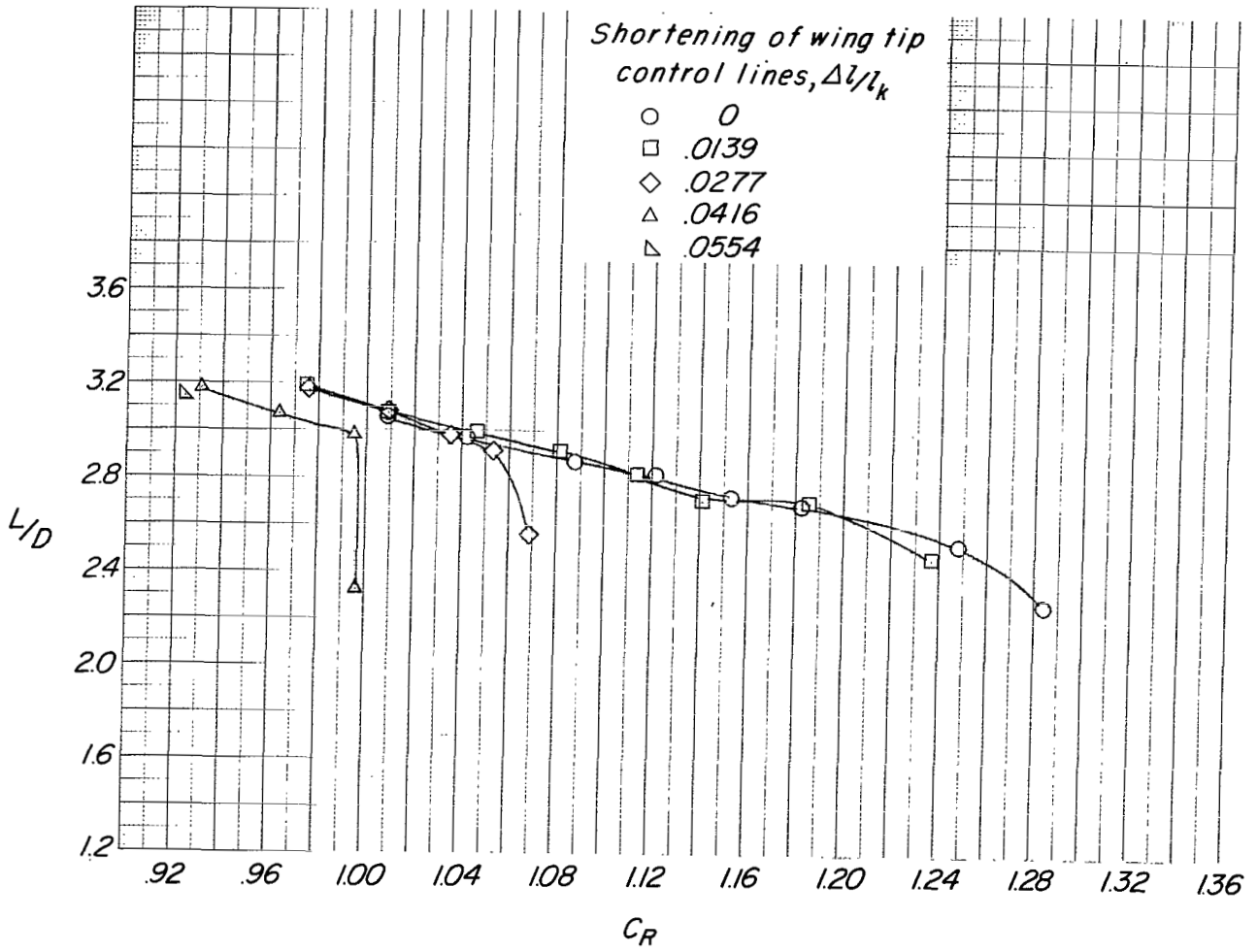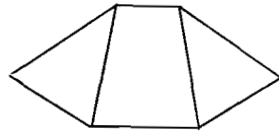
Figure 28.- Variation of L/D with C_R for same configuration as that used for figure 27.
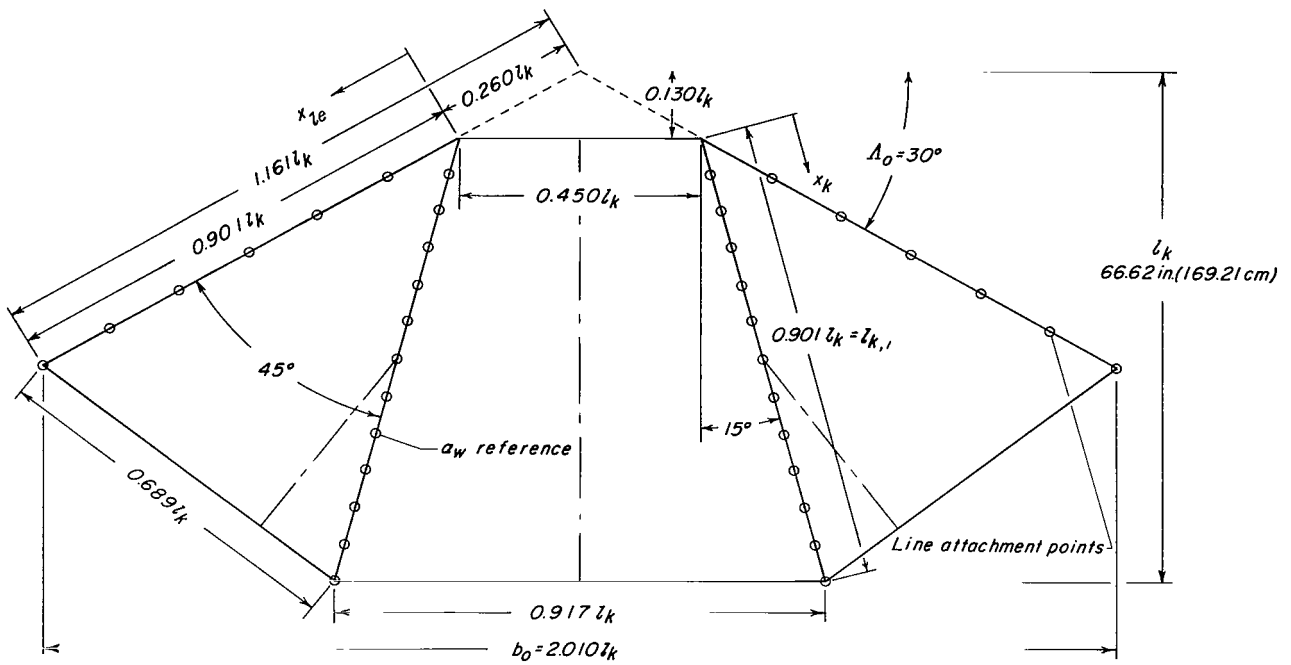
Figure 29.- Flat planform details of twin-keel parawing model 21.

The figure contains the following labels and dimensions:

x_{le}, $1.16 l_k$, $0.901 l_k$, $0.260 l_k$, $0.130 l_k$, $0.450 l_k$, $\Lambda_0 = 30°$, l_k 66.62 in.(169.21 cm), $45°$, a_w reference, $0.901 l_k = l_{k,1}$, $15°$, x_k, Line attachment points, $0.689 l_k$, $0.917 l_k$, $b_0 = 2.010 l_k$

Line attachment location table ($x/l_{k,1}$):

Keel	Leading edge
0.083	0.167
.167	.333
.250	.500
.333	.667
.417	.833
.500	1.000
.583	
.667	
.750	
.833	
.917	
1.000	

Line attachment location
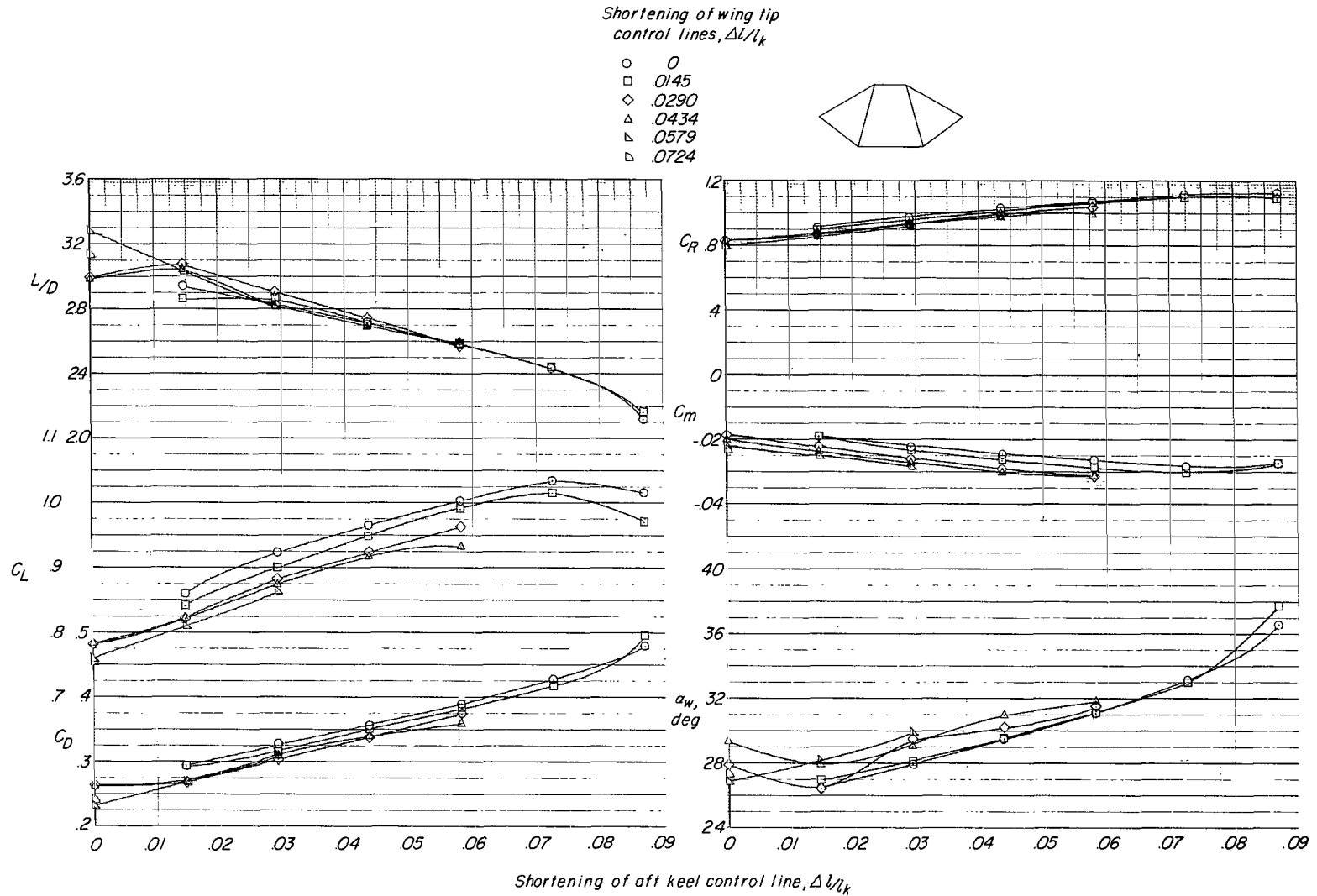
Figure 30.- Effect of aft keel control line shortening on the longitudinal aerodynamic characteristics of twin-keel model 21, 15° canted keels. Keel-to-payload separation distance ≈ $1.00l_k$.
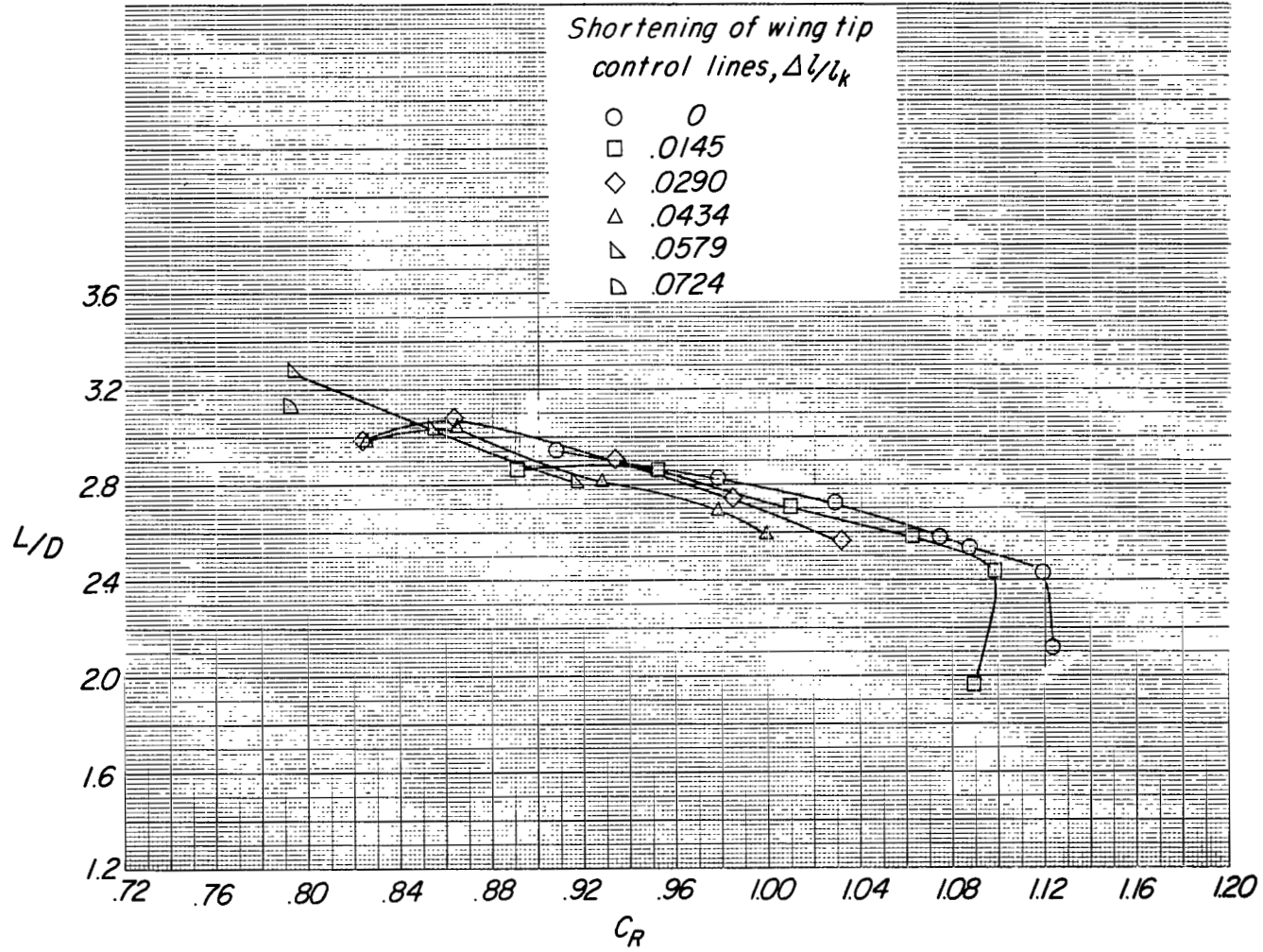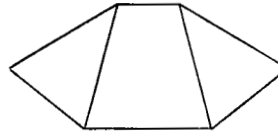
Figure 31.- Variation of L/D with C_R for same configuration as that used for figure 30.
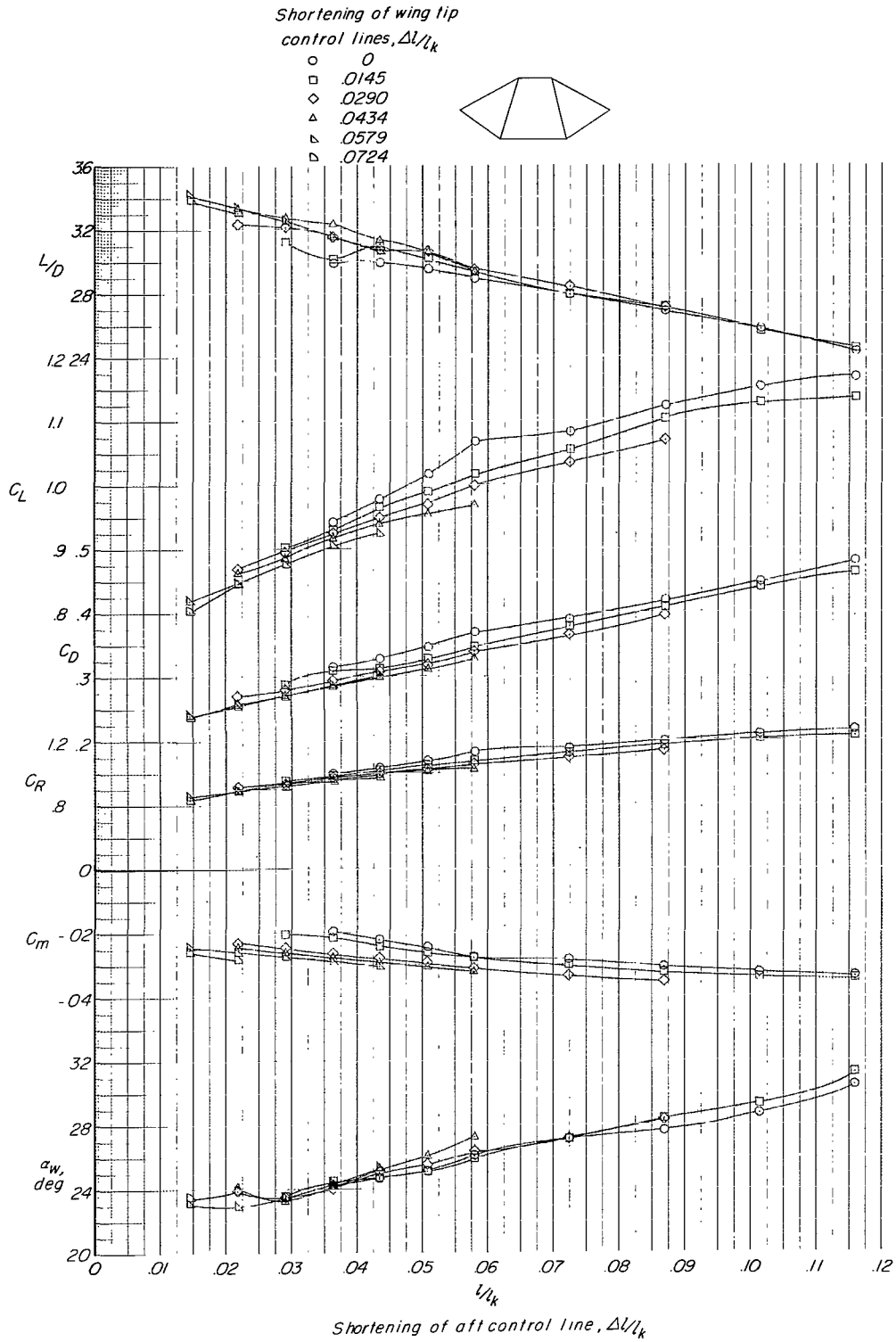
Figure 32.- Effect of aft keel control line shortening on the longitudinal aerodynamic characteristics of twin-keel model 21, 15⁰ canted keels. Keel-to-payload separation distance $\approx 1.25 l_k$.
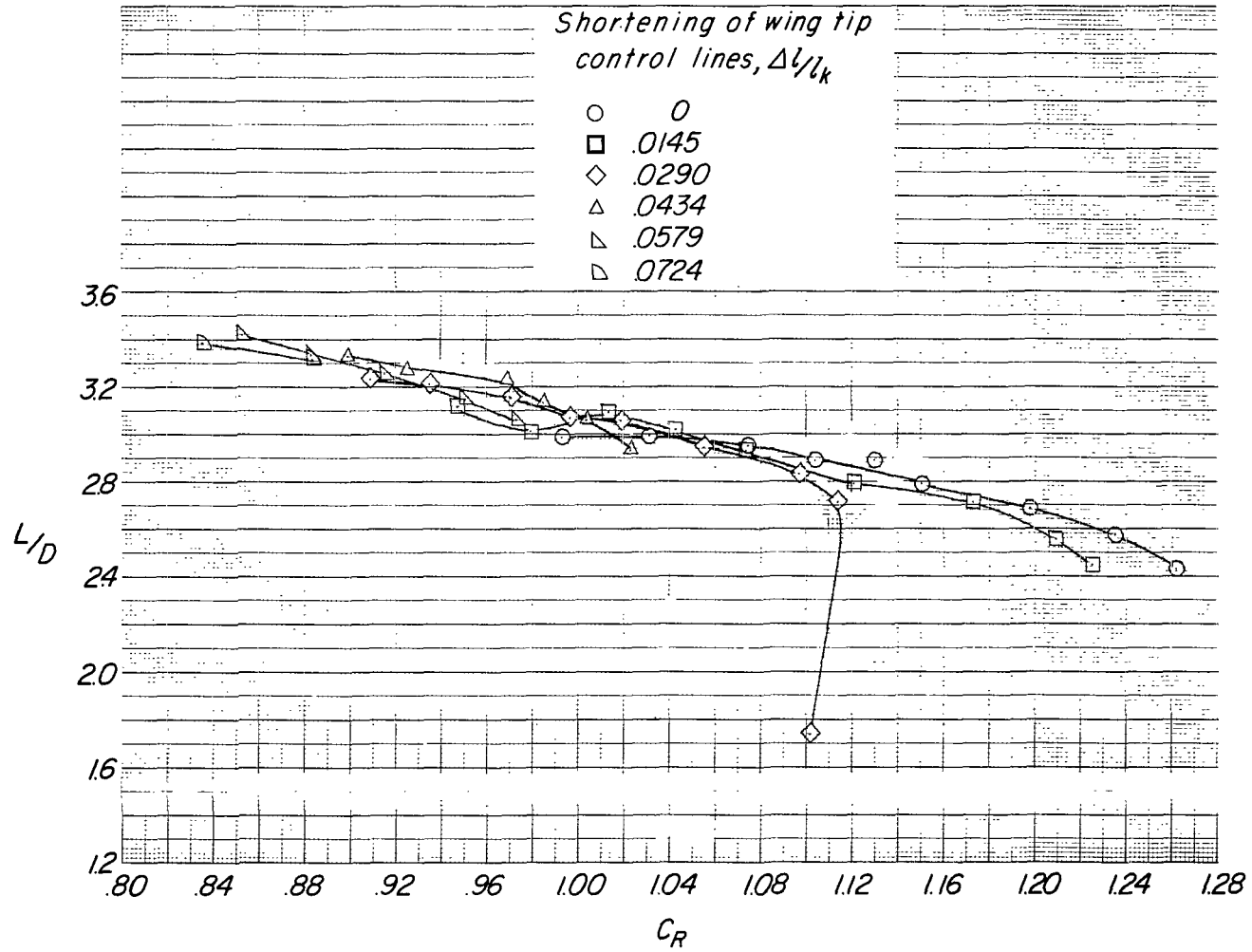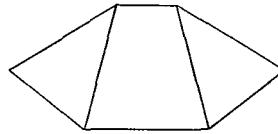
Figure 33.- Variation of L/D with C_R for same configuration as that used for figure 32.
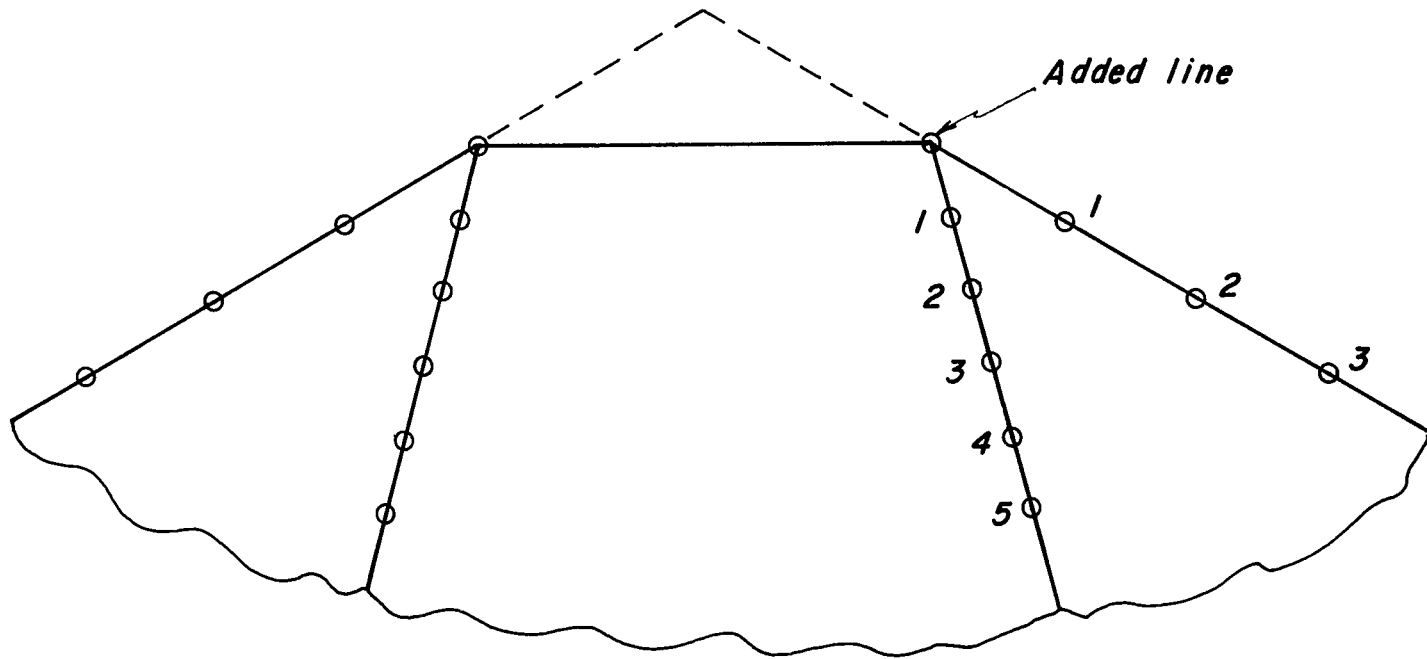
Figure 34.- Flat planform details of twin-keel parawing model 21 showing modified line arrangement at the nose. Added nose line.
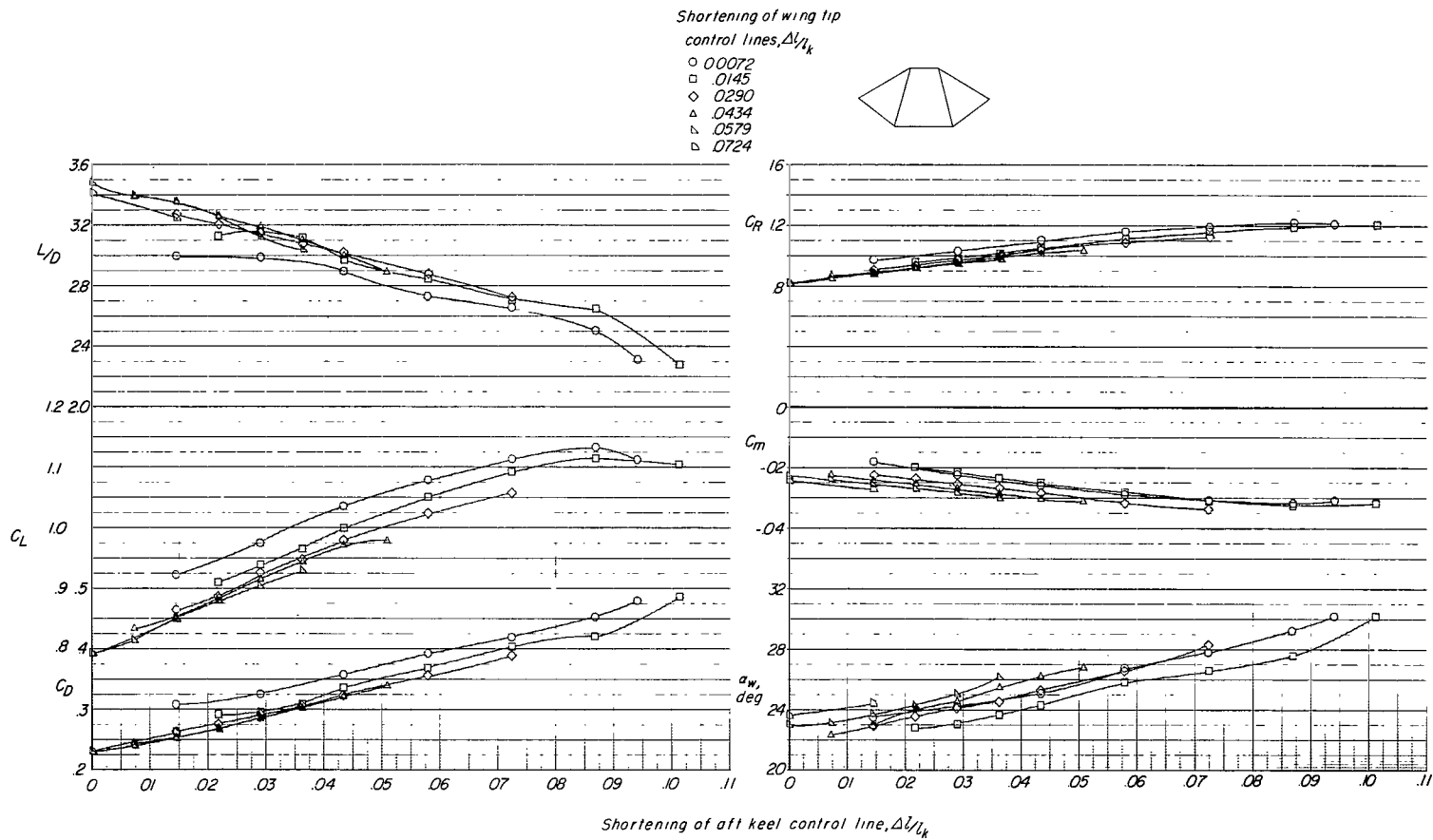
Figure 35.- Effect of aft keel control line shortening on the longitudinal aerodynamic characteristics of twin-keel model 21, 15° canted keels, with modified line arrangement at nose. Keel-to-payload separation distance ≈ $1.25l_k$.
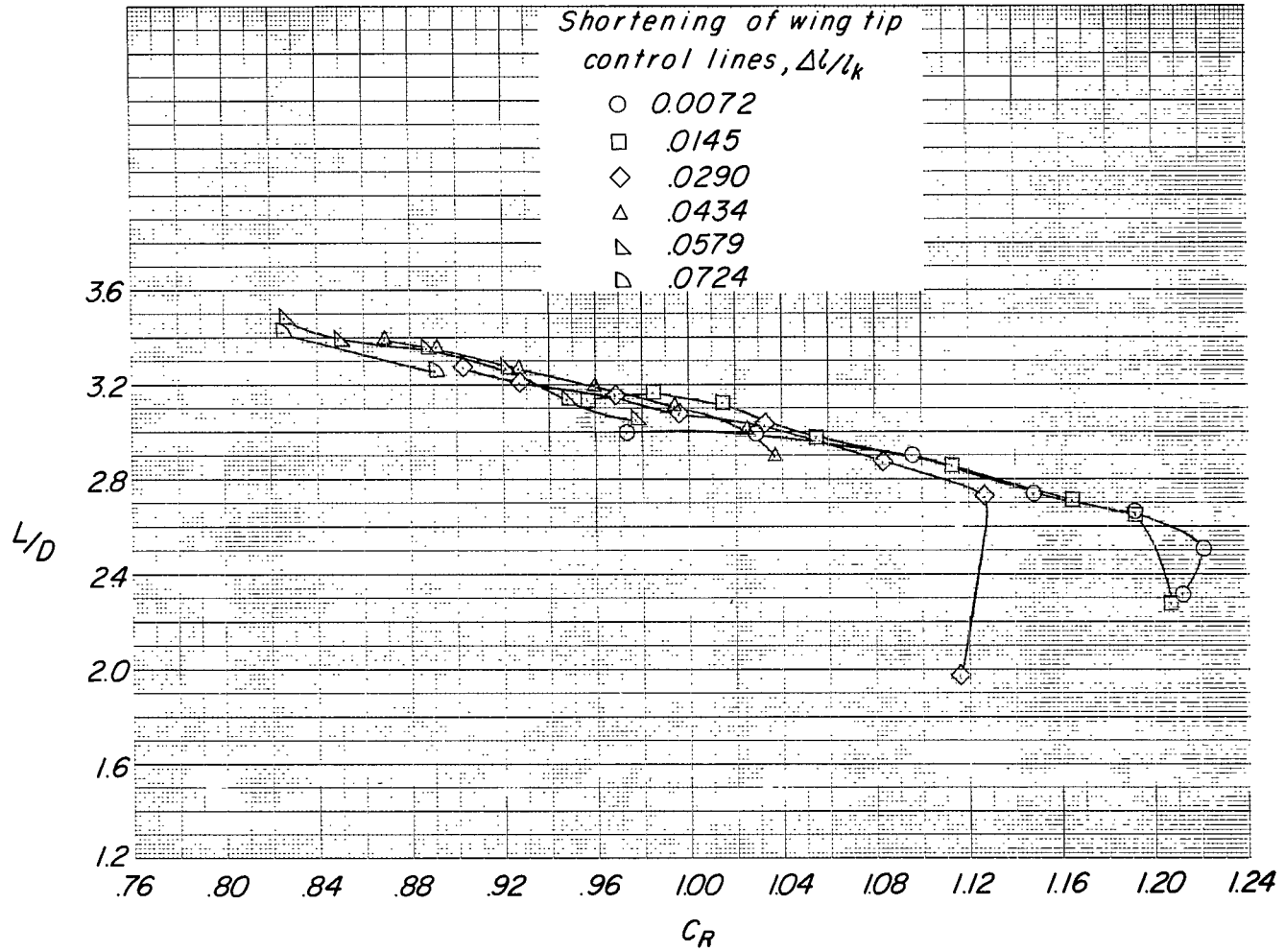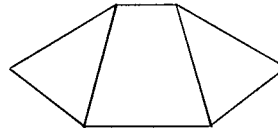
Figure 36.- Variation of L/D with C_R for same configuration as that used for figure 35.
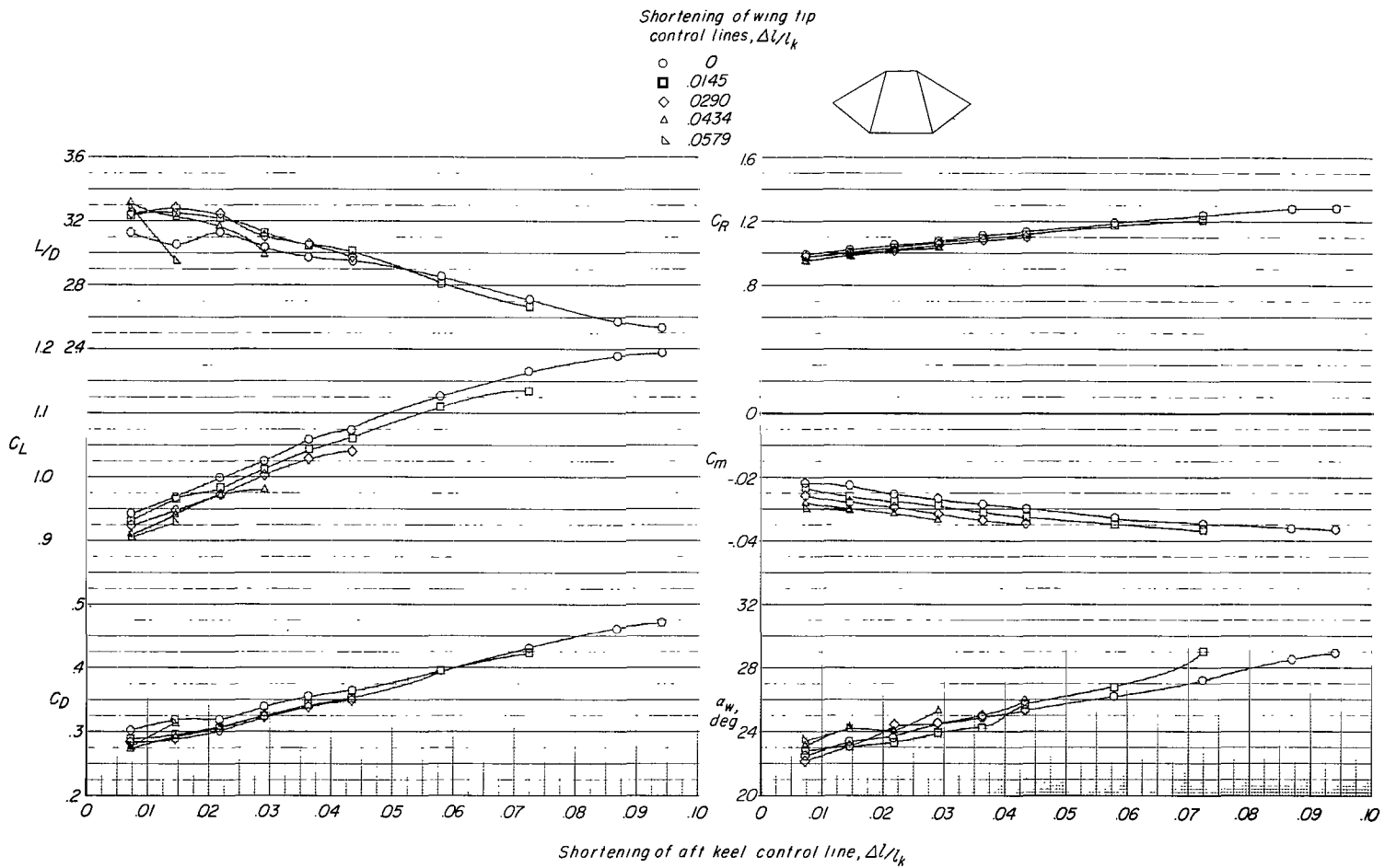
Figure 37.- Effect of aft keel control line shortening on the longitudinal aerodynamic characteristics of twin-keel model 21, 15⁰ canted keels, with modified line arrangement at nose. Keel-to-payload separation distance ≈ $1.50l_k$.
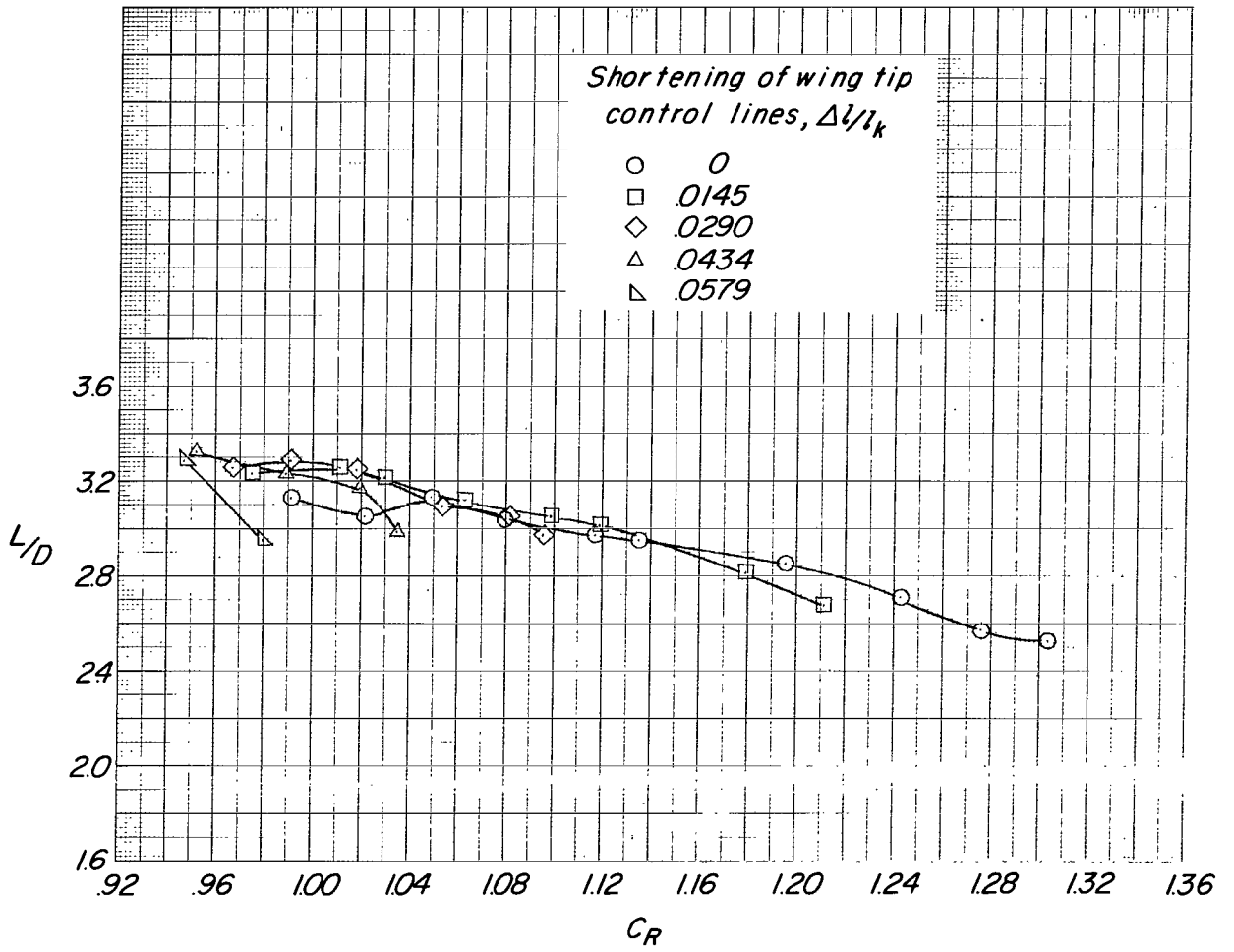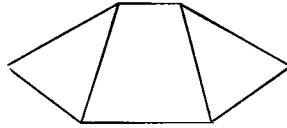
Figure 38.- Variation of L/D with C_R for same configuration as that used for figure 37.
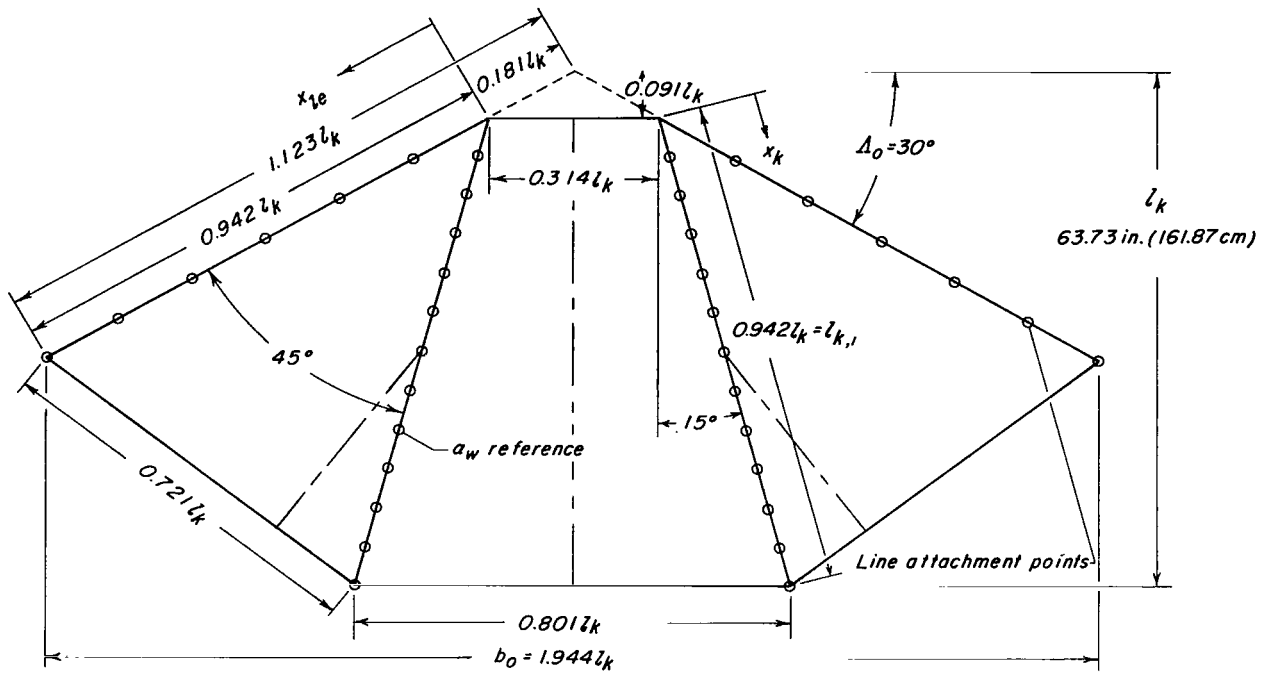
Figure 39.- Flat planform details of twin-keel parawing model 22, 15° canted keels with narrowed center panel.

The figure includes the following labels and dimensions:

x_{le}

$0.181 l_k$

$0.091 l_k$

$1.123 l_k$

x_k

$\Lambda_o = 30°$

$0.942 l_k$

$0.314 l_k$

l_k

63.73 in. (161.87 cm)

45°

a_w reference

$0.942 l_k = l_{k,l}$

$0.721 l_k$

15°

Line attachment points

$0.801 l_k$

$b_o = 1.944 l_k$

| Keel	$x/l_{k,l}$	Leading edge
0.083		0.167
.167		.333
.250		.500
.333		.667
.417		.833
.500		1.000
.583		
.667		
.750		
.833		
.917		
1.000		

Line attachment location
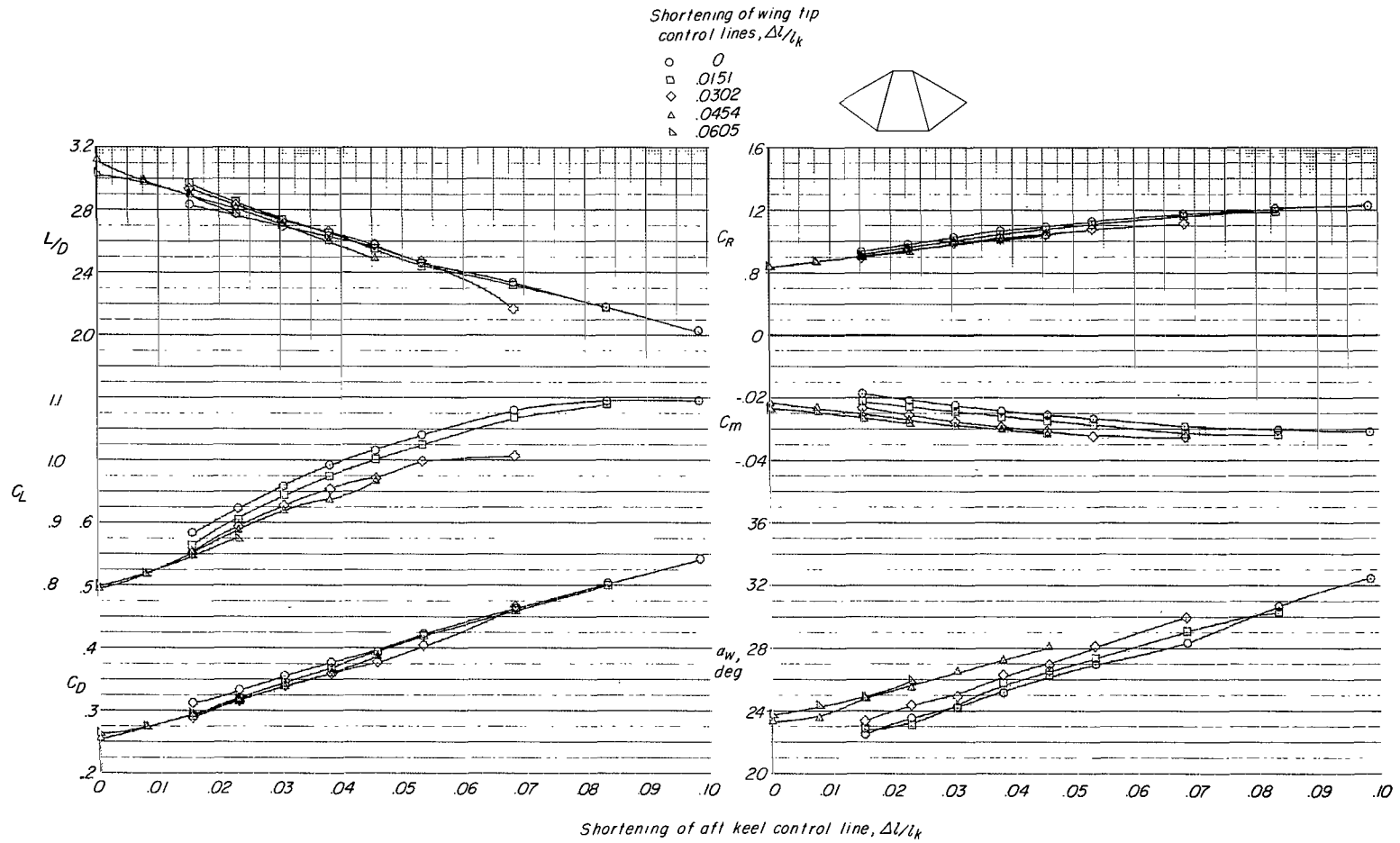
Figure 40.- Effect of aft keel control line shortening on the longitudinal aerodynamic characteristics of twin-keel model 22, 15° canted keels with narrowed center panel. Keel-to-payload separation distance ≈ $1.00l_k$.
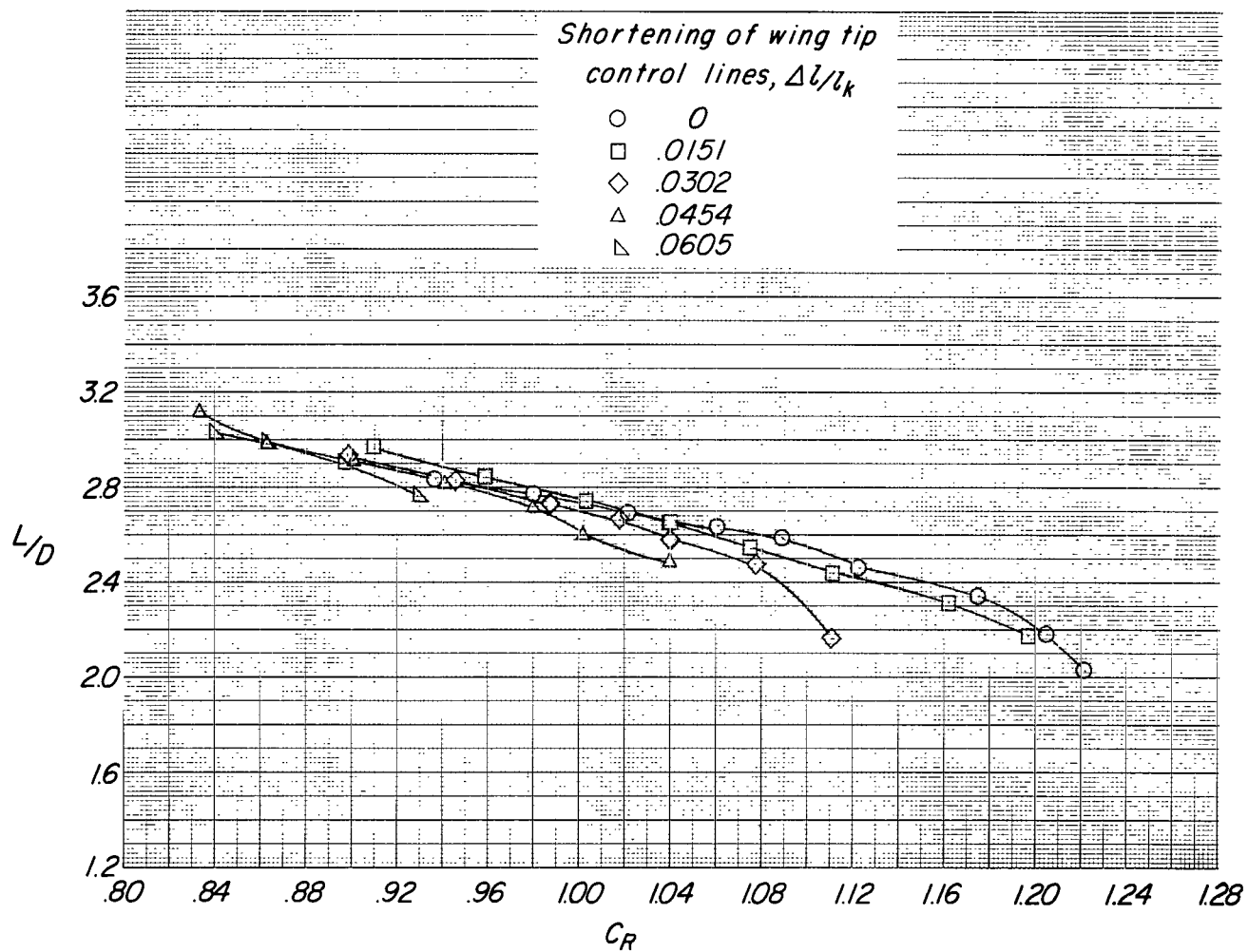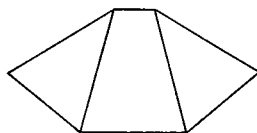
Figure 41.- Variation of L/D with C_R for same configuration as that used for figure 40.

Figure 42.- Flat planform details of twin-keel parawing model 23, 15⁰ canted keels with widened center panel.

$x/l_{k,1}$	
Keel	Leading edge
0.083	0.167
.167	.333
.250	.500
.333	.667
.417	.833
.500	1.000
.583	
.667	
.750	
.833	
.917	
1.000	

Line attachment location

Figure 43.- Effect of aft keel control line shortening on the longitudinal aerodynamic characteristics of twin-keel model 23, 15° canted keels with widened center panel. Keel-to-payload separation distance ≈ 1.00l_k.
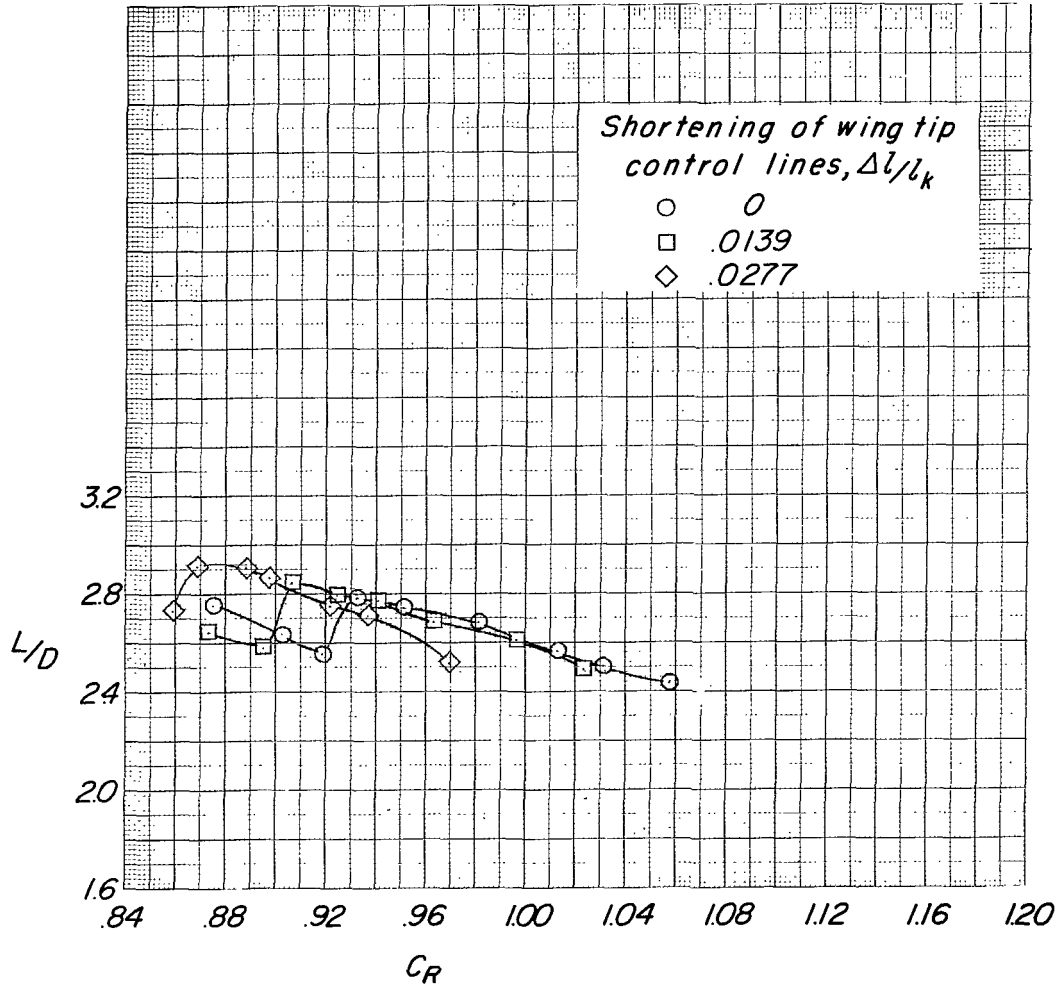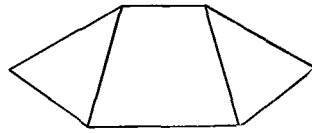
Figure 44.- Variation of L/D with C_R for same configuration as that used for figure 43.
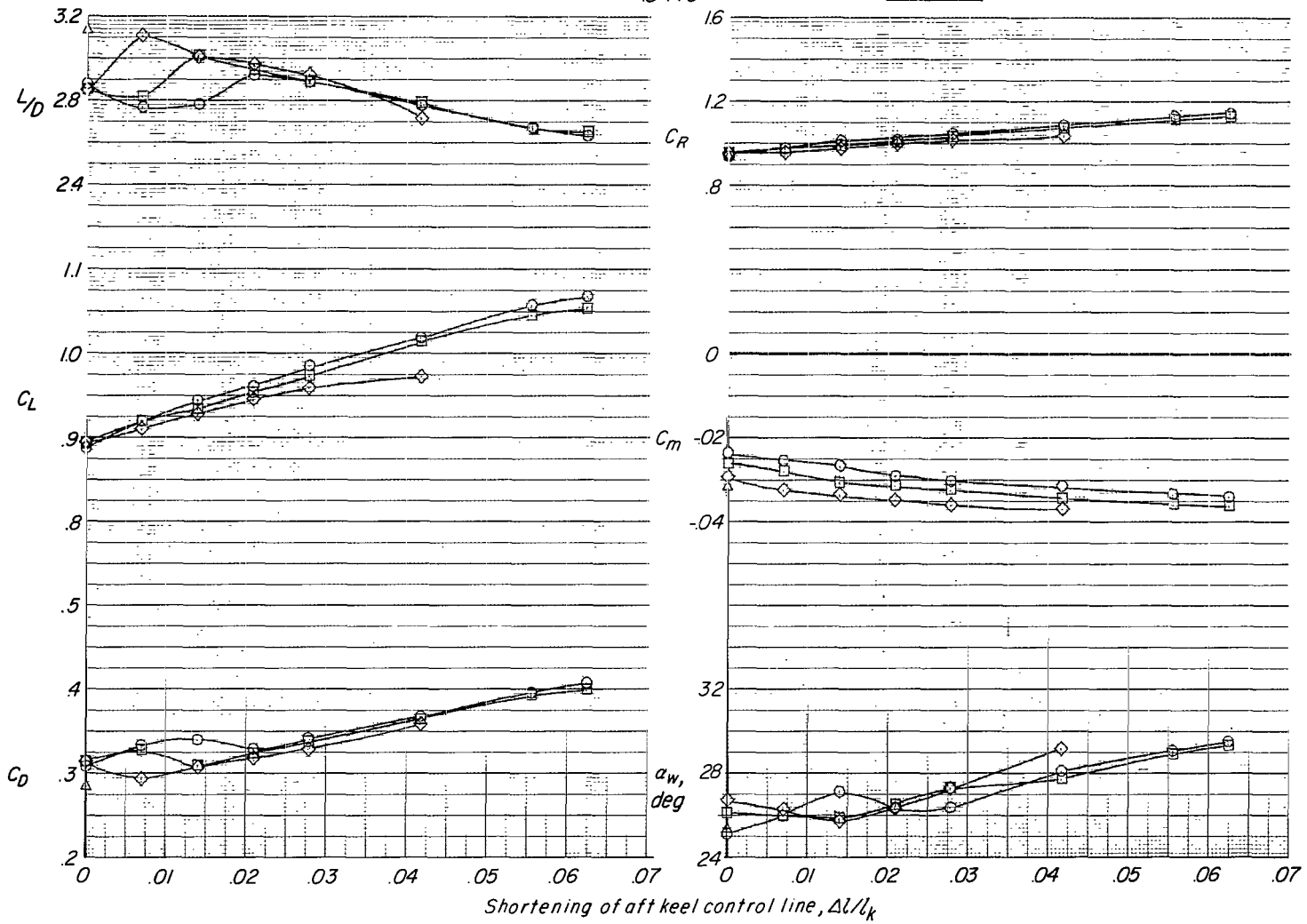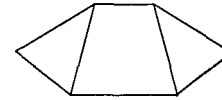
Figure 45.- Effect of aft keel control line shortening on the longitudinal aerodynamic characteristics of twin-keel model 23, 15^0 canted keels with widened center panel. Keel-to-payload separation distance $\approx 1.25 l_k$.
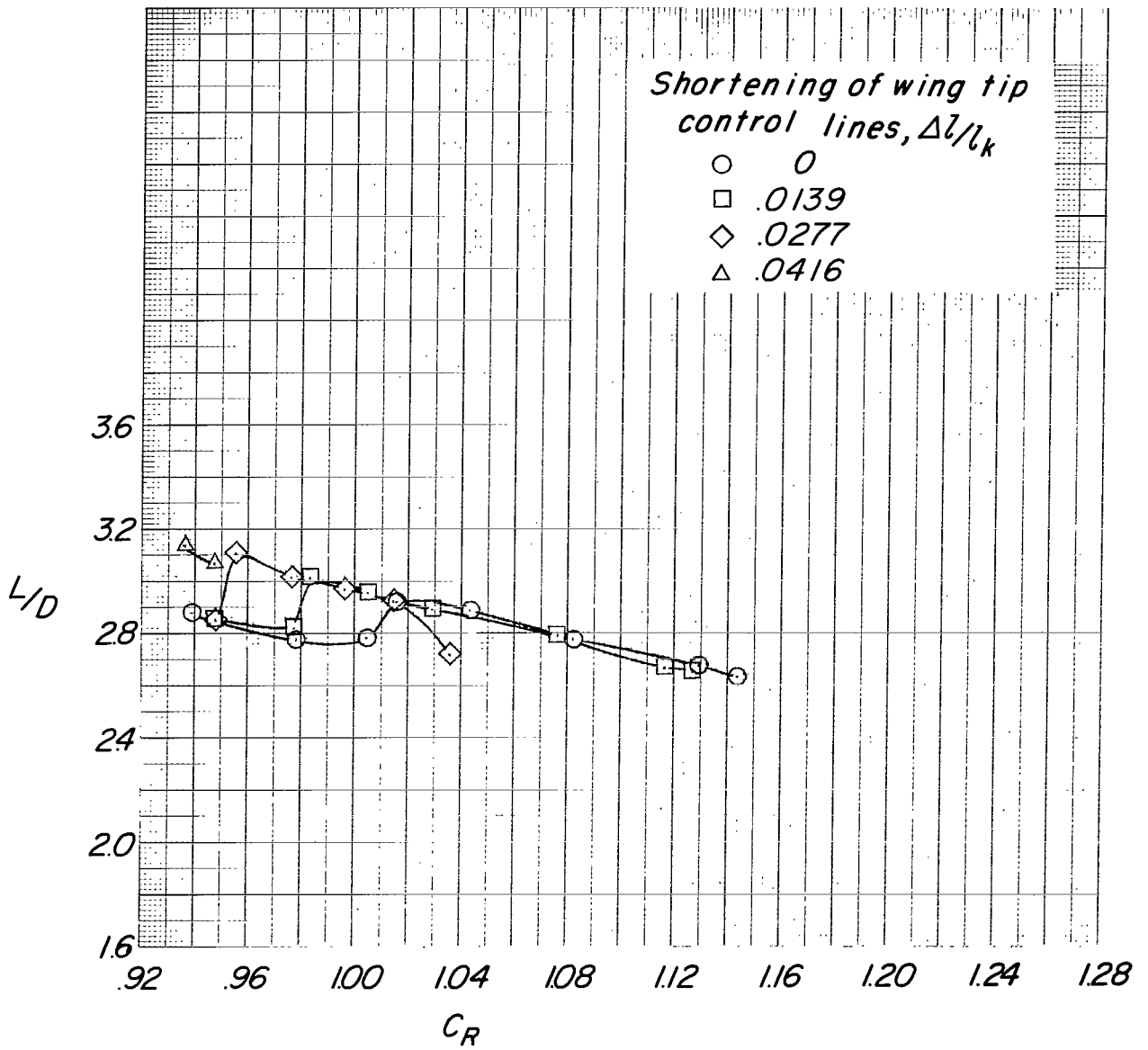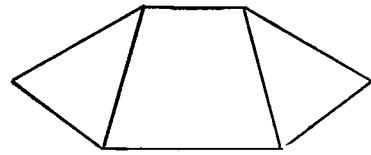
Figure 46.- Variation of L/D with C_R for same configuration as that used for figure 45.
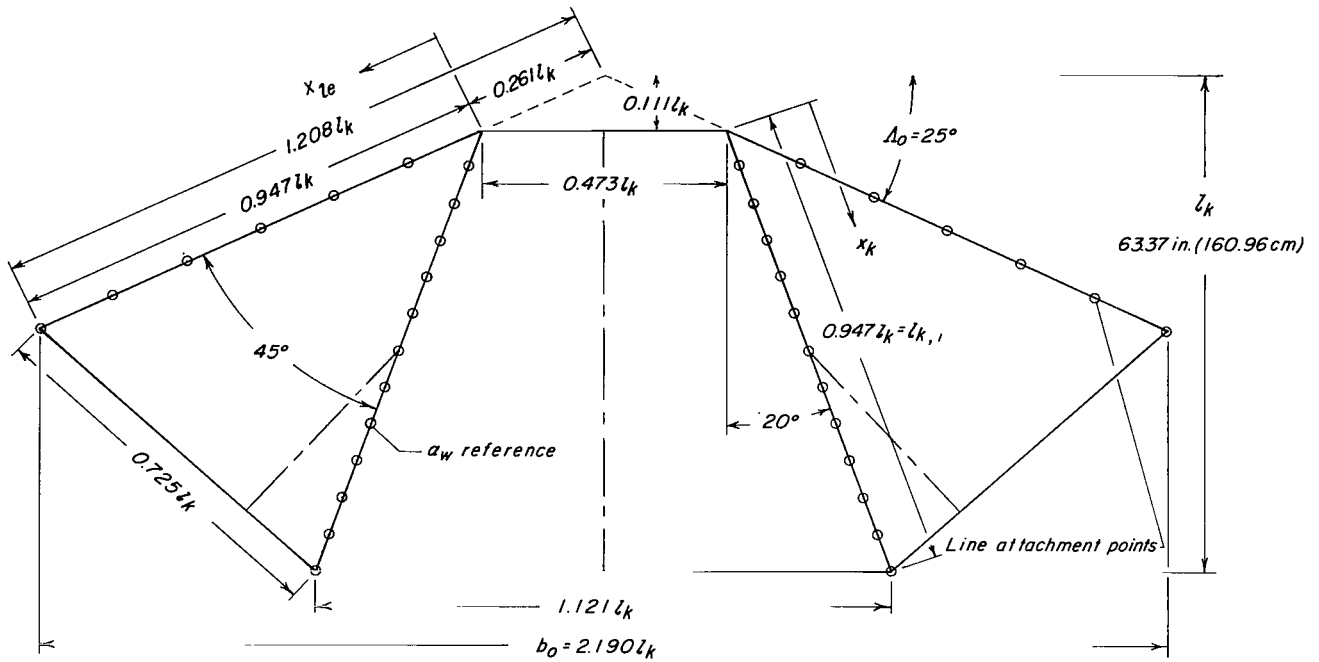
Figure 47.- Flat planform details of twin-keel model 24.
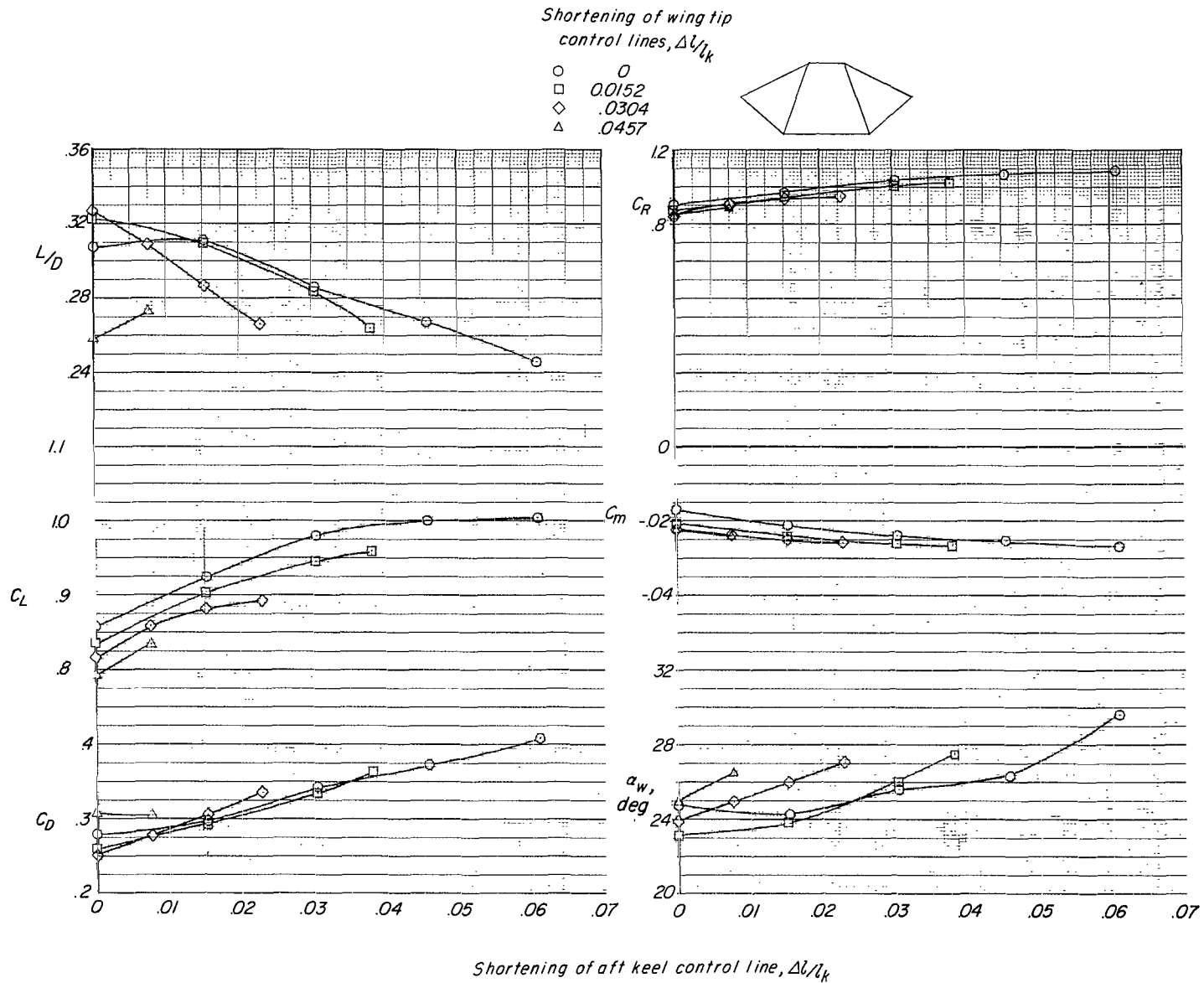
Figure 48.- Effect of aft keel control line shortening on the longitudinal aerodynamic characteristics of twin-keel model 24, 20° canted keels. Keel-to-payload separation distance ≈ $1.25l_k$.
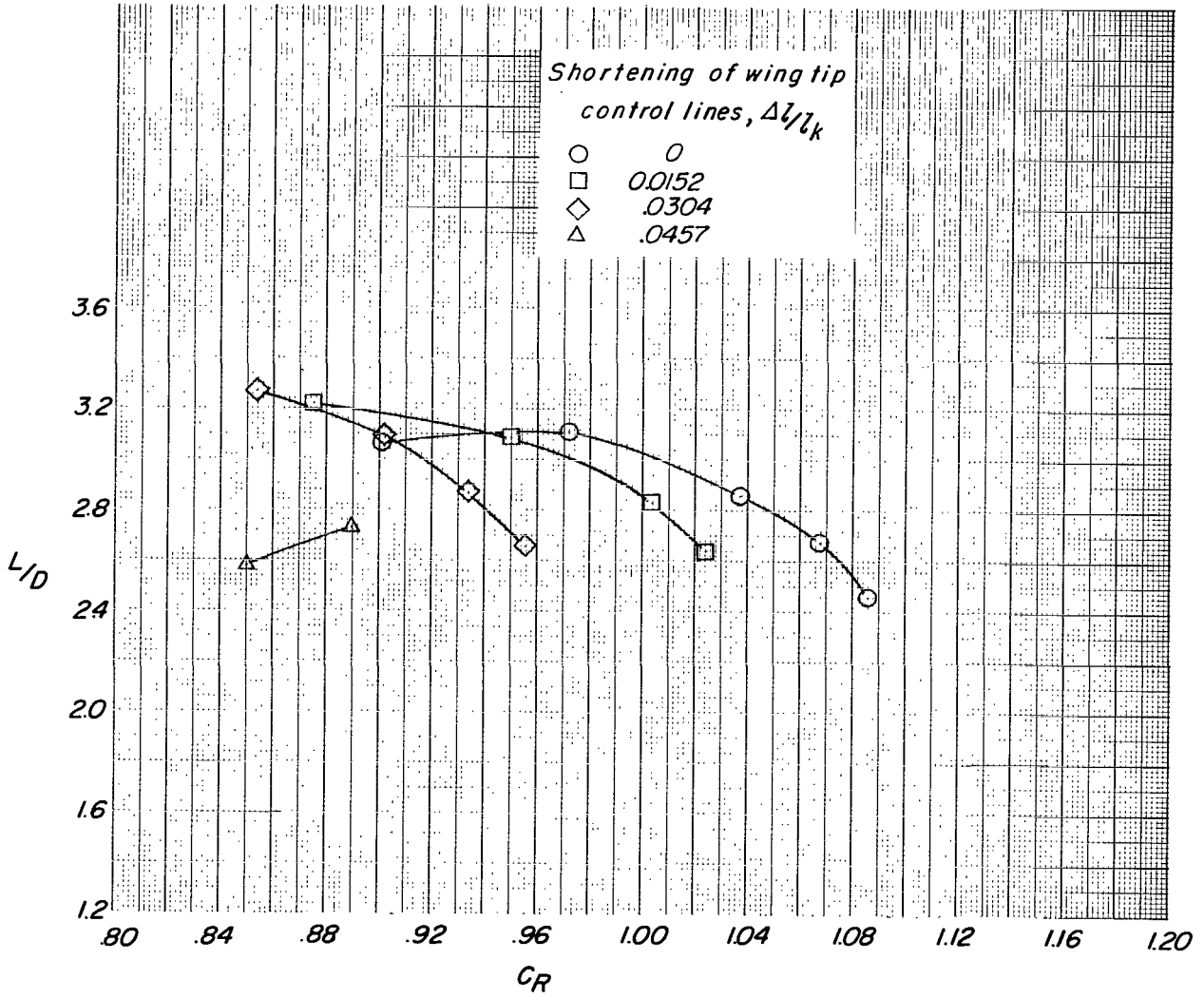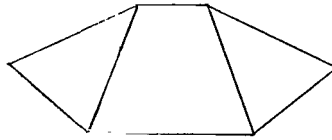
Figure 49.- Variation of L/D with C_R for same configuration as that used for figure 48.
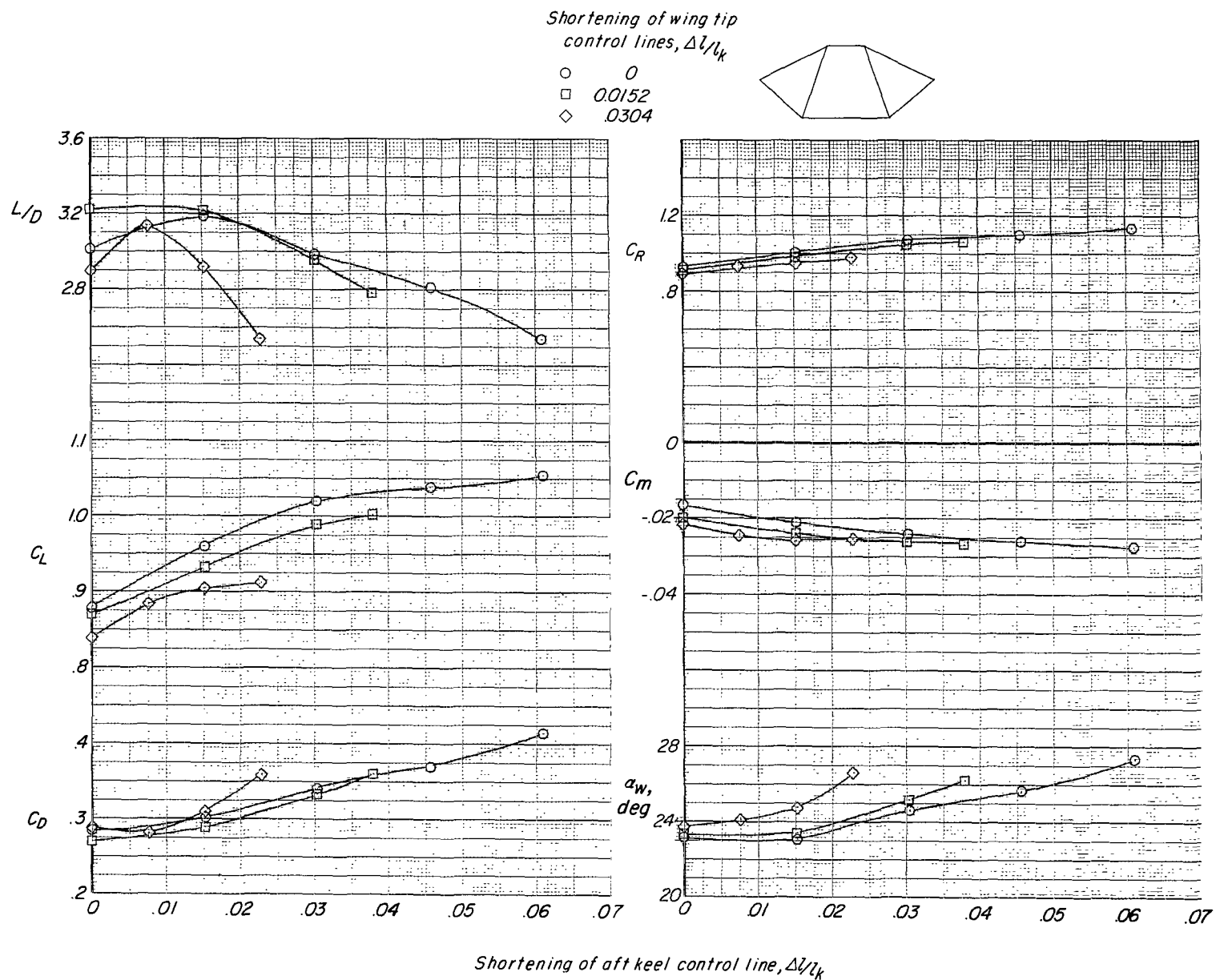
Figure 50.- Effect of aft keel control line shortening on the longitudinal aerodynamic characteristics of twin-keel model 24, 20^0 canted keels. Keel-to-payload separation distance $\approx 1.50 l_k$.
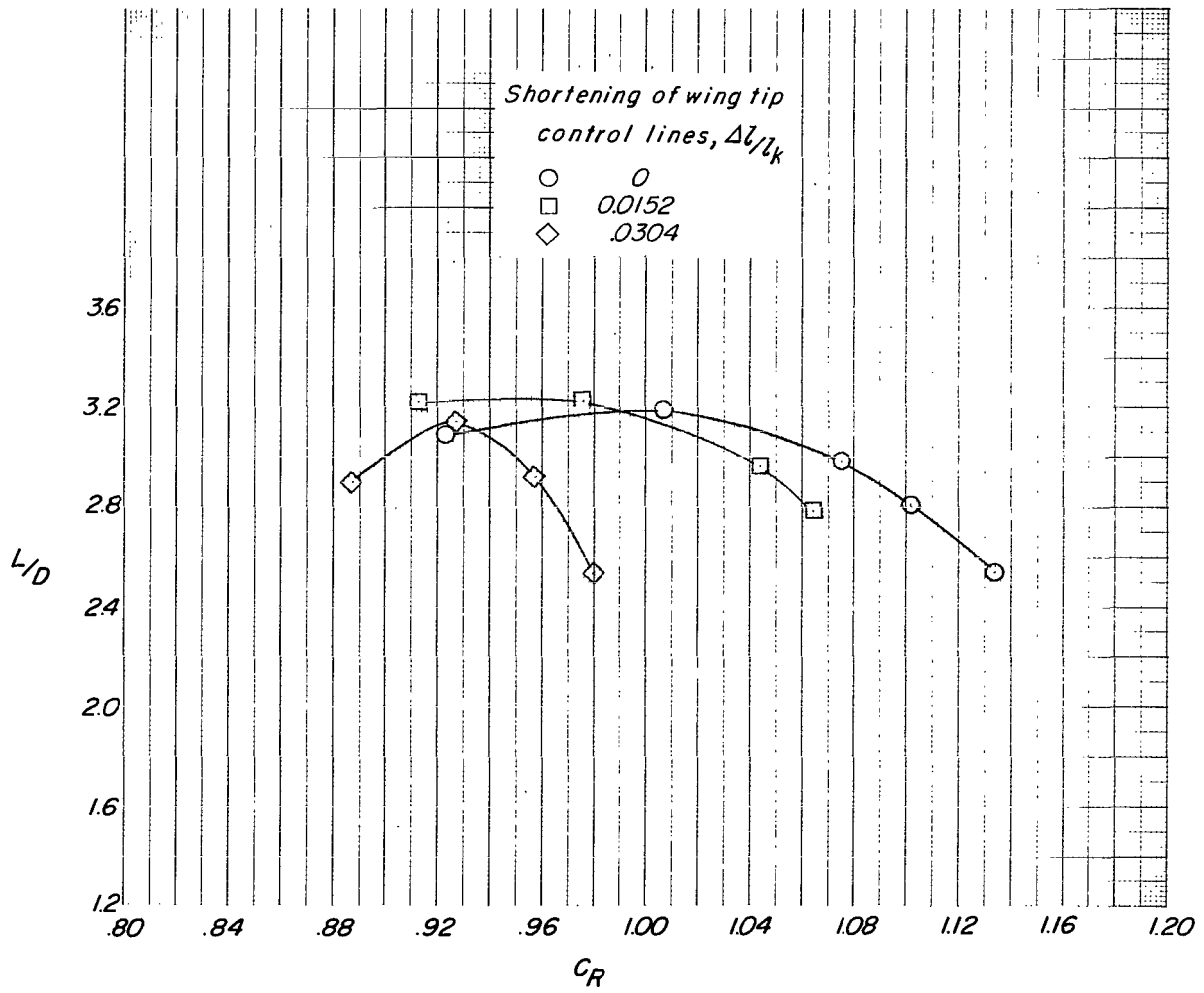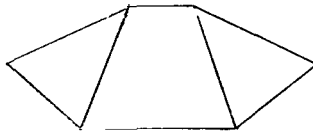
Figure 51.- Variation of L/D with C_R for same configuration as that used for figure 50.
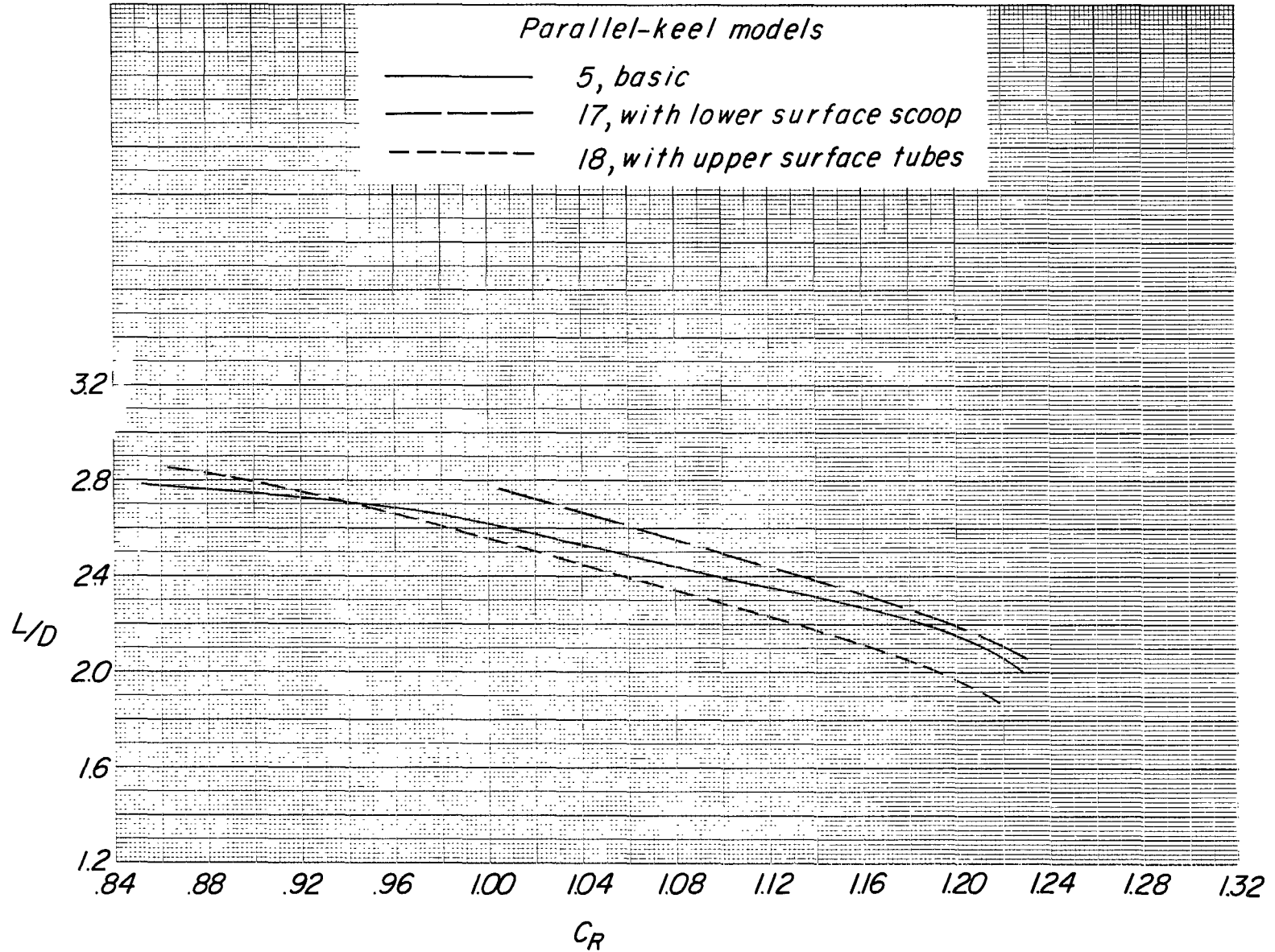
Figure 52.- Effect of addition of a ram-air-inflated scoop on lower surface and ram-air-inflated tubes on upper surface at the keels on the variation of L/D with C_R for a model having parallel keels. Keel-to-payload separation distance $\approx 1.00\ell_k$.

Keel cant angle, deg
———————— 0
— — — — — 5
— — — — — — 10
— — — — — — 15

L/D

C_R
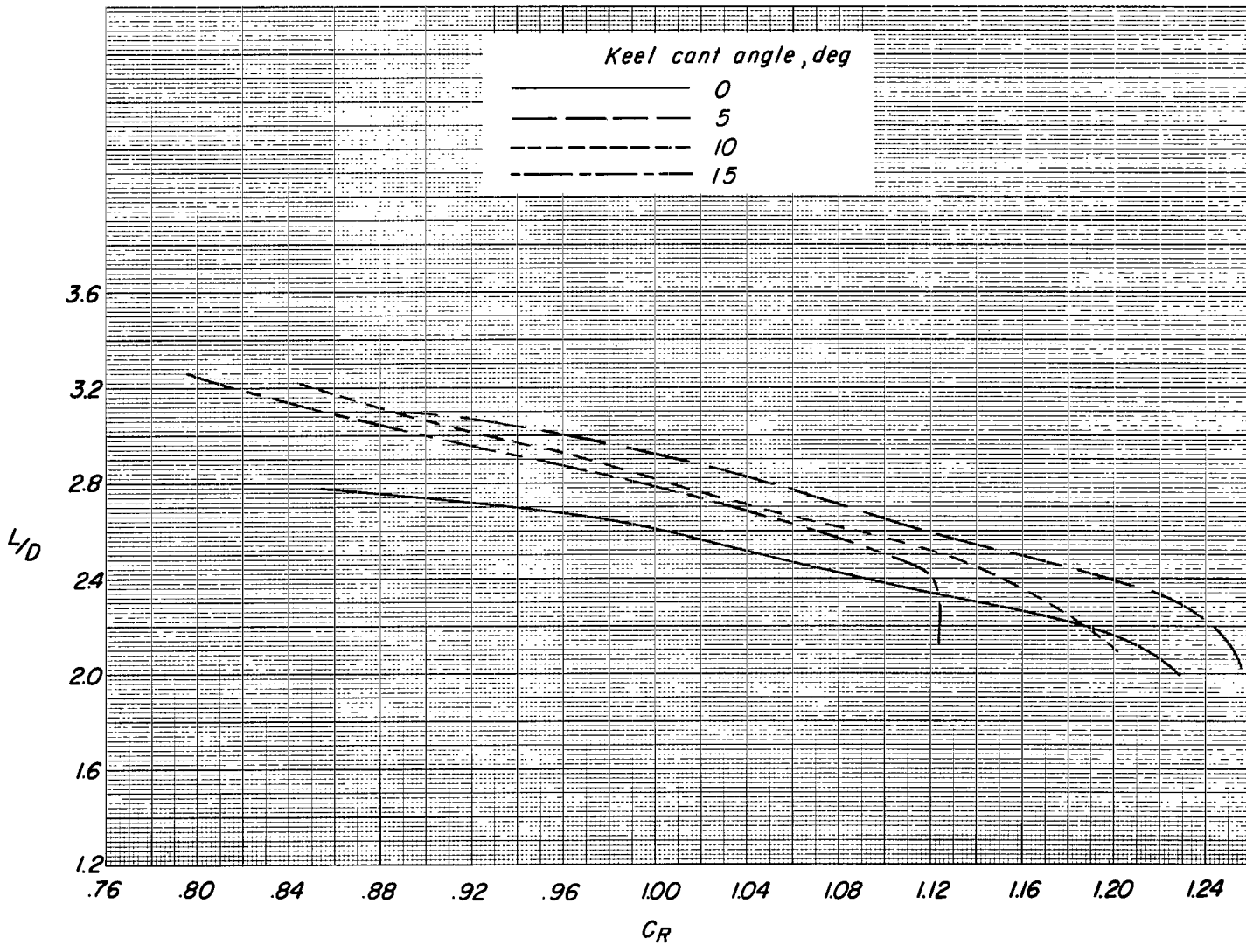
(a) $\frac{l}{l_k} \approx 1.00$.

Figure 53.- Effect of keel cant angle on the variation of L/D with C_R for models having the same center-panel width at the nose.
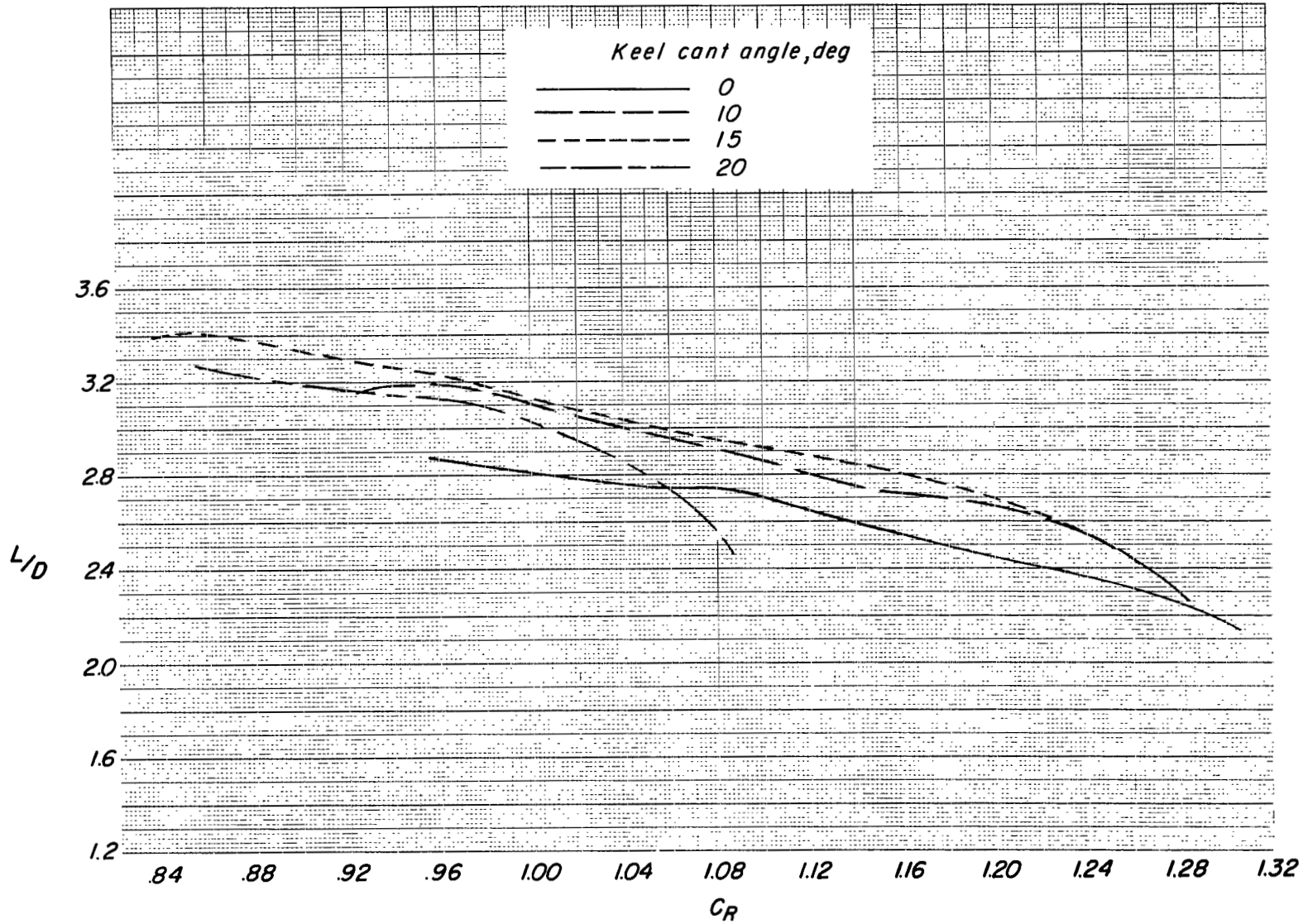
(b) $\dfrac{l}{l_k} \approx 1.25$.

Figure 53.- Concluded.
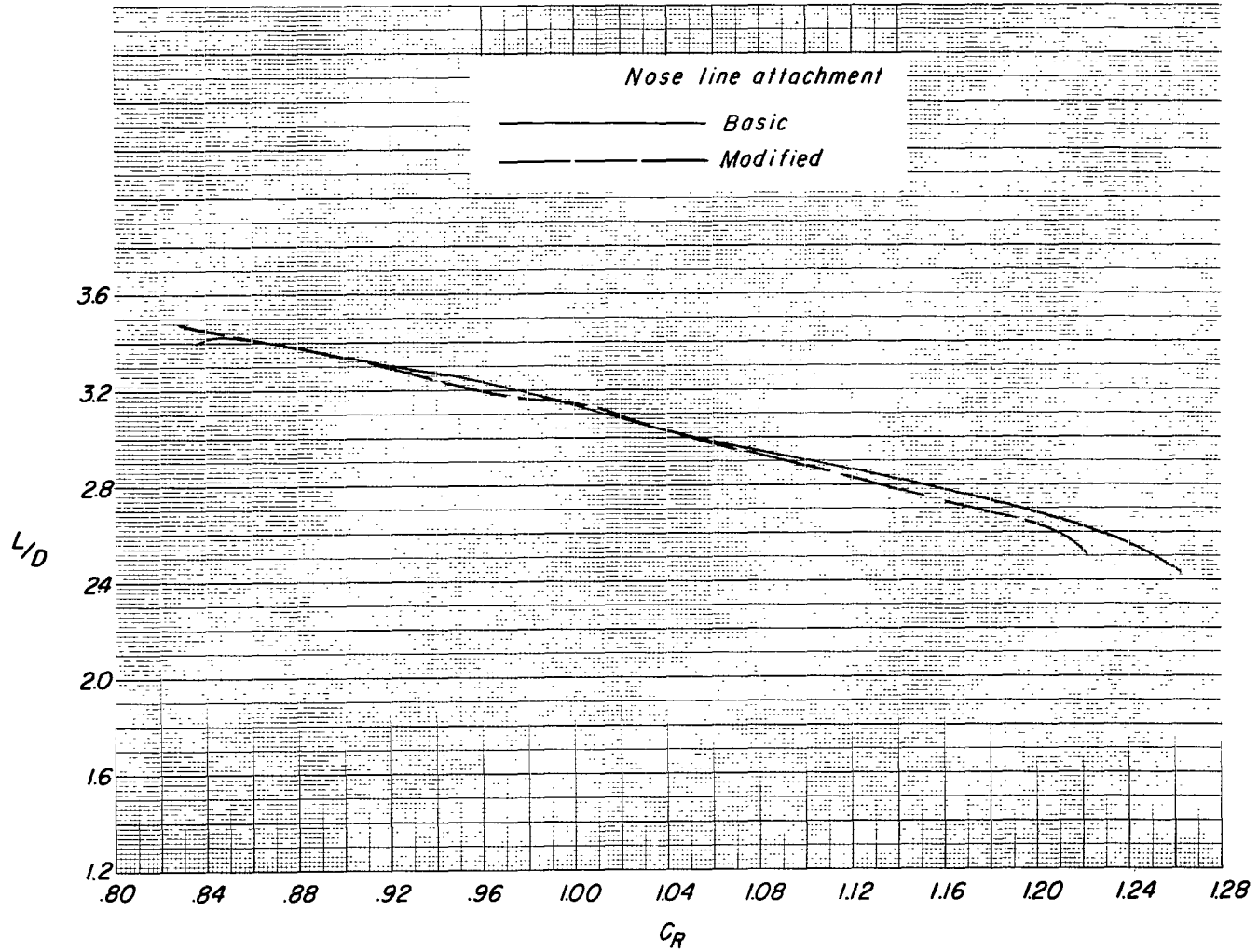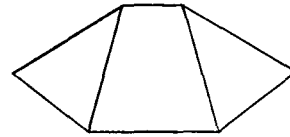
Figure 54.- Effect of nose line attachment modification for model 21. Keel-to-payload separation distance ≈ $1.25 l_k$.
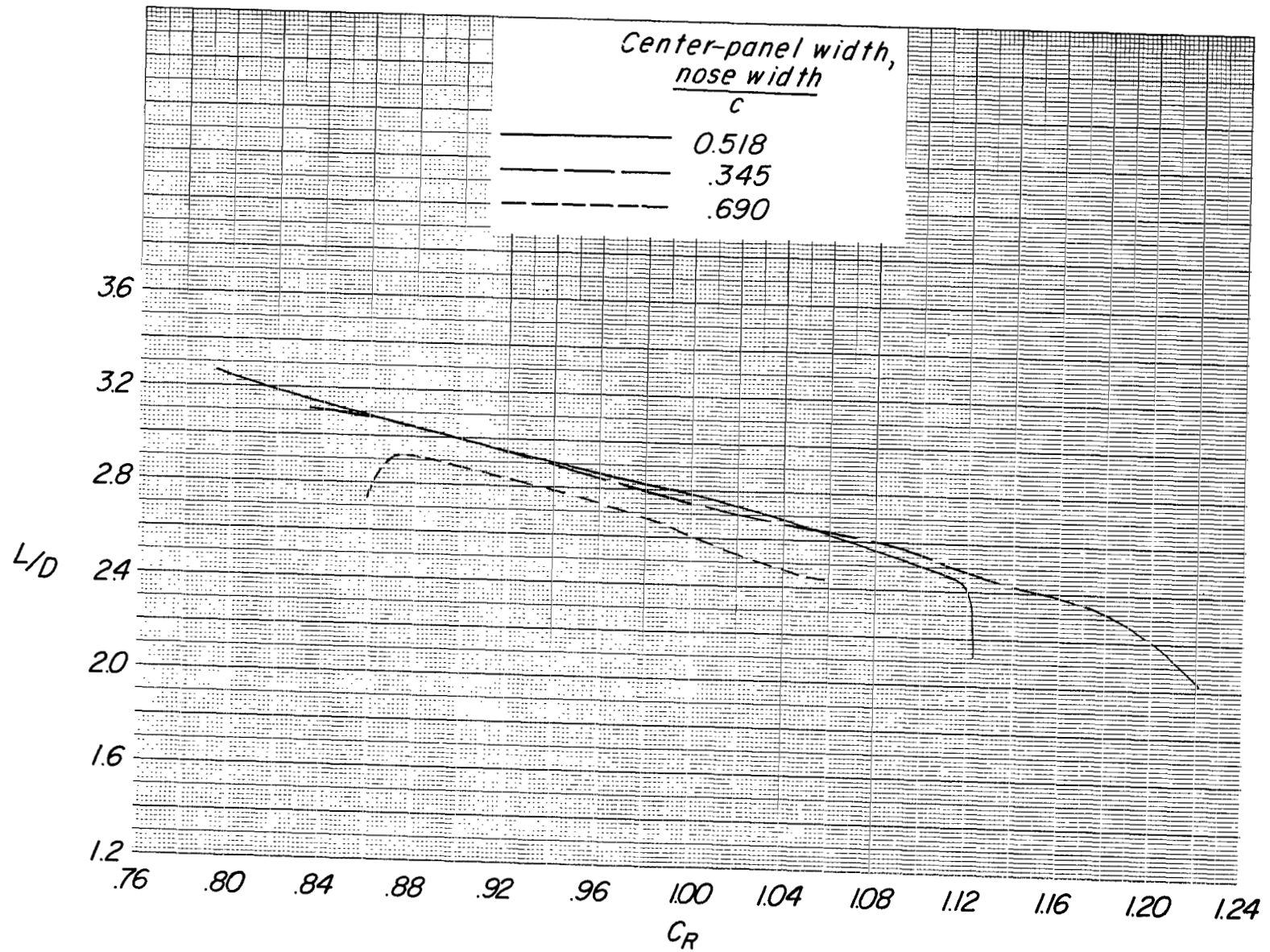
Figure 55.- Effect of center-panel width on the variation of L/D with C_R for models having 15° canted keels. Keel-to-payload separation distance $\approx 1.00 l_k$.
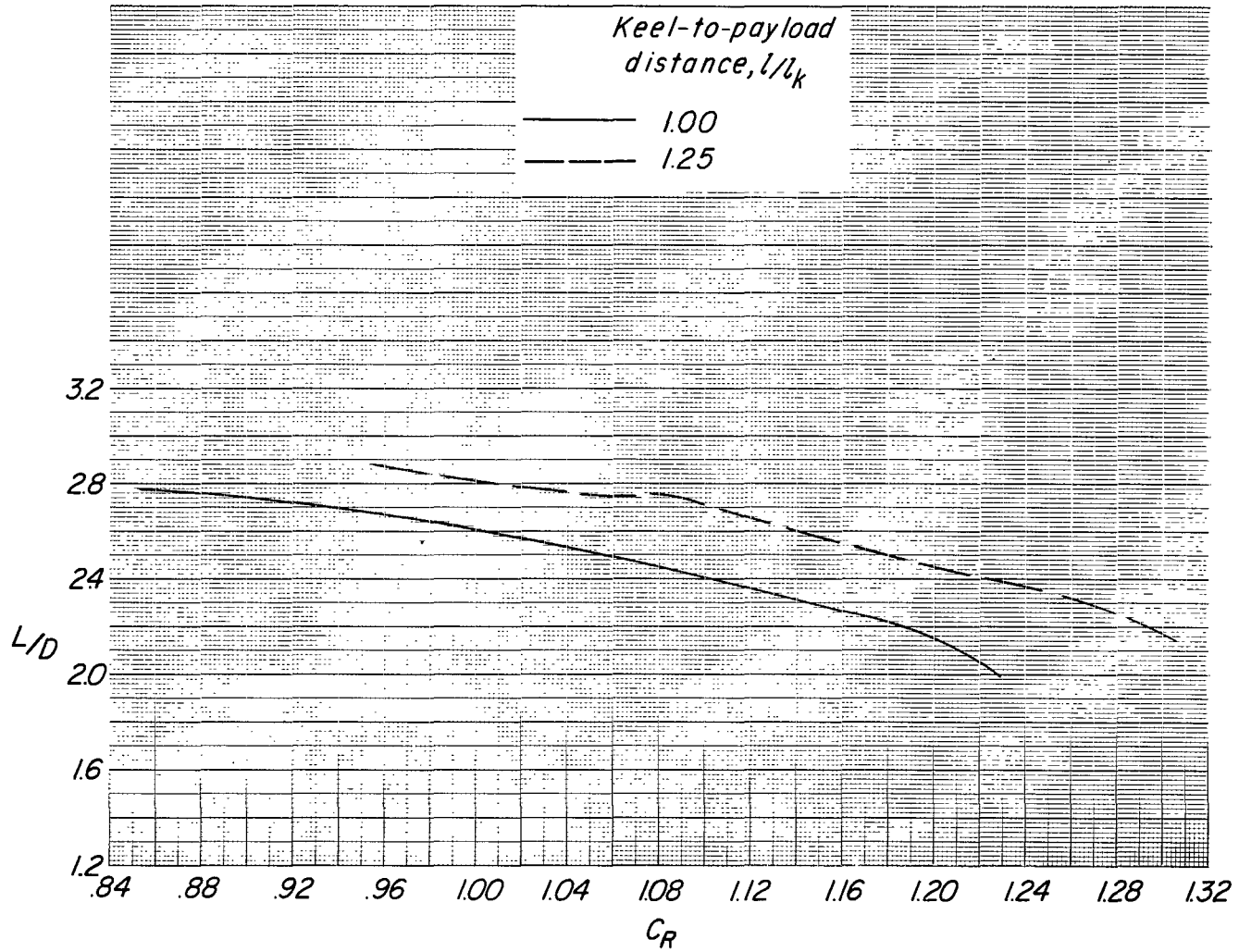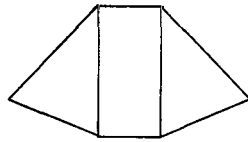
Figure 56.- Effect of keel-to-payload separation distance on the variation of L/D with C_R for model 5.
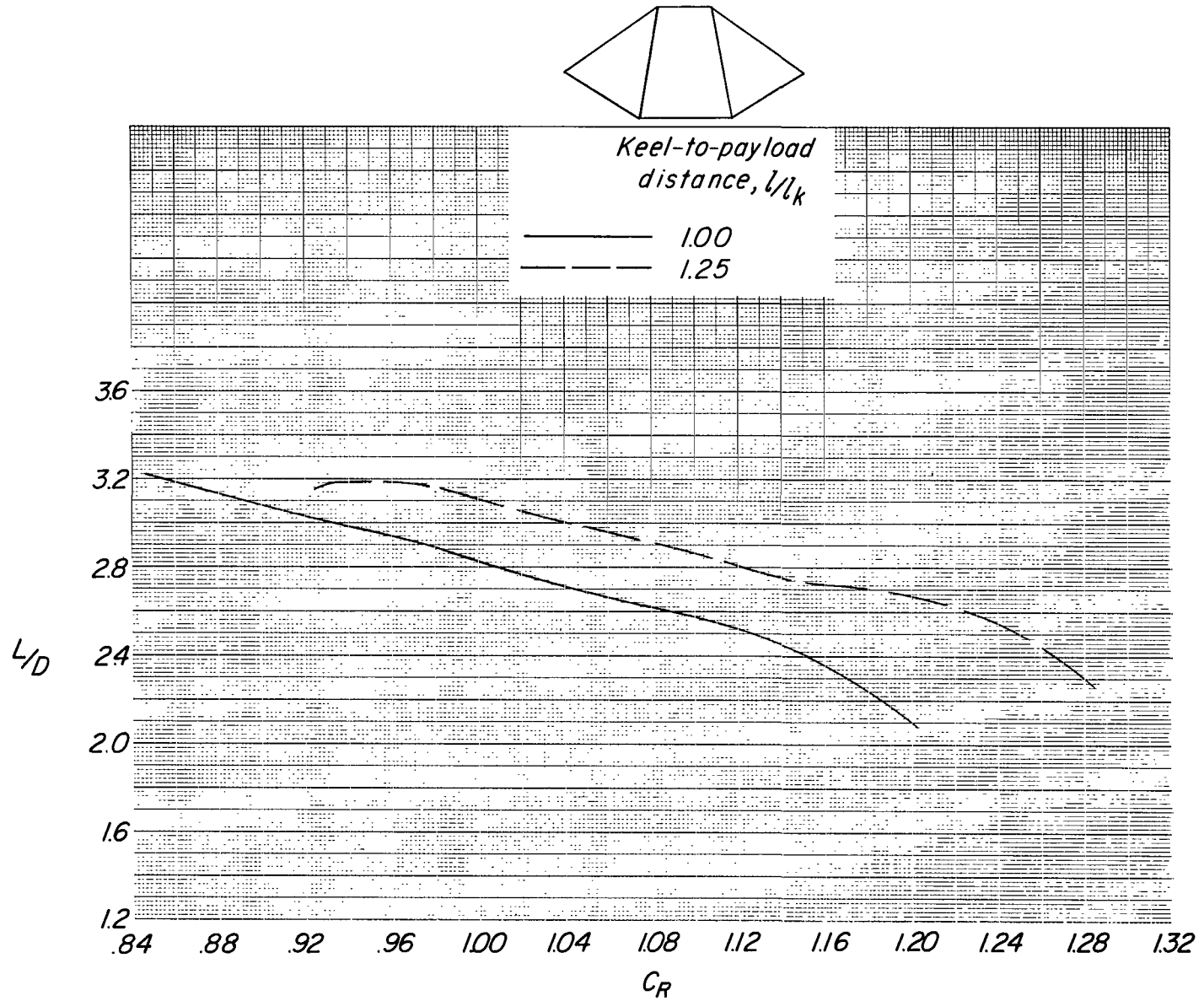
Figure 57.- Effect of keel-to-payload separation distance on the variation of L/D with C_R for model 20.
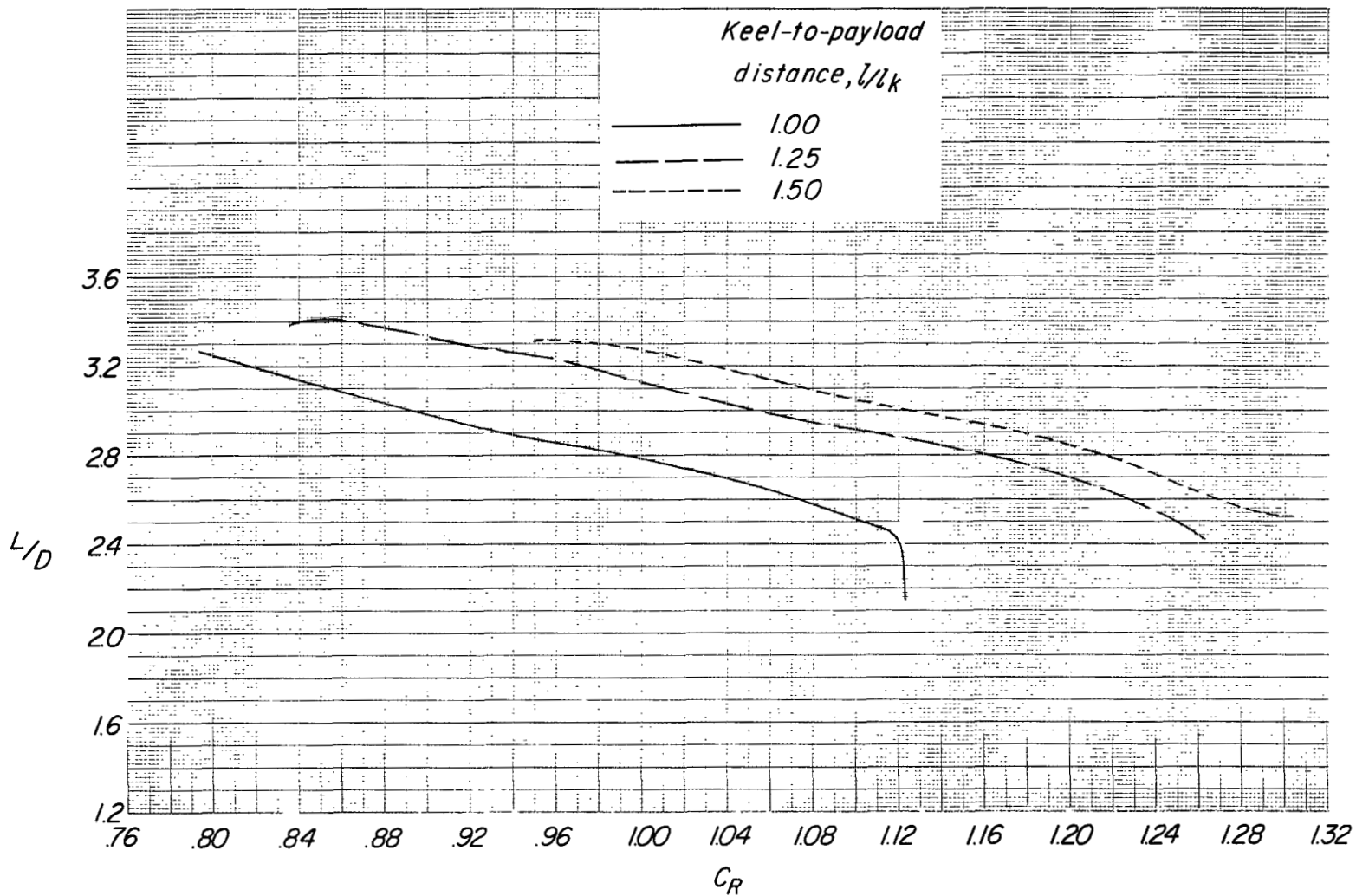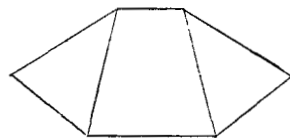
Figure 58.- Effect of keel-to-payload separation distance on the variation of L/D with C_R for model 21.
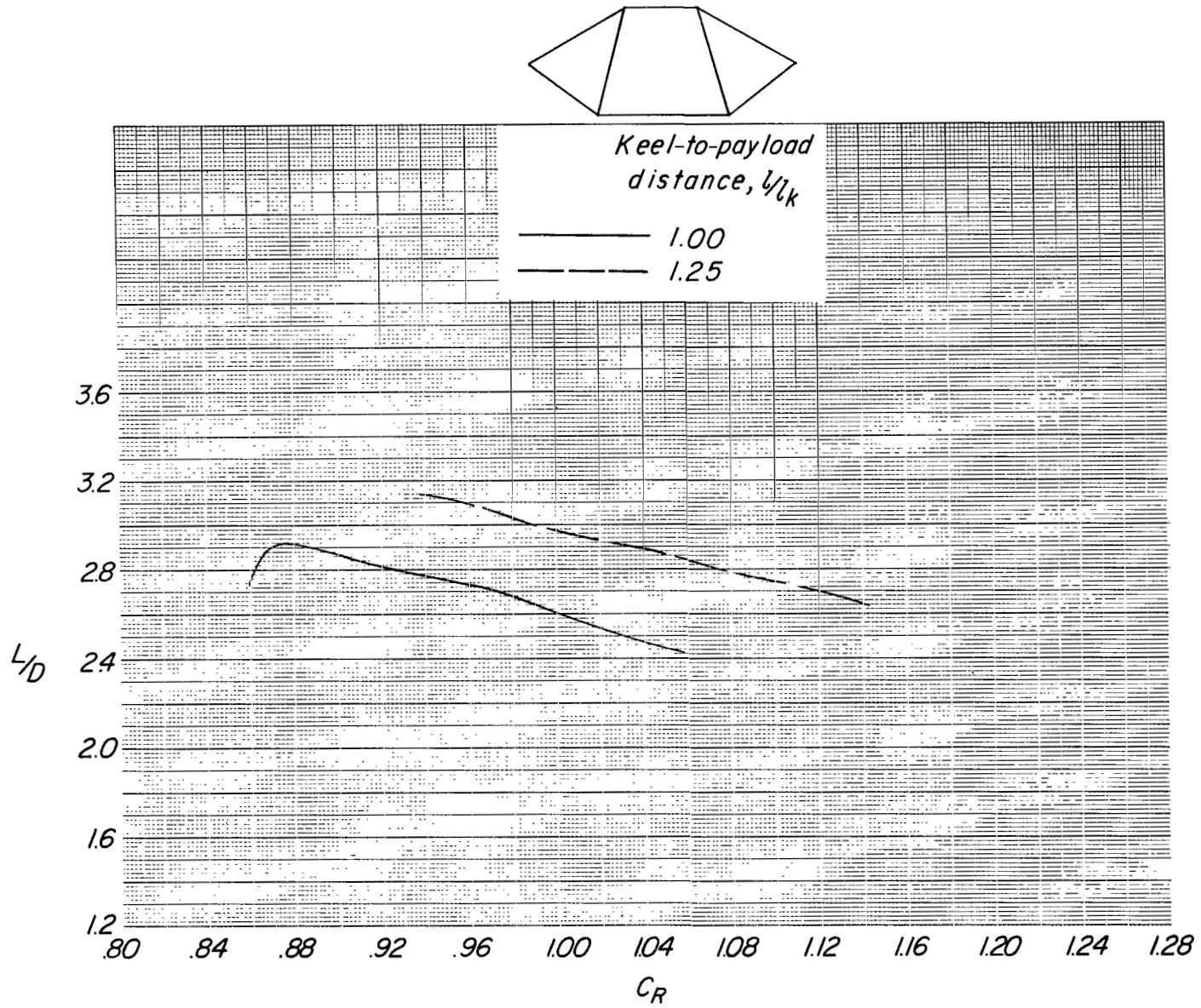
Figure 59.- Effect of keel-to-payload separation distance on the variation of L/D with C_R for model 23.
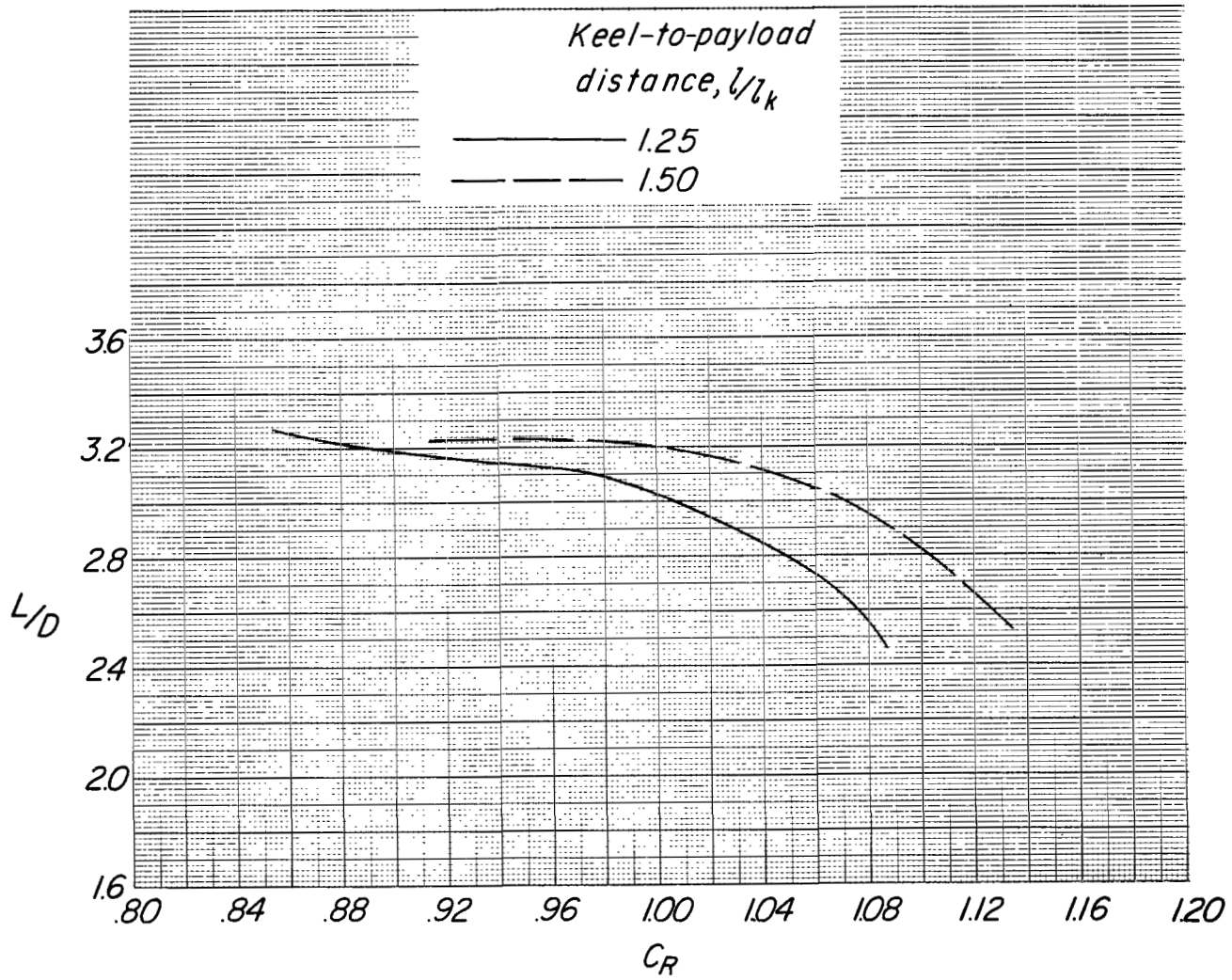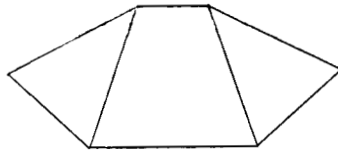
Figure 60.- Effect of keel-to-payload separation distance on the variation of L/D with C_R for model 24.
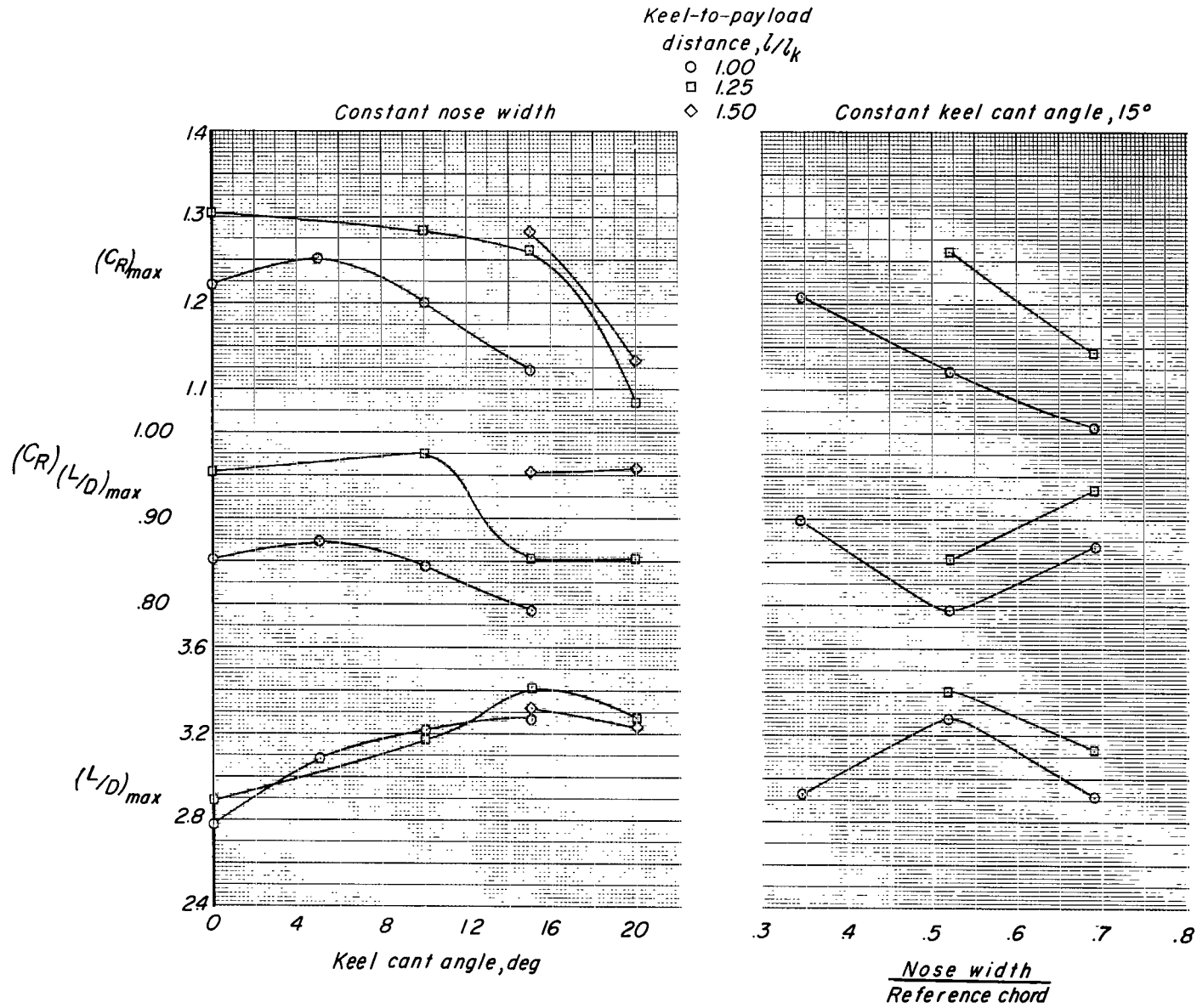
Figure 61.- Effect of keel cant angle and center-panel width on $(L/D)_{max}$, C_R for $(L/D)_{max}$, and $(C_R)_{max}$.

"The aeronautical and space activities of the United States shall be conducted so as to contribute . . . to the expansion of human knowledge of phenomena in the atmosphere and space. The Administration shall provide for the widest practicable and appropriate dissemination of information concerning its activities and the results thereof."

— NATIONAL AERONAUTICS AND SPACE ACT OF 1958

NASA SCIENTIFIC AND TECHNICAL PUBLICATIONS

TECHNICAL REPORTS: Scientific and technical information considered important, complete, and a lasting contribution to existing knowledge.

TECHNICAL NOTES: Information less broad in scope but nevertheless of importance as a contribution to existing knowledge.

TECHNICAL MEMORANDUMS: Information receiving limited distribution because of preliminary data, security classification, or other reasons.

CONTRACTOR REPORTS: Scientific and technical information generated under a NASA contract or grant and considered an important contribution to existing knowledge.

TECHNICAL TRANSLATIONS: Information published in a foreign language considered to merit NASA distribution in English.

SPECIAL PUBLICATIONS: Information derived from or of value to NASA activities. Publications include conference proceedings, monographs, data compilations, handbooks, sourcebooks, and special bibliographies.

TECHNOLOGY UTILIZATION PUBLICATIONS: Information on technology used by NASA that may be of particular interest in commercial and other non-aerospace applications. Publications include Tech Briefs, Technology Utilization Reports and Notes, and Technology Surveys.

Details on the availability of these publications may be obtained from:

SCIENTIFIC AND TECHNICAL INFORMATION DIVISION

NATIONAL AERONAUTICS AND SPACE ADMINISTRATION

Washington, D.C. 20546